AUSTRAL

JOURNAL OF IMAGING

REVISTA CHILENA DE RADIOLOGÍA

Indexed in: SciELO, Scopus, EMBASE, DOAJ, LATINDEX Catálogo 2.0, MIAR, Bibliovigilance, Dialnet
ISSN: 2810-6954 / e-ISSN: 2810-708X
VOLUME 32. ISSUE 4, OCTOBER-DECEMBER 2026

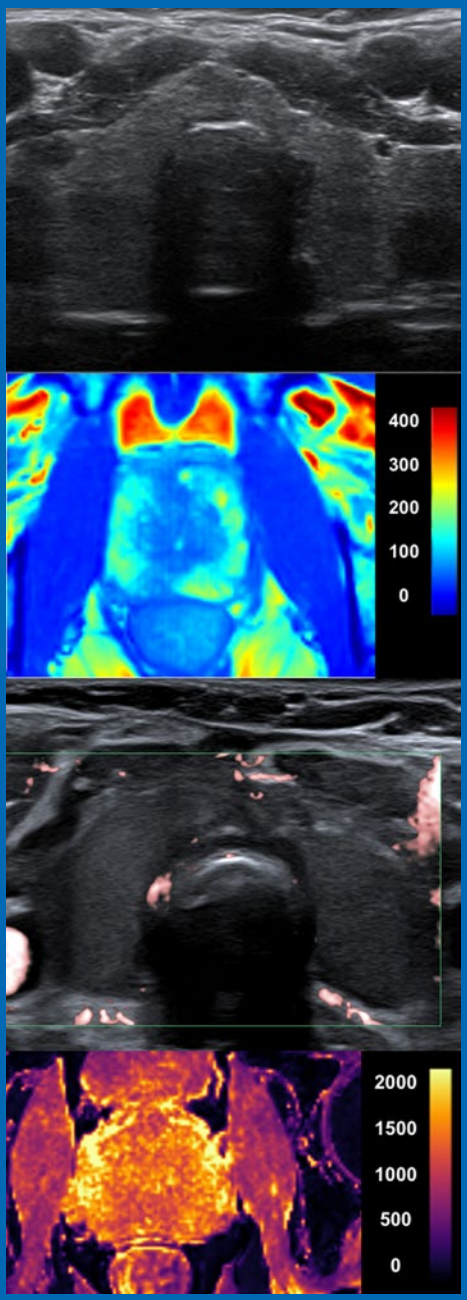

To seek the truth, one must doubt everything, as far as possible

Analysis of T1/T2 parametric maps with DESPO+ sequence in suspected prostate cancer

Copper filters in angiography and secondary radiation: an experimental study

Healthy lifestyles among students of radiology and diagnostic imaging technology

Bibliometric analysis of the *Revista Chilena de Radiología/Austral Journal of Imaging* (1995-2025)

Protection of the lens in fluoroscopic procedures: international standards, implementation gaps, and roadmap for Chile

Radiomics in lung cancer: advances and challenges in clinical practice

Postoperative pseudothyroid on ultrasound: avoiding misinterpretation of the surgical bed

PERMANYER
www.permanyer.com

www.resochradi.com

AUSTRAL
JOURNAL OF IMAGING
REVISTA CHILENA DE RADIOLOGÍA

Indexed in: SciELO, Scopus, EMBASE, DOAJ, LATINDEX Catálogo 2.0, MIAR, Bibliovigilance, Dialnet
ISSN: 2810-6954 / e-ISSN: 2810-708X
VOLUME 32. ISSUE 4, OCTOBER-DECEMBER 2026

Editorial Board

Editor in Chief

Patricia Guzmán Falcón
Hospital San Juan de Dios, Universidad Diego Portales, Santiago, Chile

National Editors

Juan P. Cruz
Clínica Santa María e Instituto de Neurocirugía, Santiago, Chile

Nicolás Sánchez Domínguez
Clínica Alemana, Universidad del Desarrollo, Santiago, Chile

Carla Sáez Tapia
Hospital Clínico, Universidad de Chile, Santiago, Chile

Claudia Astudillo Abarca
Clínica Las Condes, Santiago, Chile

Jorge Contardo Pérez
Hospital Clínico, Universidad de Chile, Santiago, Chile

Carlos Toledo
Hospital las Higueras, Talcahuano, Bío Bío, Chile

David Ladrón de Guevara Hernández
IRAM y Hospital San Juan de Dios, Universidad Diego Portales, Santiago, Chile

Eduardo Bravo Rius
Hospital de niños Dr. Luis Calvo Mackenna, Santiago, Chile

Felipe Allende Nuñez
Universidad Mayor y Universidad de San Sebastián, Santiago, Chile

Felipe Zumaeta Valenzuela
Hospital Regional de Iquique, Iquique, Chile

International Editors

Sonia Bermúdez Muñoz
Hospital Universitario Fundación Santa Fe de Bogotá, Bogotá, Colombia

Janio Szklaruk
MD Anderson Cancer Center, Houston, TX, Estados Unidos

Marcel Koenigkam Santos
Hospital das Clínicas de Bauru, Universidad de São Paulo, São Paulo, Brasil

Araceli Cué Castro
Hospital General Dr. Enrique Cabrera, Ciudad de México, México

Cristina García Villar
Hospital Universitario Puerta del Mar de Cádiz, Cádiz, España

Advisory Editorial Board

Julieta Aránguiz Ramírez
Bioestadística e Investigación Biomédica, Universidad Diego Portales, Santiago, Chile

Rolando Cocio
Salud Pública, Clínica Alemana, Universidad del Desarrollo, Santiago, Chile

Pablo Del Río López
Protección Radiológica, Hospital Militar de Santiago, Universidad Mayor, Santiago, Chile

PERMANYER
www.permanyer.com

www.resochradi.com

11902ACHI264

AUSTRAL JOURNAL OF IMAGING
REVISTA CHILENA DE RADIOLOGÍA

PERMANYER

Check for updates

EDITORIAL

To seek the truth, one must doubt everything, as far as possible[1]

Para investigar la verdad es preciso dudar, en cuanto sea posible, de todas las cosas[1]

Patricia Guzmán-Falcón

Editor in Chief, Austral Journal of Imaging/Revista Chilena de Radiología, Santiago, Chile

René Descartes, *Principios de la filosofía*, Parte I, §1 (1644).
Translation from the original Latin

We are living through a period of profound transformation in which artificial intelligence has become a central player, permeating activities ranging from the simple and everyday tasks to the production of knowledge. It is a clearly useful tool, capable of facilitating and accelerating processes that are repetitive, cumbersome, and often time-consuming.

In our own editorial experience, an increasing number of manuscripts declare the use of artificial intelligence, at least as a support tool for orthographic or linguistic review. Resisting this transformation seems unreasonable. The relevant discussion is probably no longer whether we will use artificial intelligence, but rather how we will use it and, especially, what we are willing to delegate to it.

At this juncture, it is worth revisiting what remains essential to the human construction of knowledge: our capacity to reflect, create, formulate questions, and, above all, doubt. Cartesian doubt takes on particular relevance here. Never has it been so easy to obtain an answer, and, for that very reason, never has it been so important to preserve the capacity to question it.

Science is built precisely upon questions. It is not enough to find a plausible answer, it is necessary to examine its origin, evaluate the supporting evidence, acknowledge its limitations, and determine the extent to which it can be considered valid. All this forms part of the daily work of science: asking ourselves not only *what we know*, but also *how we know what we believe we know*.

Metacognition, understood as the ability to observe and evaluate our own thought processes, is another equally important dimension. Recognizing what we know and what we ignore, identifying when an explanation is insufficient, determining when to seek new evidence, or even recognizing when our own biases are shaping a conclusion, all constitute fundamental aspects of learning, research, and professional judgment.

In this context, critical thinking does not simply consist of rejecting answers, but rather it involves comparing, substantiating, and scrutinizing them. Doubting everything, as far as possible, as proposed by Descartes[1], does not imply permanent distrust or a form of defiant contrarianism, but rather it signifies a willingness to withhold acceptance of anything as true until it has been sufficiently examined.

Generative artificial intelligence introduces a new tension here, as it can formulate arguments, synthesize evidence, propose interpretations, and produce texts with apparent coherence and certainty. The risk, perhaps, lies not in the act of using it, but in ceasing to perform ourselves, some of the cognitive operations we increasingly entrust to it, amounting to a form of cognitive surrender, akin to concepts described in the

Correspondence:
Patricia Guzmán-Falcón
E-mail: patricia.guzman.f@redsalud.gob.cl

Date of reception: 01-08-2026
Date of acceptance: 28-08-2026
DOI: 10.24875/AJI.M26000041

Available online: 26-10-2026
Austral J. Imaging. (Engl. ed.). 2026;32(4):161-162
www.resochradi.com

2810-708X / © 2026 Sociedad Chilena de Radiología. Published by Permanyer. This is an open access article under the CC BY-NC-ND license (https://creativecommons.org/licenses/by-nc-nd/4.0/).

literature as "*cognitive offloading*" or "*cognitive outsourcing*": the transfer of tasks to external tools that previously required our own mental effort. This delegation is not necessarily detrimental, as not all cognitive tasks are equivalent. Delegating a spelling correction is not the same as delegating the formulation of a question; summarizing information is not the same as interpreting it, and, above all, arriving at a conclusion does not mean having gone through the often arduous, intellectual process required to understand, question, or defend it.

The challenge posed by generative artificial intelligence may not be to preserve intact every traditional way of doing things, but rather to recognize which of our cognitive processes are worth protecting precisely because they are an integral part of learning, creation, and the construction of knowledge.

Reference

1. Descartes R. Principia philosophiae. Amstelodami: apud Ludovicum Elzevirium; 1644. Pars 1, Art. 1.

AUSTRAL JOURNAL OF IMAGING
REVISTA CHILENA DE RADIOLOGÍA

PERMANYER

Check for updates

ORIGINAL ARTICLE

Analysis of T1/T2 parametric maps with DESPO+ sequence in suspected prostate cancer

Análisis de mapas paramétricos T1/T2 con secuencia DESPO+ en sospecha de cáncer de próstata

José M. González-del-Valle[1], Ronal Coronado[2,3], Pablo Irarrázaval[3,4], Marcelo Andía[1,3], Javier Domínguez[5], and Cecilia Besa[3,6]*

[1]Radiology Department, Faculty of Medicine, Pontificia Universidad Católica de Chile; [2]Engineering and Business Faculty, Universidad de Las Américas; [3]Millennium Institute for Intelligent Healthcare Engineering (iHEALTH); [4]Department of Electrical Engineering, Faculty of Engineering; [5]Urology Department; [6]Radiology Department, Biomedical Imaging Center. Faculty of Medicine, Pontificia Universidad Católica de Chile. Santiago, Chile

Abstract

Introduction: *Prostate cancer (PCa) is the most common malignancy among men in Chile. Multiparametric MRI has improved its detection; however, substantial interobserver variability persists. Quantitative T1 and T2 parametric maps offer additional tissue characterization, but their clinical use has been limited by long acquisition times and frequent artifacts in the prostate region.* **Objective:** *To evaluate the DESPO+ technique in patients with suspected PCa, determining whether the values obtained from T1 and T2 parametric maps agree with published reference ranges and whether they distinguish healthy tissue from biopsy-proven lesions.* **Material and methods:** *Forty men with clinical suspicion of PCa were included (mean age 63 ± 7 years; PSA 7 ± 9 ng/mL). Fifty percent presented PI-RADS ≥ 3 lesions, mainly in the peripheral zone, all confirmed histologically.* **Results:** *T1/T2 maps obtained with DESPO+ showed no relevant artifacts, and the quantitative values agreed with those reported in the literature. Significant differences were found across anatomical regions: in the peripheral zone both T1 and T2 values were lower in tumor tissue compared with healthy tissue, and no significant differences were observed in the transition zone.* **Conclusions:** *DESPO+ demonstrated clinical feasibility and potential to enhance the quantitative characterization of PCa. Larger cohorts and external validation are needed.*

Keywords: *Prostatic neoplasms. Magnetic resonance imaging. Multiparametric magnetic resonance imaging. Image processing.*

Resumen

Introducción: *El cáncer de próstata (PCa) es la neoplasia más frecuente en los hombres en Chile. La resonancia magnética multiparamétrica ha mejorado su detección y caracterización, aunque persiste una importante variabilidad interobservador. Los mapas paramétricos T1 y T2 aportan información cuantitativa complementaria, pero su uso clínico ha sido limitado por los largos tiempos de adquisición y los artefactos en la región prostática.* **Objetivo:** *Evaluar la técnica DESPO+ en pacientes con sospecha de PCa, determinando si los valores cuantitativos T1/T2 concuerdan con lo descrito en la literatura y permiten diferenciar tejido sano de lesiones confirmadas.* **Material y métodos:** *Se incluyeron 40 hombres con sospecha clínica de PCa (edad 63 ± 7 años; APE 7 ± 9 ng/ml). El 50% presentaron lesiones PIRADS ≥ 3, predominantemente en la*

***Correspondence:**
José M. González-del-Valle
E-mail: jmgonzalez11@uc.cl

Date of reception: 27-06-2025
Date of acceptance: 19-03-2026
DOI: 10.24875/AJI.25000048

Available online: 26-10-2026
Austral J. Imaging. (Engl. ed.). 2026;32(4):163-172
www.resochradi.com

2810-708X / © 2026 Sociedad Chilena de Radiología. Published by Permanyer. This is an open access article under the CC BY-NC-ND license (https://creativecommons.org/licenses/by-nc-nd/4.0/).

zona periférica, todas confirmadas por histología. **Resultados:** *Los mapas T1/T2 adquiridos con DESPO+ no mostraron artefactos relevantes y tuvieron valores compatibles con los rangos publicados. Se observaron diferencias significativas entre regiones anatómicas: en la zona periférica, los valores T1 y T2 fueron menores en tejido tumoral que en tejido sano, y en la zona transicional no se identificaron diferencias significativas.* **Conclusiones:** *DESPO+ demostró viabilidad clínica y potencial para fortalecer la caracterización del PCa. Se requieren estudios con mayor tamaño muestral y validación externa.*

Palabras clave: *Neoplasias prostáticas. Resonancia magnética. Resonancia magnética multiparamétrica. Procesamiento de imágenes.*

Introduction

Prostate cancer (PCa) is a major health problem. Currently, approximately 10 million men in the United States are living with a diagnosis of prostate cancer (PCa), the metastatic stage of the disease being the cause of more than 400,000 deaths annually, a figure expected to double by 2040.[1] In 2022, the Global Cancer Observatory reported that PCa in Chile presented an incidence of over 9,000 cases and was associated with approximately 2,000 deaths, making it the cancer with the highest incidence and mortality among the male population.[2]

Multiparametric magnetic resonance imaging (mpMRI) is currently the imaging modality of choice for evaluating patients with suspected prostate cancer (PCa). The diagnostic algorithm begins with identifying risk factors, performing a clinical assessment via digital rectal examination, and determination of prostate-specific antigen (PSA) levels. In the event of abnormal findings, mpMRI enables the detection and characterization of lesions suspicious for PCa and also guides biopsy procedures. Its use is supported by international guidelines.[3–5] and studies, such as PROMIS, which have demonstrated its efficacy in increasing the detection of clinically significant cancer while reducing the overdiagnosis of indolent tumors.[6,7]

The PI-RADS (Prostate Imaging–Reporting and Data System) v2.1, used to classify and interpret prostate mpMRI, correlates well with the histological presence of PCa.[3] However, as it is a qualitative system, it presents inter-observer variability. Studies have reported moderate to adequate agreement among radiologists, with kappa coefficients of 0.7[8] and 0.593 in the peripheral zone (PZ) for PI-RADS ≥ 4 lesions[9], highlighting the need for strategies to reduce this diagnostic variability.

A promising alternative is the use of quantitative imaging, such as T1 and T2 parametric maps, which allow for more precise tissue characterization.[10] Nevertheless, its clinical implementation faces limitations, such as long 3D acquisition times and *off-resonance* artifacts. One solution for this is the DESPO+ (driven equilibrium single pulse observation of T1/T2 plus) technique, which not only enables the reconstruction of T1 and T2 3D maps, but also reduces acquisition time and corrects the aforementioned artifacts (Fig. 1).[10]

Our study group has previously developed and applied the DESPO+ technique in a cohort of 14 healthy patients, obtaining T1 and T2 parametric maps with results comparable to those reported in the literature.[10] These initial findings support the technical feasibility and reproducibility of the method. However, it is essential to evaluate its performance in patients with suspected PCa.

Therefore, the objective of this study is to evaluate the performance of the DESPO+ technique in patients with suspected PCa through quantitative analysis of T1 and T2 parametric maps. We aim to verify whether the obtained values align with ranges described in the literature and to determine whether they allow for the differentiation of healthy tissue from lesions diagnosed as PCa. In doing so, we explore the technique's potential clinical usefulness as a complement to mpMRI and the PI-RADS system, providing a quantitative tool that contributes to reducing diagnostic variability.

Material and methods

Patients

This prospective, single-center study utilized a database from our research group (*Fondecyt Regular* 1210468) and was approved by the Ethics Committee of the *Pontificia Universidad Católica de Chile* (Approval Number 200612004). Written informed consent was obtained from all participants. The study included patients with suspected PCa between October 2022 and January 2024, who were referred by the urology team at the *Red de Salud UC Christus* (UC Christus Health Network). Clinical suspicion of PCa was defined by elevated PSA, a family history of PCa, or an abnormal digital rectal examination.

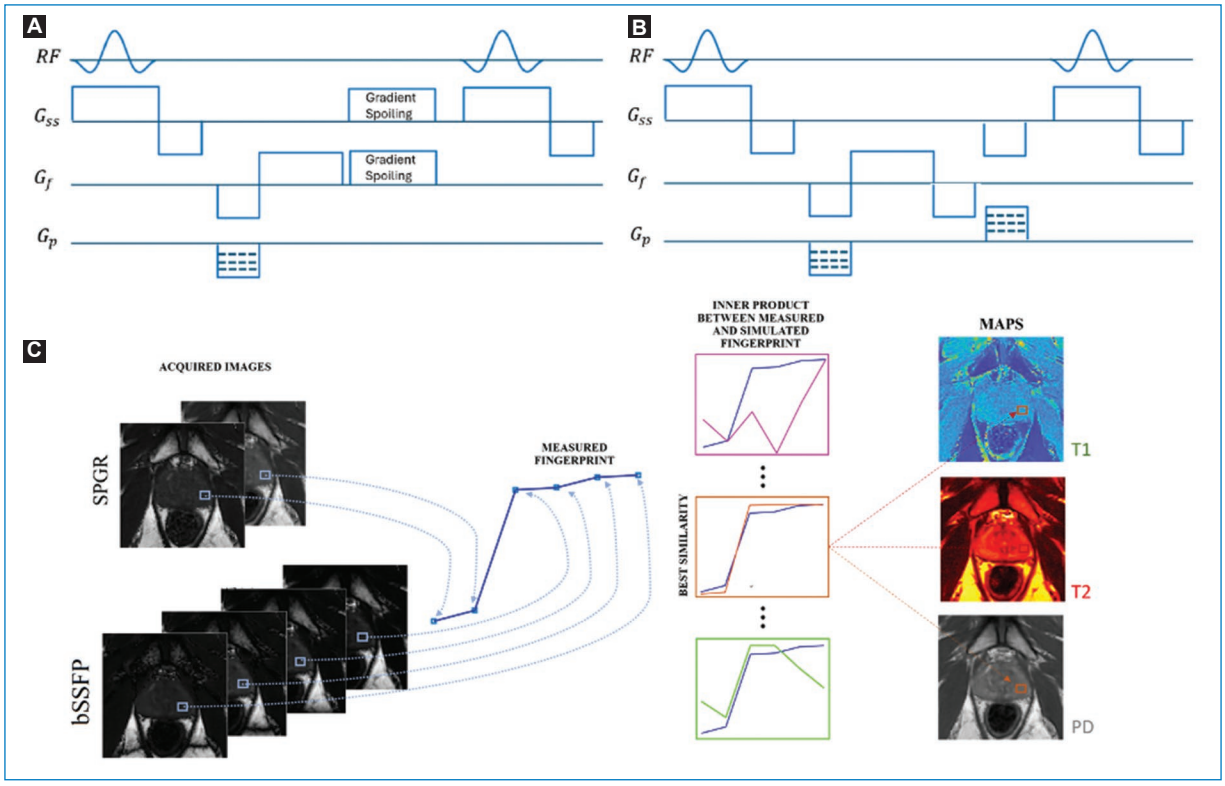

Figure 1. Magnetic resonance imaging sequences used: SPGR **(A)** and bSSFP **(B)**. DESPO+, the reconstruction method used in **(C)**, enables the generation of T1 and T2 parametric maps from rapid acquisitions using SPGR (*spoiled gradient echo sequences*) and bSSFP (*balanced steady-state free precession imaging*) sequences in the prostate region. The acquired data generate a "measurement fingerprint" that is processed by an artificial intelligence algorithm, which not only allows for the reconstruction of parametric maps but also corrects the *off-resonance* artifacts.

All patients included in the study underwent 3T mpMRI prior to biopsy, in cases where the latter was clinically indicated. Patients were excluded if they had claustrophobia, a history of prior PCa treatment (surgery, radiotherapy, or hormonal therapy), incomplete mpMRI sequences, or severe artifacts preventing accurate lesion segmentation. In addition, eight patients were excluded who did not have biopsy results available by September 2024.

Cohort characterization

The following variables were analyzed: demographic variables (age); clinical history (family history of PCa, PSA level at study entry, or abnormal digital rectal exam); radiological variables (mpMRI-derived volume, mpMRI-derived PSA density, PI-RADS v2.1 score, lesion size and location within the prostate, presence of local extraprostatic extension, defined as involvement of the adjacent neurovascular bundle or seminal vesicles, or distant extension defined as lymphadenopathy in the iliac chains or bone marrow involvement); and histopathological variables (Gleason score or presence of PCa).

mpMRI sequences

A 3.0 T Ingenia MRI system (Philips, Best, The Netherlands) scanner was used, and included standard high-resolution axial T2 (T2HR), diffusion-weighted imaging (DWI), and apparent diffusion coefficient (ADC) mapping sequences, as well as the DESPO+ research protocol sequences, which included T1/T2 parametric maps and high-resolution synthesized axial T2 imaging (HR T2synt) (Fig. 2).[10] No intravenous contrast medium was used in this protocol. Table 1 summarizes the relevant parameters used during the acquisition.

Analysis of PCa lesions

Images were interpreted using the PI-RADS v2.1 classification system by a radiologist expert in abdominopelvic imaging (15 years of experience). Lesions or

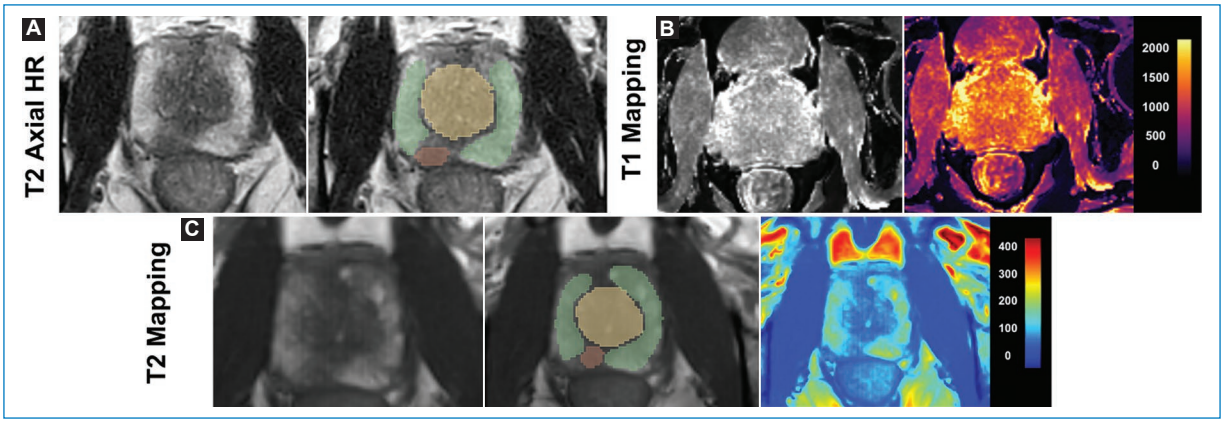

Figure 2. Images obtained from the research protocol, including clinical sequences and parametric maps from the DESPO+ sequence. **A:** corresponds to an axial high-resolution (HR) T2 image and its segmentation of healthy tissue in the peripheral zone (green) and transition zone (yellow), and a lesion in the right peripheral zone (red), respectively. **B:** corresponds to a parametric T1 map image in grayscale and with a color scale. **C:** corresponds to a parametric T2 map image, its segmentation, and color-scale representation of healthy tissue in the peripheral zone (green) and transition zone (yellow), and a lesion in the right peripheral zone (red), respectively.

Table 1. Acquisition parameters for the magnetic resonance imaging sequences used

Protocol	Sequence	TE (ms)	TR (ms)	α:(º)	Time (mins)
DESPO+	SPGR1	3.1	8.0	4	3.6
	SPGR2	3.1	8.0	15	
	bSSFP1	1.7	3.4	15	
	bSSFP2	2.1	4.2	30	
	bSSFP3	3.4	6.8	60	
SE	T1w	7	795	90	7.1
	T2w	110	4229	90	
Traditional SE-EPI	DWI b (s/mm^2): {100,500 1000,2000}	100	6900	90	17.7

α: flip angle; bSSFP: balanced steady-state free precession; DESPO+: driven equilibrium single pulse observation of T1/T2 plus; DWI: diffusion-weighted imaging; SE: spin echo; SE-EPI: spin echo-echo planar imaging; SPGR: spoiled gradient echo; T1w: T1-weighted; T2w: T2-weighted; TE: echo time; TR: repetition time.

abnormalities PI-RADS ≥ 3 were evaluated for referral to biopsy using transrectal MRI-guided ultrasound, based on clinical assessment by the urology team. A pathologist specializing in the genitourinary tract reviewed each patient's samples to confirm the PCa diagnosis. Each tumor was assigned a Gleason score based on the International Society of Urological Pathology (ISUP) grading system.[11]

The reference standard was established based on histopathological findings obtained through a combination of systematic transrectal ultrasound-guided biopsies and mpMRI-targeted biopsies of the suspicious index lesions. Any cancer with a Gleason score ≥ 7, a volume ≥ 0.5 ml, or extraprostatic extension was considered clinically significant.

Image segmentation and analysis

The prostate gland was segmented volumetrically (3D) on T1 and T2 maps by a radiologist specializing in abdominal imaging (15 years of experience). Additionally, the peripheral zone (PZ) was divided into three levels -base, mid-gland, and apex- and the transition zone (TZ) into two levels -base and mid-gland-. Lesions with histological confirmation were also segmented. This was performed following the

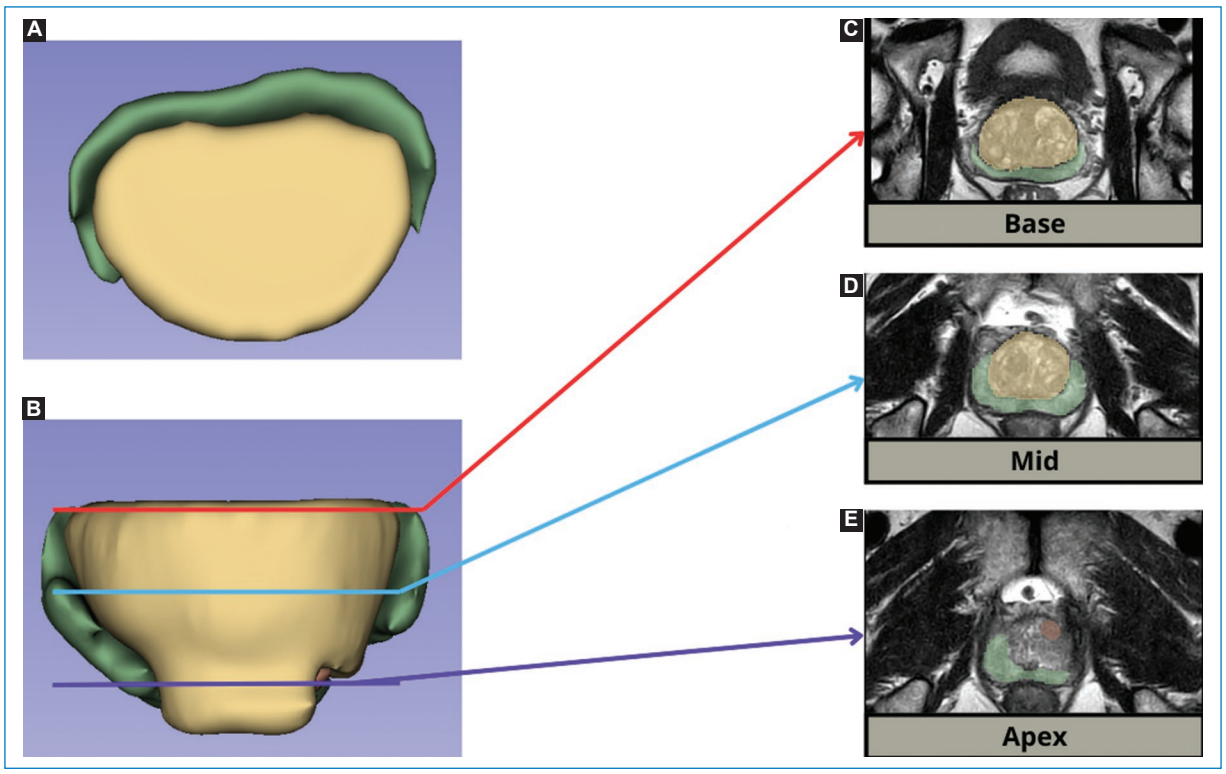

Figure 3. Segmentations performed on healthy tissue and prostate cancer lesions. The image on the left shows volumetric segmentation in axial **(A)** and coronal **(B)** views, identifying the prostatic gland base in red, the mid-gland in light blue, and the apex in purple. Note the identification of a lesion in the left transition zone (burgundy). On the right, segmentation of the transition zone (yellow), peripheral zone (green), and prostate cancer lesion (burgundy) is shown at the base **(C)**, mid-gland **(D)**, and apex **(E)** of the gland.

methodology of De Oliveira et al.[12] using 3DSlicer software (v5.6.1) (Fig. 3). The TZ was not segmented at the apex due to its small size and anatomical overlap. An average analysis of healthy tissue was performed on both a zonal and volumetric basis. A comparison was also made between the suspicious lesion and the healthy tissue contralateral to the lesion.

The statistical analysis was conducted using unpaired parametric tests for continuous variables and the chi-square (χ^2) test for discrete variables, with significance established at a p-value ≤ 0.05 in Prism.

The graphs were generated using R and Prism.

Results

Patients

Forty patients with suspected PCa were included, with a mean age of 63 ± 7 years and a mean PSA of 7 ± 9 ng/mL. Tables 2 and 3 describe the demographic variables of the cohort. Fifty percent of the patients presented with PI-RADS v2.1 lesions ≥ 3.

Characterization of suspicious lesions

Of the 20 suspicious lesions, 14 were found in the PZ (mean size: 11 ± 5 mm), with one case showing extracapsular extension and three showing distant dissemination. The remaining six were in the TZ (mean size: 13 ± 6 mm) and showed no signs of local or distant extension. Ten lesions in the PZ were biopsied: 30% had a Gleason score < 7, 60% had a Gleason score of 3 + 4, and 10% had a Gleason score of 4 + 3. Four lesions in the TZ were biopsied: 75% had a Gleason score < 7 and 25% had a Gleason score of 4 + 3. There were no lesions with a Gleason score ≥ 8. All biopsies confirmed PCa.

Parametric maps

None of the parametric maps presented artifacts that would prevent their interpretation. Figure 4A and B illustrate the mean values for healthy tissue. Figure 5 shows the segmental and volumetric analysis, whose specific values are listed in Tables 4 and 5.

Table 2. Description of the demographic, radiological, and histological variables for the cohort

Category	Variable	Cohorte (n = 40)	PCa in PZ (n = 14)	PCa in TZ (n = 6)	No PCa (n = 20)	p
Clinical-demographic factors	Age, years	63 ± 7	64 ± 6	66 ± 8	61.5 ± 7	0.18* 0.22†
	PSA, ng/ml	7 ± 9	10 ± 16	6.8 ± 2	6.3 ± 3.3	0.32* 0.72†
	Family history of PCa, % (n)	50% (20/40)	64% (9/14)	33% (2/6)	45% (9/20)	0.4* 0.3†
	Abnormal digital rectal exam % (n)	10% (4/40)	14% (2/14)	0% (0/6)	10% (2/20)	0.7* 0.8†
Radiological characteristics	Prostate volume by MRI, ml	50 ± 29	40 ± 22	29 ± 10	55 ± 22	0.37* 0.11†
	PSA density, ng/ml/cc	0.25 ± 0.6	0.5 ± 1.2	0.2 ± 0.04	0.12 ± 0.05	0.18* 0.003†
	Size of suspicious lesions, mm	12 ± 5	11 ± 5	13 ± 6	-	-

Continuous data are expressed as mean ± standard deviation.
*p-value for PCa in TZ vs. no PCa.
†p-value for PCa in PZ vs. no PCa.
PSA: prostate-specific antigen; PCa: prostate cancer; PZ: peripheral zone; MRI: magnetic resonance imaging; TZ: transition zone.

Table 3. Description of discrete demographic, radiological, and histological variables for the cohort: patients with prostate cancer in the peripheral zone or transition zone, and patients without prostate cancer

Category	Variable	Cohorte (n = 40)	PCa in PZ (n = 14)	PCa in TZ (n = 6)
Radiological characteristics: classification PI-RADS V2.1	PI-RADS 1, n (%)	0% (0/40)	0% (0/14)	0% (0/6)
	PI-RADS 2, n (%)	50% (20/40)	0% (0/14)	0% (0/6)
	PI-RADS 3, n (%)	15% (6/40)	14% (2/14)	66% (4/6)
	PI-RADS 4, n (%)	22% (9/40)	57% (8/14)	16% (1/6)
	PI-RADS 5, n (%)	13% (5/40)	28% (4/14)	16% (1/6)
Radiological characteristics: signs of dissemination	Signs of local extension*, n (%)	3% (1/40)	8% (1/14)	0% (0/6)
	Signs of distant extension†, n (%)	8% (3/40)	21% (3/14)	0% (0/6)
Histopathology	Biopsies performed based on PI- RADS ≥ 3, n (%)	75% (14/20)	71% (10/14)	66% (4/6)
	Gleason < 7, n (%)	35% (5/14)	30% (3/10)	75% (3/4)
	Gleason 3 + 4, n (%)	50% (7/14)	60% (6/10)	0% (0/10)
	Gleason 4 + 3, n (%)	14% (2/14)	10% (1/10)	25% (1/4)

*Involvement of the adjacent neurovascular bundle or seminal vesicles.
†Lymphadenopathy in the iliac chains or involvement of the bone marrow included in the field of view.
PCa: prostate cancer; PZ: peripheral zone; TZ: transition zone.

T1 values in healthy tissue

In the PZ, all 40 patients showed values within the reference range found in the literature (1037-2000 ms). In the TZ, 36 cases fell within the reference interval (1050-1800 ms) or presented a minimal difference (less than 50 ms); the remaining four cases showed values below the lower limit.

The segmental T1 analysis showed mean T1 values of 1422 ± 190 ms at the base, 1386 ± 202 ms in the mid-zone, and 1302 ± 194 ms at the apex of the PZ, with a global value of 1383 ± 177 ms, with significant

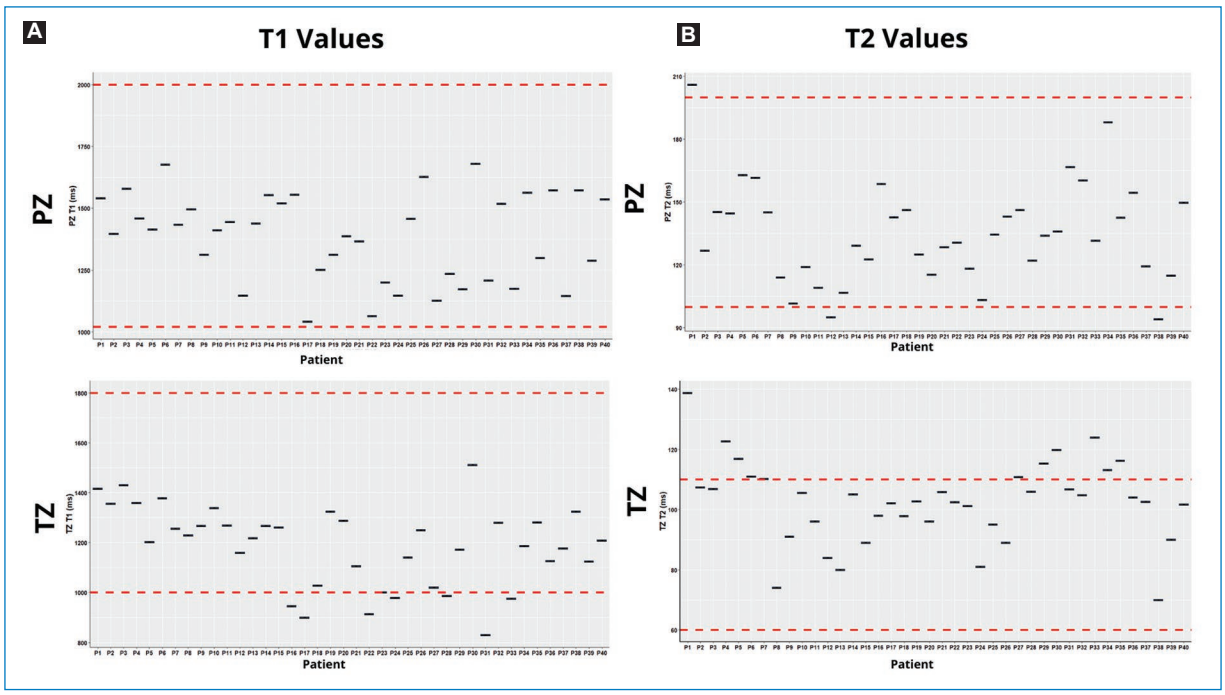

Figure 4. A: box plots showing mean T1 values for healthy tissue volume in the peripheral zone (PZ) and transition zone (TZ) in 40 patients. Red dotted lines represent the maximum (PZ: T1 2000 ms; TZ: T1 1800 ms) and minimum (PZ: T1 1037 ms; TZ: T1 1050 ms) values reported in the literature[10]. **B:** box plots showing mean T2 values for healthy tissue volume in the PZ and TZ, obtained from T2 parametric maps in 40 patients. Red dotted lines represent the maximum (PZ: T2 200 ms; TZ: T2 110 ms) and minimum (PZ: T2 105 ms; TZ: T2 60 ms) values reported in the literature[10].

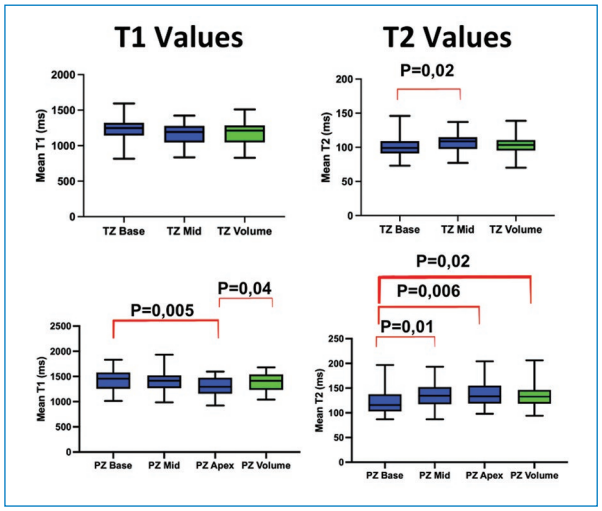

Figure 5. Box plots showing mean volumetric values and values for the different prostatic zones (base, mid-gland, and apex) of healthy tissue obtained from the transition zone and peripheral zone for T1 and T2 parametric maps. Brackets indicate statistically significant differences found when comparing the various values.

differences between the apex and the base (p = 0.005) and between the apex and the total volume (p = 0.04). No statistically significant differences based on zone were observed in the TZ.

T2 values in healthy tissue

In the PZ, 38 patients stayed within the 105-200 ms range, and the remaining two presented values below the lower limit. In the TZ, 32 patients stayed within the 60-110 ms range or showed values slightly above the range (less than 5 ms above the upper limit), and the remaining eight presented values above the upper limit.

The segmental analysis showed in the PZ some mean values of 122 ± 25 ms at the base, 136 ± 24 ms in the mid-zone, and 137 ± 24 ms at the apex, with a volumetric value of 135 ± 23 ms, observing significant differences between the apex and the base (p = 0.006), between the mid-zone and the base (p = 0.01), and between the total volume and the base (p = 0.02). In

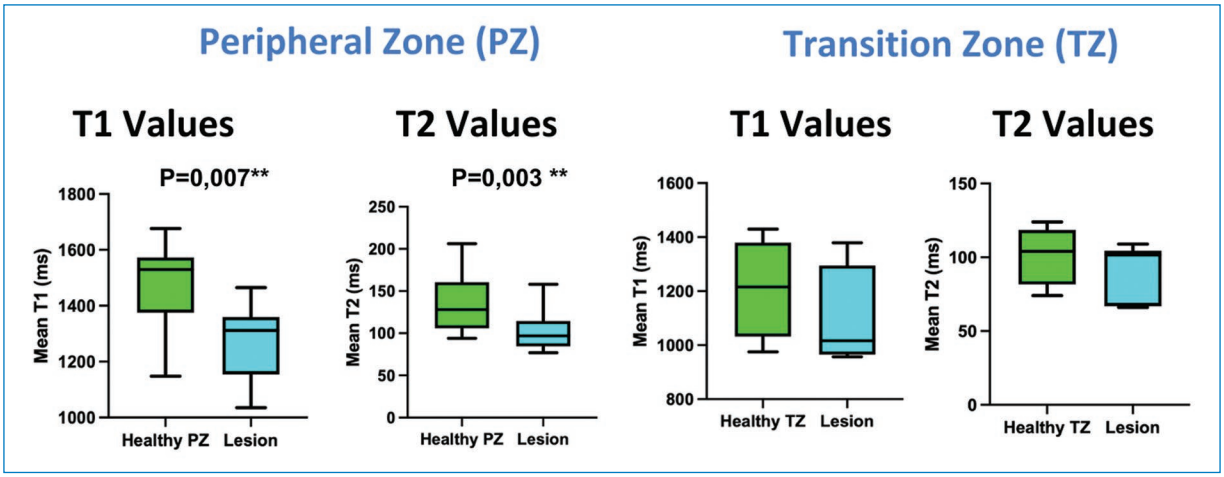

Figure 6. Box plots with the mean volumetric values for both healthy prostatic tissue and tissue suspected of harboring a tumor lesion for the T1 and T2 parametric maps.

Table 4. T1 and T2 values obtained from DESPO + parametric maps for healthy control tissue and prostate cancer lesions in the peripheral zone

Sample type	Prostatic segment	T1 Values (ms)	T2 Values (ms)
Control	Base	1422 ± 190	122 ± 25
	Middle (Mid)	1386 ± 202	136 ± 24
	Apex	1302 ± 194	137 ± 24
Control	Volumetric	1383 ± 177	135 ± 23
Lesion	Volumetric	1284 ± 130	102 ± 22
p (comparison of healthy tissue vs. lesion)		0.007	0.003

Data are expressed as mean ± standard deviation.

Table 5. T1 and T2 values obtained from DESPO + parametric maps for healthy prostatic tissue and prostate cancer lesions in the transition zone

Sample type	Prostatic segment	Parametric map T1 (ms)	Parametric map T2 (ms)
Control	Base	1222 ± 202	99 ± 14
	Middle (Mid)	1164 ± 159	106 ± 14
Control	Volumetric	1138 ± 174	102 ± 13
Lesion	Volumetric	1092 ± 194	91 ± 19
p (comparison of healthy tissue vs. lesion)		0.39	0.47

Data are expressed as mean ± standard deviation.

the TZ, values were 99 ± 14 ms at the base, 106 ± 14 ms in the mid-zone, and 102 ± 13 ms for the total volume, with significant differences between the mid-zone and the base (p = 0.02).

T1 and T2 values in suspicious lesions

Regarding tumor tissue, it was observed that the mean T1 and T2 values were consistently lower compared to healthy tissue in the PZ (Fig. 6).

In the PZ, the mean value for suspicious tissue was 1284 ± 130 ms for T1 (p = 0.007) and 102 ± 22 ms for T2 (p = 0.003). In the TZ, the mean value for suspicious tissue was 1092 ± 194 ms for T1 (p = 0.39) and 91 ± 19 ms for T2 (p = 0.47).

Discussion

Our study prospectively evaluated a cohort of Chilean patients with suspected PCa using 3T mpMRI, incorporating the new quantitative DESPO+ sequence, which enables the acquisition of T1/T2 parametric maps of the prostate gland. This technique proved to be clinically feasible and consistent with values reported in the literature, reinforcing its potential for integration with mpMRI and the clinical and histopathological parameters.

One of the key findings was the adequate agreement between T1 and T2 values obtained in healthy tissue and reference ranges, particularly in the peripheral zone (PZ) (100% for T1 and 90% for T2).[10] Cases falling outside the T2 range tended to show an underestimation, which aligns with studies highlighting the technical

limitations of SSFP (*steady-state free precession*)-based sequences, which are susceptible to banding and *off-resonance* artifacts, that can potentially lead to T2 estimation errors[13-15], as well as magnetization transfer effects and concomitant gradients that can underestimate T2 values .[16,17]

Less agreement was observed in the transition zone (TZ) (77% for T1 and 80% for T2), with a tendency toward T1 underestimation and T2 overestimation. These discrepancies may be linked to the multicompartmental complexity of this zone and the methodological limitations of DESPO+, specifically, where the spoiled gradient echo-based T1 mapping methods can be prone to bias caused by rapid exchange between compartments with differing relaxation times.[18] This can lead to a systematic underestimation of T1 in regions rich in glandular components, such as the TZ.

The T2 overestimation observed in the TZ could be explained by the radiofrequency pulse profile and B1 field homogeneity, which are critical factors in SSFP sequences.[19] Taken together, these findings reinforce the need to consider the specific tissue characteristics and technical limitations of each DESPO+ sequence.

Significant segmental variability within the prostate was evident. In the PZ, significant differences were observed for T1 values between the apex and the base, and between the apex and the total volume, whereas for T2 differences were observed between the apex and the base, between the mid-gland and the base, and between the total volume and the base. These findings align with previous studies that have reported varying values due to histological differences in glandular and stromal components.[12] In the TZ, significant differences in T2 values were detected between the mid-gland portion and the base, with no significant differences in T1 maps, which reflects greater glandular homogeneity.[12,20]

These observations are consistent with the literature, which describes marked discrepancies between zones (PZ vs. TZ) and more subtle intra-zonal variations[12,18-21], since the PZ exhibits higher values than the TZ in both healthy and pathological prostate tissue[12,18-21], key factors when establishing reliable diagnostic thresholds.

Suspicious lesions showed lower and more homogeneous T1 and T2 values compared to healthy tissue. In the PZ, lesions presented decreased T2 values and also significant differences in T1 values. These results are consistent with various studies[22-30] that have demonstrated the usefulness of distinguishing between healthy tissue and tissue suspicious for PCa.

This reduction is attributed to higher cellular density and lower free water content in tumor tissue. Similarly, in the TZ the values associated with cancer are lower than those observed in benign conditions, such as hyperplasia or prostatitis.[24,26,29,30] Additionally, T2 values have shown diagnostic usefulness in distinguishing between PCa and chronic prostatitis, with areas under the curve comparable to those of ADC maps.[26-30]

In the TZ, no statistically significant differences were observed between healthy tissue and lesions. This lack of differentiation may be due to the reduced sample size or less contrast in the relaxation properties.[31]

Limitations

This study presents some limitations. Firstly, the sample size was small, which could limit the ability to extrapolate the findings. Secondly, there was no external validation cohort, so reproducibility and clinical applicability in other contexts remain to be evaluated. Thirdly, processing the acquired images requires robust computing hardware, which may pose a barrier for its implementation in centers with limited technical resources. Finally, generalizing this technique to different MRI systems –particularly across field strengths (1.5 T vs. 3 T) and manufacturers– will require further studies.

Conclusions

This study prospectively validates the DESPO+ technique for the study of prostate cancer (PCa), which offers shorter acquisition times, provides quantitative data, and reduces variability in clinical interpretation, proving useful for distinguishing between healthy and pathological tissue. Furthermore, the study proposes population-based reference values, both volumetrically and in the specific prostatic sectors.

Funding

The authors declare that they have received funding for this study under grant numbers Fondecyt Regular 1210468 and ANID-IHEALTH ICN 2021_004.

Conflicts of interest

The authors declare no conflicts of interest.

Ethical considerations

Protection of human subjects and animals. The authors declare that the procedures followed were in accordance with the ethical standards of the

responsible committee on human experimentation and with the World Medical Association and the Declaration of Helsinki. The procedures were authorized by the Institutional Ethics Committee.

Confidentiality, informed consent, and ethical approval. The authors have followed their institution's confidentiality protocols, obtained informed consent from all patients, and secured approval from the Ethics Committee. SAGER guidelines have been followed as applicable to the nature of the study.

Declaration on the use of artificial intelligence. The authors declare that no generative artificial intelligence was used in the writing or creation of the content of this manuscript.

References

1. Sandhu S, Moore CM, Chiong E, Beltran H, Bristow RG, Williams SG. Prostate cancer. Lancet. 2021;398:1075-90
2. Global Cancer Observatory: Cancer Today (version 1.1). Lyon: International Agency for Research on Cancer; 2024. (Consulted 10-03-2025.) Available from: https://gco.iarc.who.int/today
3. Cornford P, van den Bergh RCN, Briers E, Van den Broeck T, Brunckhorst O, Darraugh J, et al. EAU-EANM-ESTRO-ESUR-ISUP-SIOG Guidelines on Prostate Cancer. Edn. presented at the EAU Annual Congress Paris 2024. Arnhem: EAU Guidelines Office; 2024. ISBN 978-94-92671-23-3. Available from: https://uroweb.org/guidelines/prostate-cancer
4. Turkbey B, Rosenkrantz AB, Haider MA, Padhani AR, Villeirs G, Macura KJ, et al. prostate imaging reporting and data system Version 2.1: 2019 Update of prostate imaging reporting and data system Version 2. Eur Urol. 2019;76:340-51.
5. Wei JT, Barocas D, Carlsson S, Coakley F, Eggener S, Etzioni R, et al. Early detection of prostate cancer: AUA/SUO guideline part I: prostate cancer screening. J Urol. 2023;210:45-53.
6. El-Shater Bosaily A, Parker C, Brown LC, Gabe R, Hindley RG, Kaplan R, et al.; PROMIS Group. PROMIS-Prostate MR imaging study: a paired validating cohort study evaluating the role of multi-parametric MRI in men with clinical suspicion of prostate cancer. Contemp Clin Trials. 2015;42:26-40.
7. Hugosson J, Godtman RA, Wallstrom J, Axcrona U, Bergh A, Egevad L, et al. Results after four years of screening for prostate cancer with PSA and MRI. N Engl J Med. 2024;391:1083-95.
8. Wei CG, Zhang YY, Pan P, Chen T, Yu HC, Dai GC, et al. Diagnostic accuracy and interobserver agreement of PI-RADS Version 2 and Version 2.1 for the detection of transition zone prostate cancers. AJR Am J Roentgenol. 2021;216:1247-56.
9. Rosenkrantz AB, Ginocchio LA, Cornfeld D, Froemming AT, Gupta RT, Turkbey B, et al. Interobserver reproducibility of the PI-RADS Version 2 Lexicon: a multicenter study of six experienced prostate radiologists. Radiology. 2016;280:793-804.
10. Coronado R, Castillo-Passi C, Besa C, Irarrazaval P. Fast and accessible T2 mapping using off-resonance corrected DESPOT2 with application to 3D prostate. Magn Reson Imaging. 2024;109:227-37.
11. van Leenders GJLH, van der Kwast TH, Grignon DJ, Evans AJ, Kristiansen G, Kweldam CF, et al.; ISUP Grading Workshop Panel Members. The 2019 International Society of Urological Pathology (ISUP) Consensus Conference on Grading of Prostatic Carcinoma. Am J Surg Pathol. 2020;44:e87-99.
12. de Oliveira E, Qiaom P, Griswold M, Chen Y, Bittencourt L. Assessment of prostate cancer with MR fingerprinting: histopathologic correlation and diagnostic performance. Radiology. 2023;307:e222287.
13. Deoni SC. Transverse relaxation time (T2) mapping in the brain with off-resonance correction using phase-cycled steady-state free precession imaging. J Magn Reson Imaging. 2009;30:411-7.
14. Jutras JD, Wachowicz K, De Zanche N. Analytical corrections of banding artifacts in driven equilibrium single pulse observation of T2 (DESPOT2). Magn Reson Med. 2016;76:1790-804.
15. Hofstetter LW, Morrell G, Kaggie J, Kim D, Carlston K, Lee VS. T2* measurement bias due to concomitant gradient fields. Magn Reson Med. 2017;77:1562-72.
16. Wu PH, Cheng CC, Wu ML, Chao TC, Chung HW, Huang TY. Effects of RF profile on precision of quantitative T2 mapping using dual-echo steady-state acquisition. Magn Reson Imaging. 2014;32:102-6.
17. Deoni SC, Rutt BK, Jones DK. Investigating the effect of exchange and multicomponent T1 relaxation on the short repetition time spoiled steady-state signal and the DESPOT1 T1 quantification method. J Magn Reson Imaging. 2007;25:570-8.
18. Yu AC, Badve C, Ponsky LE, Pahwa S, Dastmalchian S, Rogers M, et al. Development of a combined MR fingerprinting and diffusion examination for prostate cancer. Radiology. 2017;283:729-38.
19. Panda A, Obmann VC, Lo WC, Margevicius S, Jiang Y, Schluchter M, et al. MR fingerprinting and ADC mapping for characterization of lesions in the transition zone of the prostate gland. Radiology. 2019;292:685-94.
20. Shiradkar R, Panda A, Leo P, Janowczyk A, Farre X, Janaki N, et al. T1 and T2 MR fingerprinting measurements of prostate cancer and prostatitis correlate with deep learning-derived estimates of epithelium, lumen, and stromal composition on corresponding whole mount histopathology. Eur Radiol. 2021;31:1336-46.
21. Hepp T, Kalmbach L, Kolb M, Martirosian P, Hilbert T, Thaiss WM, et al. T2 mapping for the characterization of prostate lesions. World J Urol. 2022;40:1455-61.
22. Klingebiel M, Schimmöller L, Weiland E, Franiel T, Jannusch K, Kirchner J, et al. Value of T2 mapping MRI for prostate cancer detection and classification. J Magn Reson Imaging. 2022;56:413-22.
23. Mai J, Abubrig M, Lehmann T, Hilbert T, Weiland E, Grimm MO, et al. T2 mapping in prostate cancer. Invest Radiol. 2019;54:146-52.
24. Cui Y, Han S, Liu M, Wu PY, Zhang W, Zhang J, et al Diagnosis and grading of prostate cancer by relaxation maps from synthetic MRI. J Magn Reson Imaging. 2020;52:552-64.
25. Baur ADJ, Hansen CM, Rogasch J, Posch H, Elezkurtaj S, Maxeiner A, et al. Evaluation of T1 relaxation time in prostate cancer and benign prostate tissue using a modified look-locker inversion recovery sequence. Sci Rep. 2020;10:3121.
26. Tamada T, Sone T, Jo Y, Toshimitsu S, Yamashita T, Yamamoto A, et al. Apparent diffusion coefficient values in peripheral and transition zones of the prostate: comparison between normal and malignant prostatic tissues and correlation with histologic grade. J Magn Reson Imaging. 2008;28:720
27. Delongchamps NB, Rouanne M, Flam T, Beuvon F, Liberatore M, Zerbib M, et al. Multiparametric magnetic resonance imaging for the detection and localization of prostate cancer: combination of T2-weighted, dynamic contrast-enhanced and diffusion-weighted imaging. BJU Int. 2011;107:1411-8.
28. Bucher AM, Egger J, Dietz J, Strecker R, Hilbert T, Frodl E, et al. Value of MRI - T2 mapping to differentiate clinically significant prostate cancer. J Imaging Inform Med. 2024;37:3304-15.
29. Kurhanewicz J, Vigneron D, Carroll P, Coakley F. Multiparametric magnetic resonance imaging in prostate cancer: present and future. Curr Opin Urol. 2008;18:71-7
30. Chen M, Dang HD, Wang JY, Zhou C, Li SY, Wang WC, et al. Prostate cancer detection: comparison of T2-weighted imaging, diffusion-weighted imaging, proton magnetic resonance spectroscopic imaging, and the three techniques combined. Acta Radiol. 2008; 49:602-10.
31. Zhang S, Wan J, Xu Y, Huo L, Xu L, Xia J, et al. Predictive value of multiparametric magnetic resonance imaging (T2-weighted imaging and apparent diffusion coefficient) for pathological grading of prostate cancer: a meta-analysis. Int Braz J Urol. 2025; 51:e20240509.

AUSTRAL JOURNAL OF IMAGING
REVISTA CHILENA DE RADIOLOGÍA

PERMANYER

Check for updates

ORIGINAL ARTICLE

Copper filters in angiography and secondary radiation: an experimental study

Filtros de cobre en angiografía y radiación secundaria: un estudio experimental

*Claudio Cuéllar-Fritis[1], Martín Abarca-Arredondo[1], Vicente Córdova-Jorquera[1], Pablo Nilo-Aguilera[1], Vicente Lobos-Valladares[1], Rocío Valdivia-Vásquez[1], Cristóbal Guerrero-Lara[1], Camila Cortés-Barrera[2], Sebastián Pereira[2], Eduardo Espinoza-Parra[3], and Marvin Querales[1,4]**

[1]Medical Technology School, Faculty of Medicine, Universidad de Valparaíso, Valparaiso; [2]Imaging Service, Hospital de Urgencia Asistencia Pública; [3]Administration Department, Protección Radiológica Ltda. Santiago; [4]Interdisciplinary Center for Biomedical Research and Health Engineering (MEDING), Universidad de Valparaíso, Valparaiso. Chile

Abstract

Introduction: *In interventional cardiology, copper filters reduce patient radiation dose; however, their impact on occupationally exposed workers remains uncertain.* **Objective:** *To evaluate the effect of copper filter utilization on the absolute percentage variations (APVs) of dose rates between the work positions of the interventional cardiologist and the radiologic technologist during interventional cardiology procedures.* **Material and methods:** *An experimental study was conducted using a polymethyl methacrylate geometric phantom and calibrated ionization chambers. Dose rates were measured at the physician and technologist positions during fluoroscopy (with filters) and cineangiography (without filters) under various angiographic projections and acquisition frequencies, and APVs were calculated for each condition.* **Results:** *Cineangiography showed the highest APVs, with no significant differences between acquisition frequencies. In fluoroscopy, APV decreased significantly with increasing copper filter thickness, whereas no changes were observed when filter thickness remained constant.* **Conclusions:** *At the experimental level, the use of copper filters in fluoroscopy is associated with a reduction in APVs between the interventional cardiologist and the radiologic technologist, suggesting a redistribution of scattered radiation. These findings provide preliminary evidence to support the optimization of occupational radiological protection and highlight the need for further validation in real clinical settings.*

Keywords: *Percutaneous coronary intervention. Radiation dosage. Occupational exposure. Fluoroscopy. Cineradiography. Radiation protection.*

Resumen

Introducción: *En cardiología intervencionista, los filtros de cobre reducen la dosis al paciente, pero su efecto sobre el trabajador ocupacionalmente expuesto es incierto.* **Objetivo:** *Evaluar el efecto del uso de filtros de cobre sobre las variaciones absolutas porcentuales (VAP) de las tasas de dosis entre los puestos de trabajo del médico y el tecnólogo médico durante procedimientos de cardiología intervencionista.* **Material y métodos:** *Se realizó un estudio experimental con un fantoma geométrico de polimetilmetacrilato y cámaras de ionización calibradas. Se midieron tasas de dosis en las posiciones del médico y del tecnólogo durante fluoroscopia (con filtros) y cineangiografía (sin filtros), en distintas proyecciones angiográficas y frecuencias, obteniendo las VAP en cada caso.* **Resultados:** *La cineangiografía presentó las mayores VAP, sin diferen-*

***Correspondence:**
Marvin Querales
E-mail: marvin.querales@uv.cl

Date of reception: 23-04-2025
Date of acceptance: 02-07-2026
DOI: 10.24875/AJI.25000026

Available online: 26-10-2026
Austral J. Imaging. (Engl. ed.). 2026;32(4):173-181
www.resochradi.com

2810-708X / © 2026 Sociedad Chilena de Radiología. Published by Permanyer. This is an open access article under the CC BY-NC-ND license (https://creativecommons.org/licenses/by-nc-nd/4.0/).

cias entre frecuencias. En fluoroscopia, la VAP disminuyó significativamente al aumentar el espesor del filtro, sin cambios cuando este se mantuvo constante. **Conclusiones:** *A nivel experimental, el uso de filtros de cobre en fluoroscopia se asocia a una reducción de las VAP entre el médico intervencionista y el tecnólogo médico, sugiriendo una redistribución de la radiación dispersa. Estos resultados aportan evidencia preliminar para la optimización de la protección radiológica ocupacional y respaldan la necesidad de estudios en escenarios clínicos reales.*

Palabras clave: *Intervención coronaria percutánea. Fluoroscopia. Cineangiografía. Dosis de radiación. Exposición ocupacional. Protección radiológica.*

Introduction

Interventional cardiology is a subspecialty of cardiology that includes, among others, angiography and hemodynamic procedures, and in which occupationally exposed workers (OEW) receive higher radiation doses compared to other hospital specialties[1]. This is primarily due to the proximity of the OEW to the X-ray tube and the source of scattered radiation generated in the patient, which constitutes the main source of occupational radiation exposure[2].

There are two primary imaging modes used in coronary interventions: fluoroscopy and cineangiography. Fluoroscopy is used in both diagnostic and therapeutic procedures; it provides real-time images using pulses per second, which implies prolonged exposures and significant cumulative doses for patients and OEW[3]. Cineangiography, in contrast, operates over much shorter timeframes, however, it employs frames per second (*frames/s*), which correspond to still images within a moving sequence[4], where the radiation dose per frame can be up to 15 times higher than in fluoroscopy[5].

During a cardiology procedure, an interventionalist may receive an effective dose ranging from 1.2 to 2.3 microsieverts (μSv), depending on the access site used[6]. While this dose may appear low, it is significant when considering the number of procedures an interventionalist performs annually. On the other hand, the effective dose received by patients varies according to the procedure's complexity and duration (as well as the operator's experience), averaging around 2 millisieverts (mSv)[7], though this figure can be substantially exceeded in complex cases. It is worth noting that both the average duration of procedures and the number of interventions have increased in recent years[8].

Given this situation, strategies have been developed to reduce the ionizing radiation dose received by patients. One such strategy, primarily within the fluoroscopy mode, involves placing filters of varying thicknesses in the path of the X-ray beam[9]. These filters, generally made of copper or aluminum, primarily attenuate low-energy X-rays, thereby homogenizing the beam's energy and reducing the dose absorbed by the patient. Although the use of filters reduces the radiation received by patients[10], there is no consensus regarding its impact on the dose received by OEW. In fact, the literature presents conflicting results: some studies indicate that filters benefit only the patient and increase scattered radiation toward the OEW[11-14]; others, however, demonstrate that the use of filters reduces scattered radiation, benefiting both the patient and the OEW[9,15].

Beyond the absolute magnitude of the dose, during interventional procedures there is a marked spatial heterogeneity in scattered radiation and its energy levels, resulting in significant differences in dose rates among the various workstations around the patient[3]. In this context, the use of copper filters may not only modify the total dose but also alter the relative distribution of scattered radiation within the lab, influencing the difference of exposure between the interventional physician and other OEW. However, this effect has been scarcely addressed. In this regard, the aim of this study was to experimentally evaluate the effect of the use and thickness of copper filters on the percentage variations of radiation dose rates between the workstations of the interventional physician and the radiologic technologist during simulated interventional cardiology procedures, under controlled conditions.

The increasing complexity and frequency of interventional cardiology procedures heighten the exposure of the OEW to ionizing radiation, which is a matter of concern given the growing number of cases of cataracts, brain cancer, and other associated diseases[1]. Therefore, evaluating the effect of copper filters on percentage variations in radiation doses between workstations provides experimental evidence to help understand how technical decisions regarding the imaging acquisition system influence the distribution of scattered radiation within the procedure room, thereby contributing to the optimization of occupational radiation protection in interventional cardiology.

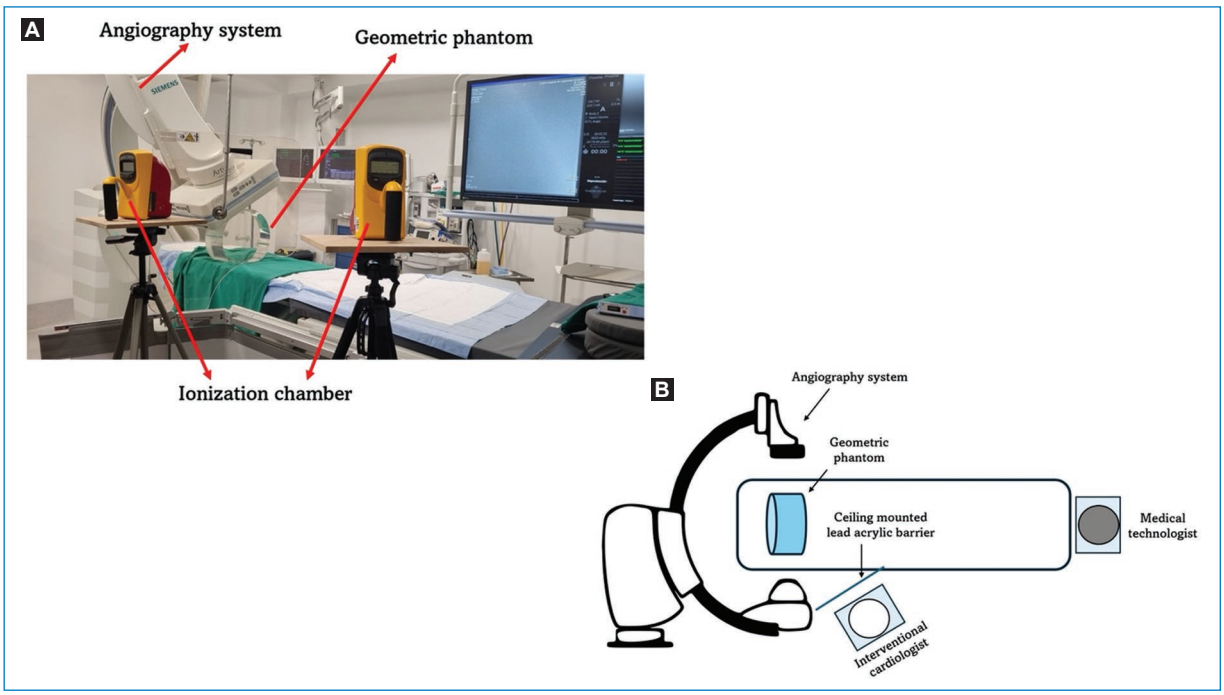

Figure 1. A: arrangement of equipment and materials used in the experimental trial. **B:** diagram showing the distribution of ionization chambers relative to the positions of the occupationally exposed workers.

Material and methods

Study design

An *in vitro* experimental study was conducted, using a geometric phantom, designed to replicate a standard coronary intervention procedure performed in the hemodynamics lab at the *Hospital de Urgencia Asistencia Pública* (HUAP) in Santiago, Chile. The experimental setup recreated the layout of the clinical procedure room (Fig. 1), incorporating the materials, equipment, and operating conditions described below, in accordance with the principles of transparency and reproducibility promoted by the EQUATOR Network.

Experimental phantom

The phantom used was a homogeneous polymethyl-methacrylate (PMMA) cylinder, 150 mm thick and 320 mm in diameter, made in Germany by PTW, model Freiburg (S/N: T40027). The material, which has an equivalent density to soft tissue (7 g/cm²), represents approximately 70% of the water content in the human body. Its use did not present any technical limitations, as the PMMA is recognized by the International Commission on Radiation Units and Measurements (ICRU) as a universal reference material in dosimetry, due to its radiological similarity to soft tissue (ICRU Reports 2, 24, and 64). Although this phantom does not replicate the length of a real patient, and may therefore overestimate the dose at distal positions, it is widely used in *in vitro* experimental studies due to its validity as a reference material and its international acceptance in dosimetric research.

Ionizing radiation-generating (X-ray) equipment and projections used

A Siemens Artis Zee angiography system belonging to the HUAP was used in the fluoroscopy and cineangiography modes. For fluoroscopy, frequencies of 7.5 and 15 pulses per second (pulses/s) were used; at these rates the equipment automatically applies a copper filter with a thickness of 0.2 or 0.3 mm, depending on the projection used, which makes it impossible to establish a fixed value *a priori* for conducting the tests. For cineangiography, frame rates of 15 and 30 frames per second (frames/s) were used; however, this mode does not employ filters on the equipment that was used.

The selected angiographic projections corresponded to those routinely used at the HUAP: 30° left anterior oblique (LAO), 30° cranial (CRAN) anteroposterior (AP), 30° right anterior oblique (RAO), 10° RAO with 30°

CRAN, 30° LAO with 30° CRAN, 45° LAO with 40° caudal (CAU), 20° RAO with 20° CAU, and 40° CAU AP. Before performing the measurements, a quality control check was conducted to verify exposure factors, such as kV, mA, exposure time and exposure dose in Gy/cm², using a RADCAL electrometer, model AccuGold+ TouchPro, with two solid-state sensors (AGMS-DM+ and DDX6-WL).

Positions of workstations of the occupationally exposed workers

The typical positions of the interventional physician and the radiologic technologist during interventional cardiology procedures at HUAP were recreated, taking into account the specific configuration of the hemodynamics lab, the equipment dimensions, and staff positioning during routine clinical practice. Distances were determined based on measurements taken from the center of the phantom to the position occupied by the OEW, adopting as average values 107 cm for the interventional physician and 250 cm for the radiologic technologist. These positions represent, respectively, the operator closest to and the one furthest from the X-ray tube during the procedure. Given that the positioning of the staff depends on the specific characteristics of each angiography lab and the type of procedure performed, the distances used in this study reflect the standard practice of the evaluated facility and are not intended to be extrapolated to other clinical settings.

Dosimetric measurements

For each acquisition mode, the dose rate in millisieverts per hour (mSv/h) at the OEW workstations was recorded in triplicate, by positioning US-made Fluke model 451P ionization chambers at the height of the OEWs' chests, defined for this study as 140 cm above the floor. These three consecutive replicates per condition were performed to ensure beam stability and mitigate instrumental variability, using the average value as the representative observation for each experimental scenario. The occupational measurements were conducted using detectors previously calibrated by the *Laboratorio de Metrología de Radiaciones Ionizantes de la Comisión Chilena de Energía Nuclear/LMRI-CCHEN* (Ionizing Radiation Metrology Laboratory of the Chilean Nuclear Energy Commission), for the operational quantity of ambient dose equivalent H*(10), with traceability to the national reference system (NPL 303/227). This quantity corresponds to the international standard used to assess the external exposure of personnel, where the value 10 indicates that the dose is estimated at a theoretical depth of 10 millimeters below the skin, a point that simulates radiation penetration into the human internal organs most sensitive to highly penetrating radiation, such as X-rays. The uncertainty associated with the measurements is inherent to the detector, in the order of 20%, and is consistent with measurements in scattered radiation fields. During each measurement, radiation was emitted for five seconds, and the collected data were tabulated in Excel spreadsheets.

Statistical analysis

The study's dependent variables correspond to the dose rates recorded at the positions of the interventional physician and the radiologic technologist, as well as the absolute percentage variation (APV) of the dose rate measured at the radiologic technologist's position relative to that of the interventional physician. Independent variables, considered as factors for analysis, included the position of the OEW, the acquisition mode (fluoroscopy and cineangiography), the X-ray pulse/frame emission frequency, the thickness of the copper filter used in fluoroscopy, and the radiologic projections.

The quantitative dose rate variable was summarized in tables via descriptive statistics, using the mean ± standard deviation, as well as the median and interquartile range, with the aim to characterize the central tendency, dispersion, and distribution of the data. For each of the eight projections and both OEW positions, dose rates were compared at different X-ray pulse/frame frequencies during acquisition (7.5 vs. 15 pulses/s in fluoroscopy; 15 vs. 30 frames/s in cineangiography) using the independent-samples Student's t-test, following verification of the assumptions of normality (Shapiro-Wilk test) and homogeneity of variance (Levene's test). A two-tailed alternative hypothesis was used to assess the existence of statistically significant differences. The assumption of independence was based on the fact that each angiographic projection and technical modality constitutes a physical and independent configuration of the C-arm, without carry-over effects or repeated measurements over time on the same sampling unit.

The APV was calculated as a percentage measure of the difference between the dose rates recorded at the radiologic technologist's and interventional physician's positions for each acquisition mode and intensity, defined as:

$$APV(\%) = \frac{\left|\bar{D}_{MT} - \bar{D}_{IP}\right|}{\bar{D}_{IP}} \times 100$$

where D_{MT} corresponds to the average dose rate recorded at the radiologic technologist's position and D_{IP} to the average dose rate obtained at the interventional physician's position. In this design, the APV acts as an index of spatial radiation asymmetry, where a value close to zero indicates that both the physician and the technologist are exposed to identical levels of scattered radiation (homogeneous distribution), whereas a high APV value reflects that one workstation receives significantly more radiation than the other due to the geometric configuration of the beam. The obtained APV values were compared across four groups defined by acquisition mode and intensity (two for fluoroscopy and two for cineangiography) using a one-way analysis of variance (ANOVA) followed by Tukey's *post hoc* test, verifying the assumptions of independence (Durbin-Watson test), normality of residuals (Shapiro-Wilk test), and homogeneity of variances (Levene's test). Sample size robustness was evaluated via a power analysis *a posteriori*, observing a large effect size (greater than 1) for a statistical power of 0.8. To satisfy the independence assumption for the ANOVA, each entered observation corresponded to the APV value calculated from the average of the triplicate measurements for each projection, thereby ensuring sample size consistency.

Additionally, a second one-way ANOVA was performed considering only the fluoroscopy mode. In this analysis, projections were grouped based on the presence or absence of variation in the thickness of the copper filter between the intensities of 7.5 and 15 pulses/s, again resulting in four comparison groups. Descriptive APV results are presented graphically using bar charts with error bars.

A 99% confidence level was established for all hypothesis tests, with the aim to minimize the probability of Type I error. Statistical analysis was performed using Microsoft Excel and the R software environment (R Core Team, 2023), via the RStudio interface.

Ethical considerations

This research did not require evaluation by a bioethics committee, as no experiments involving human beings or animals were conducted. Throughout the study, the research team acted ethically and adhered to the principles of scientific integrity. Furthermore, good practices were followed during the entire research process, in accordance with the European Code of Conduct for Research Integrity issued by *All European Academies* (ALLEA)[16].

Results

Table 1 shows that, across all projections, the cineangiography mode exhibited significantly higher dose rates at both positions (physician and radiologic technologist) when operating at 30 frames/s. Regarding fluoroscopy, results were divided according to filter thickness (Tables 2 and 3), showing that, in all cases, the dose was significantly higher at 15 pulses/s.

The APV results, considering all projections, are shown in figure 2. It was observed that the percentage differences in dose rates between the physician's and radiologic technologist's workstations were greater in cineangiography compared to both fluoroscopy intensities. However, no statistically significant differences were found between 15 and 30 frames/s. In contrast, significant differences were evident in fluoroscopy: the percentage differences at 15 pulses/s (with 0.2 mm and 0.3 mm copper filters, depending on the projection) were significantly lower than those observed at 7.5 pulses/s, where a fixed 0.2 mm copper filter was used.

Considering only the fluoroscopy mode (Fig. 3), in projections where the filter thickness was modified across the different X-ray emission frequencies (pulses/s), the APV values were statistically higher than those obtained in projections where the thickness remained constant. However, within the group of projections involving a change in thickness, a statistically significant reduction in APV was observed when a greater filter thickness (0.3 mm) was used. On the contrary, when comparing the different frequencies in projections with the same filter thickness, no statistically significant differences were found between them.

Discussion

This study used an experimental design to analyze the effect of using copper filters on the absolute percentage variations (APV) of the dose rates between the workstations of the interventional physician and the radiologic technologist in interventional cardiology. Overall, the dose rates at both stations were observed to increase significantly when using higher frames/s and pulses/s, during both cineangiography and fluoroscopy, respectively. However, the study's primary analysis focused on determining whether the magnitude of

Table 1. Dose rate (mSv/h) recorded by the ionization chamber located at the interventional physician's and radiologic technologist's positions with the cineangiography mode at different projections (without the use of copper filters)

Projection	Position: interventional physician			Position: radiologic technologist		
	15 frames/s	30 frames/s	p	15 frames/s	30 frames/s	p
LAO 30°	3.200 ± 0.000 3.200 (3.200-3.201)	3.400 ± 0.000 3.400 (3.400-3.401)	< 0.001	15.000 ± 0.000 15.000 (15.000-15.001)	16.000 ± 0.000 16.000 (16.000-16.001)	< 0.001
CRAN AP 30°	3.467 ± 0.058 3.500 (3.450-3.500)	3.633 ± 0.058 3.600 (3.600-3.650)	< 0.001	15.267 ± 0.289 15.100 (15.100-15.350)	15.933 ± 0.231 15.800 (15.800-16.000)	< 0.001
RAO 30°	2.767 ± 0.058 2.800 (2.750-2.800)	2.903 ± 0.006 2.900 (2.900-2.905)	< 0.001	10.433 ± 0.153 10.400 (10.350-10.500)	11.433 ± 0.058 11.400 (11.400-11.450)	< 0.001
RAO 10°-CRAN 30°	4.220 ± 0.026 4.210 (4.205-4.230)	4.500 ± 0.000 4.500 (4.500-4.501)	< 0.001	18.633 ± 0.252 18.600 (18.500-18.750)	19.967 ± 0.058 20.000 (19.950-20.000)	< 0.001
LAO 30°-CRAN 30°	4.067 ± 0.058 4.100 (4.050-4.100)	4.300 ± 0.000 4.300 (4.300-4.301)	< 0.001	17.667 ± 0.306 17.600 (17.500-17.800)	18.733 ± 0.153 18.700 (18.650-18.800)	< 0.001
LAO 45°-CAU 40°	2.690 ± 0.139 2.620 (2.610-2.735)	3.110 ± 0.010 3.100 (3.105-3.116)	< 0.001	8.700 ± 0.346 8.900 (8.600-8.900)	10.000 ± 0.100 10.000 (9.950-10.050)	< 0.001
RAO 20°-CAU 20°	3.717 ± 0.029 3.700 (3.700-3.725)	3.783 ± 0.029 3.800 (3.775-3.800)	< 0.001	13.500 ± 0.100 13.500 (13.450-13.550)	14.767 ± 0.115 14.700 (14.700-14.800)	< 0.001
CAU AP 40°	2.133 ± 0.153 2.100 [2.050-2.200]	3.200 ± 0.000 3.200 [3.200-3.201]	< 0.001	6.533 ± 0.252 6.500 [6.400-6.650]	9.167 ± 0.058 9.200 [9.150-9.200]	< 0.001

Results are presented as mean ± standard deviation and median [interquartile range], derived from three independent experimental replicates for each combination of projection and technical frequency.
p values less than 0.01 indicate statistically significant differences between frequencies, determined using Student's t-test.
LAO: left anterior oblique; CRAN: cranial; AP: anteroposterior; RAO: right anterior oblique; CAU: caudal.

Table 2. Dose rate (mSv/h) recorded by the ionization chamber located at the position of the interventional physician and the radiologic technologist, using the fluoroscopy modes with different projections and copper filter thicknesses

Projection	Position: interventional physician			Position: radiologic technologist		
	7.5 pulses/s (filter thickness = 0.2 mm)	15 pulses/s (filter thickness = 0.3 mm)	p	7.5 pulses/s (filter thickness = 0.2 mm)	15 pulses/s (filter thickness = 0.3 mm)	p
LAO 30°	0.178 ± 0.003 0.178 (0.177-0.180)	0.210 ± 0.000 0.210 (0.210-0.211)	< 0.001	0.693 ± 0.006 0.690 (0.690-0.695)	0.763 ± 0.006 0.760 (0.760-0.765)	< 0.001
CRAN AP 30°	0.174 ± 0.004 0.176 (0.173-0.177)	0.235 ± 0.005 0.234 (0.232-0.237)	< 0.001	0.095 ± 0.001 0.095 (0.095-0.096)	0.104 ± 0.001 0.104 (0.104-0.105)	< 0.001
RAO 30°	0.149 ± 0.001 0.149 (0.149-0.150)	0.176 ± 0.003 0.177 (0.175-0.1789	< 0.001	0.667 ± 0.006 0.670 (0.665-0.670)	0.740 ± 0.010 0.740 (0.735-0.745)	< 0.001

Results are presented as mean ± standard deviation and median [interquartile range], derived from three independent experimental replicates for each combination of projection and technical frequency.
p values less than 0.01 indicate statistically significant differences between frequencies, determined using Student's t-test.
LAO: left anterior oblique; CRAN: cranial; AP: anteroposterior; RAO: right anterior oblique.

the percentage difference between the two stations, expressed as APV, varied based on the acquisition mode, X-ray pulse emission frequency, and the filter thickness used.

These results are noteworthy, as smaller differences between the workstations were expected during cineangiography, given that this mode uses higher kilovoltage, and thus, higher-energy photons, which would reduce the attenuation capacity of the lead-acrylic shield[17]. This should translate into a higher dose at the physician's station and, consequently, a smaller difference relative to the radiologic technologist. On the contrary, in fluoroscopy, since a lower kilovoltage is used, a lower radiation transmission through the acrylic shield was expected, and therefore, a greater difference of exposure for the radiologic technologist. Consequently,

Table 3. Dose rate (mSv/h) recorded by the ionization chamber located at the position of the interventional physician and the radiologic technologist during the fluoroscopy modes at different projections, but with the same filter thickness

Projection	Position: interventional physician			Position: radiologic technologist		
	7.5 pulses/s (filter thickness = 0.2 mm)	15 pulses/s (filter thickness = 0.2 mm)	p	7.5 pulses/s (filter thickness = 0.2 mm)	15 pulses/s (filter thickness = 0.2 mm)	p
RAO 10°-CRAN 30°	0.126 ± 0.005 0.128 (0.124-0.129)	0.242 ± 0.003 0.241 (0.241-0.243)	< 0.001	0.086 ± 0.001 0.085 (0.085-0.086)	0.118 ± 0.005 0.121 (0.117-0.121)	< 0.001
LAO 30°-CRAN 30°	0.098 ± 0.003 0.099 (0.097-0.100)	0.185 ± 0.002 0.185 (0.184-0.186)	< 0.001	0.070 ± 0.000 0.070 (0.070-0.071)	0.101 ± 0.001 0.101 (0.100-0.101)	< 0.001
LAO 45°-CAU 40°	0.443 ± 0.012 0.450 (0.440-0.450)	0.893 ± 0.012 0.900 (0.890-0.900)	< 0.001	0.273 ± 0.006 0.270 (0.270-0.275)	0.543 ± 0.006 0.540 (0.540-0.545)	< 0.001
RAO 20°-CAU 20°	0.081 ± 0.001 0.080 (0.080-0.081)	0.154 ± 0.004 0.154 (0.152-0.156)	< 0.001	0.480 ± 0.026 0.470 (0.465-0.490)	0.817 ± 0.006 0.820 (0.815-0.820)	< 0.001
CAU AP 40°	0.348 ± 0.008 0.350 (0.345-0.353)	0.703 ± 0.015 0.700 (0.695-0.710)	< 0.001	0.169 ± 0.002 0.169 (0.168-0.170)	0.323 ± 0.006 0.320 (0.320-0.325)	< 0,001

Results are presented as mean ± standard deviation and median [interquartile range], derived from three independent experimental replicates for each combination of projection and technical frequency.
p values less than 0.01 indicate statistically significant differences between frequencies, determined using Student's t-test.
LAO: left anterior oblique; CRAN: cranial; AP: anteroposterior; RAO: right anterior oblique.

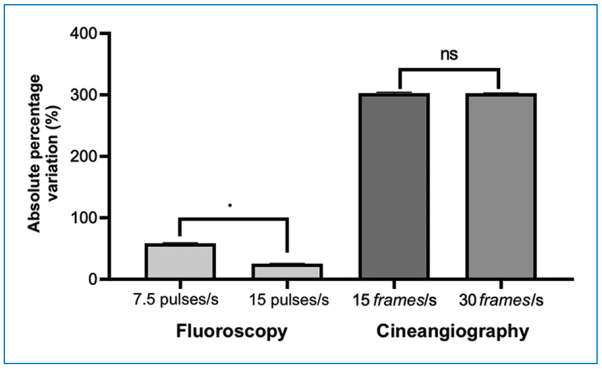

Figure 2. Absolute percentage variation of dose rates recorded by the ionization chamber at the radiologic technologist's position, compared to the one at the interventional physician's position, considering all projections in fluoroscopy and cineangiography modes. *Statistically significant difference. ns: statistically non-significant difference.

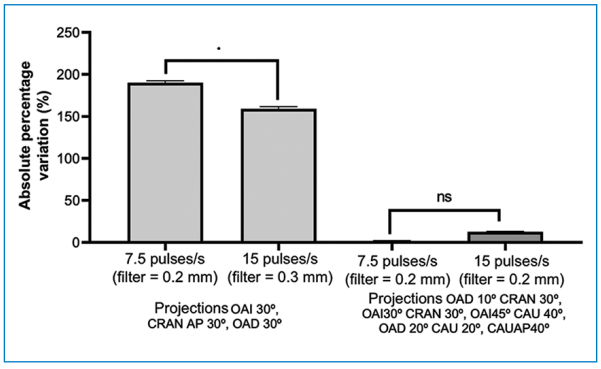

Figure 3. Absolute percentage variation of dose rates recorded by the ionization chamber at the radiologic technologist's position compared to the one at the interventional physician's position, differentiating the projections based on whether or not the copper filter thickness was modified in fluoroscopy mode. *Statistically significant difference. LAO: left anterior oblique; CRAN: cranial; AP: anteroposterior; RAO: right anterior oblique; CAU: caudal; ns: statistically non-significant difference.

and considering that the Siemens angiography system reports the use of copper filters only in fluoroscopy mode and not in cineangiography, these results suggest that the filtration may be a relevant technical factor in the magnitude of the relative differences in occupational exposure between the two workstations.

Analyzing this approach further, in fluoroscopy, by using filters, it generates a homogenization and hardening of the incident beam, allowing a higher proportion of high-energy photons within the kV range used by the angiography system, to pass through[18]. This beam hardening displaces the radiation spectrum toward higher energies, which could also generate a more energetic scattered radiation. As a result, a higher percentage of photons would be able to pass through the leaded acrylic shield that protects the interventional physician versus the number of photons striking that protective device, causing the received dose

rate to more closely resemble that of the radiologic technologist's workstation in the fluoroscopy mode, where the technologist does not have such a shield. However, this interpretation should be understood as a hypothesis consistent with the physical principles of radiation interaction, and not as a direct causal demonstration.

Another point worth noting is that, although the APV is lower in projections using the same filter thickness across the different X-ray emission frequencies, this result could also be influenced by the orientation of the X-ray tube in the analyzed projections[19]. In this regard, not only do filter thicknesses affect the APV, but also in the projections considered, the direction of the incident beam may also pass through varying thicknesses of the phantom, resulting in differing beam attenuations and, consequently, variations in scattered radiation dose rates measured at the workstations of the analyzed OEW.

The results obtained are difficult to compare with existing literature, as there are no studies evaluating the dose differences between OEW workstations based on the presence or absence of filters. Studies such as those by Vano et al.[20] and Varghese[21] do not evaluate differences between OEWs, but they do note that adding filtration in the fluoroscopy mode reduces the dose rate for the personnel, indicating that collimation and filtration can effectively reduce exposure. Therefore, further research is needed to analyze in more detail the potential impact of using copper filters, where the analysis conducted in this research can be replicated and the consistency of the main findings compared.

According to Dudhe et al.[9], strategies for reducing radiation exposure in image-guided procedures are based on the ALARA principle, which promotes maintaining doses as low as reasonably possible without compromising diagnostic quality. In interventional cardiology, the use of technical parameters, such as the use of copper filters, is a common optimization strategy aimed primarily at reducing the dose to the patient. However, the results of this study suggest the advisability of evaluating these strategies comprehensively, also considering their potential impact on occupational exposure, particularly in highly complex settings such as hemodynamics labs. In this scenario, the dose optimization should consider not only the reduction of individual exposure per procedure, but also the cumulative exposure of the personnel, in order to gain deeper insight into the management of risks associated with both deterministic and stochastic effects.

Regarding this study's limitations, it should be taken into consideration that the phantom used was a geometric type, which simulates a density similar to that of the human body, but it does not fully reflect actual patient anatomy. Therefore, the recorded dose rates represent a preliminary experimental approximation and do not directly correspond to a real clinical setting, as the generated scattered radiation might behave differently within a human thorax. Another limitation of the study was the inability to repeat the procedure and take new measurements at another facility using a different angiography system, which would have provided relevant information to demonstrate the influence of the various variables discussed. Finally, the inability to manually change the equipment's filters limited the ability to study in greater detail the potential specific effects of different filter configurations.

Key strengths of this study include the use of a controlled experimental design, based on equipment and materials that are widely validated in radiation protection, alongside the replication of operational conditions and clinical projections commonly employed in coronary procedures. Furthermore, the approach adopted provides experimental evidence that has been little explored in the literature by focusing on the analysis of percentage differences in exposure across different workstations, which contributes to a better understanding of the technical factors influencing the distribution of scattered radiation and the optimization of occupational radiation protection.

However, it must be acknowledged that the behavior of the recorded dose rates is determined by the interaction of multiple factors, in addition to the presence and thickness of the copper filters, such as the type of phantom used, the irradiation field, and the configuration of radiation protection devices, including the acrylic screen and leaded drape used exclusively at the physician's position. In this context, the results presented allow for the identification of relevant trends under controlled conditions, but they also highlight the need for additional experimental studies and clinical observations that systematically incorporate these variables, in order to proceed cautiously with occupational risk management and the optimization of operational procedures in the hemodynamic unit.

Conclusion

This study demonstrated that, under controlled experimental conditions for the fluoroscopy mode, increasing the thickness of the copper filters is associated with a decrease

in the APV of the dose rate between the simulated positions of the interventional physician and the radiologic technologist. These results preliminarily suggest that the use of varying filtration thicknesses could influence not only absolute dose rates, but also the spatial distribution of scattered radiation within the hemodynamics lab.

From a practical perspective, the findings underscore the importance of considering the configuration of the copper filters as a technical factor of interest in future analysis strategies for occupational radiation protection in interventional cardiology. Thus, the systematic evaluation of appropriate filtration configurations could contribute to optimizing protection across different workstations, in accordance with the ALARA principle. Finally, there is a need for future research in real-world and more complex clinical scenarios, incorporating anthropomorphic phantoms, various angiography system models, and variable configurations, in order to validate and extend these preliminary findings to routine clinical practice.

Funding

The authors declare that they have not received funding.

Conflicts of interest

The authors declare no conflicts of interest.

Ethical considerations

Protection of human subjects and animals. The authors declare that no experiments on humans or animals were performed for this research.

Confidentiality, informed consent, and ethical approval. This study does not involve personal patient data, medical records, or biological samples, and does not require ethical approval. SAGER guidelines do not apply.

Declaration on the use of artificial intelligence. The authors declare that no generative artificial intelligence was used in the writing or creation of the content of this manuscript.

References

1. Montalvo TR, Chavarín ESU. Rol de la protección radiológica en procedimientos de cardiología intervencionista. The Journal of Engineering and Exact Sciences. 2021;7(4):13102-15e.
2. Cousins C, Miller DL, Bernardi G, Rehani MM, Schofield P, Vañó E, et al. ICRP PUBLICATION 120: Radiological Protection in Cardiology. Annals of the ICRP. 2013;42(1):1-125.
3. Cuellar-Fritis C, Guerrero C, Cortés C, Pereira S, Ramos-Avasola S, Querales M, et al. Impacto de las proyecciones en las tasas de dosis de radiación recibidas por trabajadores expuestos durante procedimientos de cardiología intervencionista. Rev Chil Cardiol. 2024;43(2):94-103.
4. Badel AE, Rico-Mesa JS, Gaviria MC, Arango-Isaza D, Hernández Chica CA. Radiación ionizante: revisión de tema y recomendaciones para la práctica. Rev Colomb Cardiol. 2018;25(3):222-9.
5. Olcay A, Guler E, Karaca IO, Omaygenc MO, Kizilirmak F, Olgun E, et al. Comparison of fluoro and cine coronary angiography: balancing acceptable outcomes with a reduction in radiation dose. J Invasive Cardiol. 2015;27(4):199-202.
6. Kobayashi T, Hirshfeld JW. Radiation exposure in cardiac catheterization. Circ Cardiovasc Interv. 2017;10(8):e005689.
7. Mahesh M, Ansari AJ, Mettler FA. Patient exposure from radiologic and nuclear medicine procedures in the United States and worldwide: 2009-2018. Radiology. 2023;307(1):e221263.
8. Kaatsch HL, Schneider J, Brockmann C, Brockmann MA, Overhoff D, Becker BV, et al. Radiation exposure during angiographic interventions in interventional radiology - risk and fate of advanced procedures. Int J Radiat Biol. 2022;98(5):865-72.
9. Dudhe SS, Mishra G, Parihar P, Nimodia D, Kumari A. Radiation dose optimization in radiology: a comprehensive review of safeguarding patients and preserving image fidelity. Cureus. 2024;16(5):e60846.
10. Davies AG, Gislason-Lee AJ, Cowen AR, Kengyelics SM, Lupton M, Moore J, et al. Does the use of additional X-ray beam filtration during cine acquisition reduce clinical image quality and effective dose in cardiac interventional imaging? Radiat Prot Dosimetry. 2014;162(4):597-604.
11. Sanchez RM, Vano E, Salinas P, Gonzalo N, Escaned J, Fernández JM. High filtration in interventional practices reduces patient radiation doses but not always scatter radiation doses. Br J Radiol. 2021;94(1117):20200774.
12. Perisinakis K, Solomou G, Stratakis J, Damilakis J. Data and methods to assess occupational exposure to personnel involved in cardiac catheterization procedures. Physica Medica. 2016;32(2):386-92.
13. Siraj M, Dalah EZ, Okasha MH, Abdel-Kader GI, Mohamed-Said MS, Kalanter RA, et al. Potentials of additional copper filtration on radiation dose and image quality for adults underwent digital chest X-ray imaging in Dubai Health Authority - UAE. Radiography. 2023;29(3):552-6.
14. Salinas P, Sanchez-Casanueva RM, Gonzalo N, A. Gil J, Salazar CH, Jimenez-Quevedo P, et al. Dose-reducing fluoroscopic system decreases patient but not occupational radiation exposure in chronic total occlusion intervention. Catheter Cardiovasc Interv. 2021;98(5):895-902.
15. Buytaert D, Eloot L, Mauti M, Drieghe B, Gheeraert P, Taeymans Y, et al. Evaluation of patient and staff exposure with state of the art X-ray technology in cardiac catheterization: a randomized controlled trial. J Interv Cardiol. 2018;31(6):807-14.
16. ALLEA - All European Academies. The European Code of Conduct for Research Integrity [Internet]. DE: ALLEA - All European Academies; 2023 [citado 22 de enero de 2026]. Available from: https://doi.org/10.26356/ECoC
17. Bushong SC. Manual de radiología para técnicos: física, biología y protección radiológica. 12a ed. Barcelona: Elsevier; 2022. 610 p.
18. Bushong SC. Emisión de Rayos X. En: Manual de radiología para técnicos: física, biología y protección radiológica. 12a ed. Barcelona: Elsevier; 2022. pp. 121-134.
19. Roh Y, Kim J, Park H, Kim J, Ryu D, Chun K, et al. Effect of exposure angulation on the occupational radiation exposure during cardiac angiography: simulation study. Int J Environ Res Public Health. 2021;18(15):8097.
20. Vano E, Sanchez RM, Fernandez JM, Bartal G, Canevaro L, Lykawka R, et al. A set of patient and staff dose data for validation of Monte Carlo calculations in interventional cardiology. Radiat Prot Dosimetry. 2015; 165(1-4):235-9.
21. Livingstone RS, Varghese A. Radiation safety culture: the way forward in practicing interventional radiology. J Clin Int Radiol ISVIR. 2017;01(2):100-6.

AUSTRAL JOURNAL OF IMAGING
REVISTA CHILENA DE RADIOLOGÍA

PERMANYER

Check for updates

ORIGINAL ARTICLE

Healthy lifestyles among students of radiology and diagnostic imaging technology

Estilos de vida saludable en estudiantes de tecnología en radiología e imágenes diagnósticas

Gustavo Díaz[1,2]* *and Marlly Rojas*[1,2]

[1]*Research Directorate, Fundación Tecnológica Autónoma de Bogotá;* [2]*Design, Computing, Competitiveness, and Health Research Group FABA-UDES;* [3]*Faculty of Sciences, Diet and Nutrition Program, Universidad FUCS. Bogota, Colombia*

Abstract

Introduction: *The combination of ionizing radiation exposure and unhealthy lifestyle habits may increase the risk of chronic diseases among radiology professionals.* **Objective:** *To describe health behaviors and modifiable risk factors among students of Radiologic and Diagnostic Imaging Technology.* **Material and methods***: A cross-sectional observational study was conducted in 93 first- and second-year students. The validated CEVJU-R questionnaire was applied, and differences by sex and academic year were analyzed.* **Results:** *Sedentary behavior (71%), alcohol consumption (83%), and cigarette use (27%) were highly prevalent in radiology students. Women reported lower levels of physical activity (39 vs. 18%; p = 0.058) but higher use of sunscreen (63 vs. 20%; p = 0.001) and contraceptives (57 vs. 21%; p = 0.003). Men showed a higher prevalence of smoking (41 vs. 14%; p = 0.015). Overall, 56% reported regular consumption of fruits and vegetables, and 43% achieved adequate hydration. Poor sleep quality was observed, particularly among second-year students (p = 0.013).* **Conclusions:** *The findings reveal inadequate lifestyle patterns that may amplify the health risks associated with occupational radiation exposure. Comprehensive university-based interventions are needed to promote healthy lifestyles among radiology students.*

Keywords: *Healthy lifestyle. Radiology. University students. Risk factors. Cancer. Health behavior.*

Resumen

Introducción: *La combinación de exposición a radiación ionizante y hábitos de vida no saludables puede potenciar el riesgo de enfermedades crónicas en profesionales de radiología.* **Objetivo:** *Describir los comportamientos de salud y factores de riesgo modificables en estudiantes de Tecnología en Radiología e Imágenes Diagnósticas.* **Material y métodos:** *se desarrolló un estudio observacional y transversal en 93 estudiantes de primer y segundo año. Se aplicó el cuestionario validado CEVJU-R y se analizaron diferencias por sexo y año académico.* **Resultados:** *El sedentarismo (71%), el consumo de alcohol (83%) y el uso de cigarrillo (27%) son prevalentes en los estudiantes de tecnología en radiología. Las mujeres presentaron menor actividad física (39 vs. 18%; p = 0,058), pero mayor uso de bloqueador solar (63 vs. 20%) (p = 0,001) y anticonceptivos (57 vs. 21%) (p = 0,003). Los hombres reportaron más consumo de tabaco (41 vs. 14%; p = 0,015). El 56% incluyó frutas y verduras en su dieta y el 43% alcanzó una adecuada hidratación. Se observó pobre calidad del sueño, especialmente en segundo año (p = 0,013).* **Conclusiones:** *Los hallazgos revelan estilos de vida inadecuados que podrían amplificar los riesgos derivados de la exposición ocupacional a radiación. Se requieren intervenciones universitarias integrales para promover estilos de vida saludables.*

Palabras clave: *Estilo de vida saludable. Radiología. Estudiantes universitarios. Factores de riesgo. Cáncer. Comportamiento de salud.*

Correspondence:
Gustavo Díaz
E-mail: gustavo.diaz@correo.faba.edu.co

Date of reception: 11-10-2025
Date of acceptance: 01-05-2026
DOI: 10.24875/AJI.25000069

Available online: 26-10-2026
Austral J. Imaging. (Engl. ed.). 2026;32(4):182-190
www.resochradi.com

2810-708X / © 2026 Sociedad Chilena de Radiología. Published by Permanyer. This is an open access article under the CC BY-NC-ND license (https://creativecommons.org/licenses/by-nc-nd/4.0/).

Introduction

Ionizing radiation is widely used in healthcare, however, it can cause changes in cellular components and, consequently, lead to tissue damage. Various studies have demonstrated that high doses of radiation can lead to cancer, cardiovascular disease, atherosclerosis, neurodegeneration, and cataracts, as well as reduce life expectancy.[1] Chronic low-dose radiation exposure is common among healthcare workers, with physicians and radiology technologists in nuclear medicine departments being the workers who experience the highest levels of exposure to ionizing radiation.[2] Based on this exposure, it has been determined that these workers face an increased risk of developing cataracts, cancer, and heart disease.[1] Given this scenario of occupational risk, healthy lifestyle choices represent a cost-effective intervention for preventing chronic diseases. For instance, cohort studies involving healthcare professionals have shown that by following healthy lifestyle patterns, life expectancy free of cardiovascular disease and cancer at age 50 is up to 35.5 years for women and 32.5 years for men.[3] Furthermore, a recent review regarding the incidence of colorectal, prostate, and breast cancers identified physical inactivity, a diet high in ultra-processed foods, smoking, and alcohol consumption as key risk factors.[4]

Due to the consistent link between lifestyle and the onset of chronic diseases, various organizations have issued recommendations for the prevention and treatment of these non-transmissible diseases at both the individual and population levels.[5] These findings underscore the need to implement educational strategies that promote healthy lifestyles from an early stage, particularly among university populations who are in the process of solidifying their lifestyle habits.

Consequently, promoting and adopting healthy attitudes is a crucial priority for universities,[6] as they include populations of late adolescents and young adults who are on the verge of establishing lasting healthy behaviors.[7] Although students in health-related fields may present adequate healthy habits,[6] it is a widespread fact that university students generally lead sedentary lives, have poor quality diets, and exhibit high levels of alcohol consumption and prevalent cigarette use.[8]

Given the indisputable evidence linking healthy lifestyles to the incidence of chronic non-transmissible diseases, combined with the shortcomings in healthy behaviors among university students, it is imperative that educational institutions develop strategies and environments that encourage students to adopt healthy lifestyles.[4,5] The objective of this research is to describe healthy behaviors and modifiable risk factors among students in the *Tecnología en Radiología e Imágenes Diagnósticas* (Radiology and Diagnostic Imaging Technology) program.

Material and methods

Study design and population

This is an observational, cross-sectional, descriptive epidemiological study conducted in October 2024, involving first- and second-year students from the Radiology and Diagnostic Imaging Technology program. This program has a duration of three years, distributed across six academic terms of four months each. Starting from the second year, the students begin practical training in work environments involving exposure to ionizing radiation.

Students who were unwilling to participate, as well as pregnant or breastfeeding women, were excluded. Student selection was carried out using non-probability sampling based on willingness to participate. Recruitment was conducted via email and in classrooms.

Ethical statement

This research adhered to local and international ethical guidelines for research involving human subjects. In accordance with local regulations, this study was classified as minimal risk and was approved by the institutional research committee.

Measurements

The "*Cuestionario de estilos de vida en jóvenes universitarios"* (CEVJU-R)[9] (Lifestyle Questionnaire for University Students), was used for this research. This questionnaire is a self-report instrument developed at the Pontificia Universidad Javeriana in Cali and validated at more than 10 universities in Colombia. It consists of 38 items covering seven dimensions or lifestyle areas (physical activity, hygiene and personal care, diet, alcohol and tobacco use, sleep habits, sexuality, and mental state), and each dimension comprises the practice itself (measured on a Likert-type scale), the motivations behind it (multiple-choice with a single correct answer), and the resources available to carry it out (multiple-choice answers).[9]

Table 1. Demographic characteristics

Variables	Total (n = 93)	Gender			Academic year		
		Male (n = 44)	Female (n = 49)	p	First (n = 30)	Second (n = 63)	p
Academic year, n (%) First Second	 30 (32.3) 63 (67.7)	 15 (34) 29 (66)	 15 (30.6) 34 (69.4)	 0.720			
Age, average (SD)	24.4 (6.2)	25 (6.2)	24 (6.1)	0.149	24.8 (7.7)	24.1 (5.4)	0.695
Socioeconomic level, n (%) 1 2 3	 16 (17.2) 49 (52.7) 28 (30.1)	 9 (20.4) 24 (54.6) 11 (25.0)	 7 (14.3) 25 (51.0) 17 (34.7)	 0.524	 10 (33.3) 16 (53.3) 4 (13.4)	 6 (9.5) 33 (52.4) 24 (38.1)	 0.004
Single, yes, n (%)	79 (85.0)	40 (91)	39 (79.6)	0.128	25 (83.3)	54 (85.7)	0.764
Employed, yes, n (%)	59 (63.4)	27 (61.4)	32 (65.3)	0.693	23 (76.7)	36 (57.1)	0.068
Place of origin, n (%) Bogotá Other cities	 55 (59.1) 38 (40.9)	 24 (54.6) 20 (45.4)	 31 (63.3) 18 (36.7)	 0.393	 17 (56.7) 13 (43.3)	 38 (60.3) 25 (39.7)	 0.738

SD: standard deviation.

In addition, demographic variables of gender, age, marital status, employment status, and semester, were characterized. The socioeconomic level was described based on housing characteristics and environment, as defined by the *Departamento Administrativo Nacional de Estadísticas* (National Administrative Department of Statistics) and the *Departamento Nacional de Planeación* (National Planning Department), classifying as follows: 1, low-low; 2, low; and 3, medium-low. All data were collected via an online Microsoft form.

Statistical analysis

Frequencies and percentages were used to describe categorical variables. Means (averages) and standard deviations were used to describe quantitative variables. An exploratory analysis of differences between groups was conducted to identify bivariate relationships within the findings. The comparison groups were gender (male/female) and program year (first/second). Pearson's chi-square test or Fisher's exact test was used to compare categorical variables. For quantitative variables, normal distribution was first assessed using the Shapiro-Wilk and Kolmogorov-Smirnov tests. Afterwards, comparisons were made using the Student's t-test or the Wilcoxon rank-sum test. P-values < 0.05 were considered statistically significant. Stata version 12 software was used.

Results

Population description

A total of 93 students participated in the study, 67.7% were second-year students, the mean age was 24.4 ± 6.2 years, and 52.7% were female. Regarding socioeconomic level, 70% were in level 1 or 2, 85% were single, 63.4% were employed, and 41.0% came from cities across the country other than the Colombian capital. Details by gender and academic year are presented in table 1.

Physical activity

Participants reported low levels of physical activity. 61% rarely or never walk or cycle as a means of transport, 78% rarely or never engage in competitive sports, and 71% do not exercise or engage in physical activity for at least 30 minutes three times a week.

These characteristics are significantly more prevalent among women than men. Conversely, regarding resource availability, a higher percentage of men than women reported having time (61% vs. 37%; p = 0.018), knowledge of how to perform activities correctly (91% vs. 47%; p = 0.001), and awareness of physical activity spaces and programs offered by the institution (66% vs. 35%; p = 0.003). At the same time, second-year students reported a higher percentage of having good health for exercising compared to first-year students (86% vs. 67%; p = 0.033) (Table 2).

Table 2. Physical activity

Variables	Total (n = 93)	Gender			Academic year		
		Male (n = 44)	Female (n = 49)	p	First (n = 30)	Second (n = 63)	p
Walk or cycle as a means of transport, n (%)							
Frequently	36 (38.7)	23 (52.3)	13 (26.5)	0.006	12 (40)	24 (38.1)	0.947
Rarely	43 (46.2)	19 (43.2)	24 (49.0)		14 (46.7)	29 (46.0)	
Never	14 (15.1)	2 (4.5)	12 (24.5)		4 (13.3)	10 (15.9)	
Participate in competitive sport, n (%)							
Frequently	20 (21.5)	16 (36.4)	4 (8.2)	0.001	8 (26.7)	12 (19.1)	0.701
Rarely	34 (36.6)	19 (43.2)	15 (30.6)		10 (33.3)	24 (38.1)	
Never	39 (41.9)	9 (20.5)	30 (61.2)		12 (40.0)	27 (42.8)	
Do exercise for 30 minutes, n (%)							
Frequently	26 (28.9)	17 (38.6)	9 (18.4)	0.058	10 (33.3)	16 (25.4)	0.367
Rarely	53 (56.0)	23 (52.3)	30 (61.2)		14 (46.7)	39 (61.9)	
Never	14 (15.1)	4 (9.1)	10 (20.4)		6 (20.0)	8 (12.7)	
Availability of resources, n (%)							
Equipment	68 (73.1)	30 (68.2)	38 (77.6)	0.309	23 (76.7)	45 (71.4)	0.594
Money	42 (45.2)	18 (40.9)	24 (49.0)	0.435	14 (46.7)	28 (44.4)	0.841
Time	45 (48.4)	27 (61.4)	18 (36.7)	0.018	15 (50.0)	30 (47.6)	0.831
Company	38 (40.9)	16 (36.4)	22 (44.9)	0.403	13 (43.3)	25 (39.7)	0.738
Skills	72 (77.4)	35 (79.6)	37 (75.5)	0.642	20 (66.7)	52 (82.5)	0.087
Good health	74 (79.6)	38 (86.4)	36 (73.5)	0.124	20 (66.7)	54 (85.7)	0.033
Knowledge	63 (67.7)	40 (90.9)	23 (46.9)	0.001	20 (66.7)	43 (68.3)	0.878
University spaces and programs	46 (49.5)	29 (65.9)	17 (34.7)	0.003	13 (43.3)	33 (52.4)	0.415
Reasons for engaging in physical activity, n (%)							
Beneficial for health	46 (49.5)	23 (52.3)	23 (46.9)	0.607	13 (43.3)	33 (52.4)	0.415
Mood improvement	17 (18.3)	10 (22.7)	7 (14.3)	0.293	3 (10.0)	14 (22.2)	0.154
Improving physique	19 (20.4)	6 (13.6)	13 (26.5)	0.124	8 (26.7)	11 (17.5)	0.303
Reasons for NOT engaging in physical activity, n (%)							
Laziness	58 (62.4)	33 (75.0)	25 (51.0)	0.017	17 (56.7)	41 (65.1)	0.434
Lack of time	12 (12.9)	5 (11.4)	7 (14.3)	0.675	3 (10.0)	9 (14.3)	0.564
Effort and fatigue	10 (10.8)	2 (4.6)	8 (16.3)	0.067	6 (20.0)	4 (6.4)	0.047

Personal care and hygiene

More than 80% of participants report frequently brushing their teeth after main meals and bathing daily. Compared to men, women frequently use sunscreen (63% vs. 20%; p = 0.001) and examine their bodies for changes (77% vs. 50%; p = 0.021). The reasons for attending to, or neglecting personal care and hygiene are similar across both genders and academic years (Table 3).

Diet

Few participants have healthy eating habits. 56% of the students consume fruits and vegetables most days; 43% drink sufficient water daily and 44% eat their main meals at regular times.

It was found that more men than women overeat when not hungry (70.4% vs. 42.9%; p = 0.025), whereas women are more likely to use laxatives or induce vomiting (12.2% vs. 0%; p = 0.028). Regarding academic year, the second-year students, compared to first-year students, show a higher frequency of consuming soft drinks and artificial beverages (36.5% vs. 10%; p = 0.009), a higher percentage of students who frequently skip meals despite being hungry (63.5% vs. 36.7%; p = 0.008), and an excessive percentage of students report having less time to eat (66.7% vs. 41.3%; p = 0.022) and less access to suitable spaces within the institution for eating (50.8% vs. 73.3%; p = 0.039) (Table 4).

Cigarette and alcohol use

Alcohol and cigarette use in the evaluated population is 82.8% and 26.9%, respectively, smoking being more common among men than women (40.9% vs. 14.3%; p = 0.015). Alcohol and cigarette consumption is attributed to the reduction of tension, anxiety, or stress

Table 3. Personal care and hygiene

Frequency over last 6 months	Total (n = 93)	Gender			Academic year		
		Male (n = 44)	Female (n = 49)	p	First (n = 30)	Second (n = 63)	p
Brushing teeth after every main meal, n (%)							
Frequently	82 (88.2)	36 (81.8)	46 (93.9)	0.069	25 (83.3)	57 (90.5)	0.324
Rarely	11 (11.8)	8 (18.2)	3 (6.1)		5 (16.7)	6 (9.5)	
Bathing every day, n (%)							
Frequently	92 (98.9)	43 (97.7)	49 (100)	0.473	30 (100)	62 (98.4)	0.677
Rarely	1 (1.1)	1 (2.3)	0		0	1 (1.6)	
Take over-the-counter medication, n (%)							
Frequently	23 (24.7)	10 (22.7)	13 (26.5)	0.865	5 (16.7)	18 (28.6)	0.449
Rarely	46 (49.5)	23 (52.3)	23 (46.9)		16 (53.3)	30 (47.6)	
Never	24 (25.8)	11 (25.0)	13 (26.6)		9 (30.0)	15 (23.8)	
Use sunscreen, n (%)							
Frequently	40 (43.0)	9 (20.5)	31 (63.3)	0.001	11 (36.7)	29 (46.0)	0.548
Rarely	36 (38.7)	23 (52.3)	13 (26.5)		14 (46.7)	22 (34.9)	
Never	17 (18.3)	12 (27.3)	5 (10.2)		5 (16.7)	12 (19.1)	
Observe and examine the body to detect any changes, n (%)							
Frequently	60 (64.5)	22 (50.0)	38 (77.6)	0.021	17 (56.7)	43 (68.3)	0.491
Rarely	29 (31.2)	19 (43.2)	10 (20.4)		11 (36.7)	18 (28.6)	
Never	4 (4.3)	3 (6.8)	1 (2.0)		2 (6.7)	2 (3.2)	
Attend check-ups in the last year, n (%)							
Medical check-up	65 (68.9)	28 (63.6)	37 (75.5)	0.213	21 (70.0)	44 (69.8)	0.988
Dental check-up	59 (63.4)	25 (56.8)	34 (69.4)	0.209	21 (70.0)	38 (60.3)	0.365
Reason for taking care of oneself, n (%)							
Maintaining or regaining health	49 (52.7)	20 (45.5)	29 (59.2)	0.363	18 (60.0)	31 (49.2)	0.268
Have a good personal appearance	15 (16.1)	9 (20.4)	6 (12.2)		6 (20.0)	9 (14.3)	
Feel good	29 (31.2)	15 (34.1)	14 (28.6)		6 (20.0)	23 (36.5)	
Reason for NOT taking care of oneself, n (%)							
Does not believe anything bad could happen	21 (22.6)	10 (22.7)	11 (22.5)	0.974	6 (20.0)	15 (23.8)	0.794
Afraid of finding something is wrong	11 (11.8)	3 (6.8)	8 (16.3)	0.206	4 (13.3)	7 (11.1)	0.742
Too lazy to do it	30 (32.3)	15 (34.1)	15 (30.6)	0.721	10 (33.3)	20 (31.8)	0.878
Available resources, n (%)							
Health insurance coverage	89 (95.7)	43 (97.7)	46 (93.9)	0.619	29 (96.7)	60 (95.2)	0.901
Money	70 (75.3)	32 (72.7)	38 (77.6)	0.591	24 (80.0)	46 (73.0)	0.466
Time	57 (61.3)	26 (59.1)	31 (63.3)	0.681	22 (73.3)	35 (55.6)	0.101
Knowledge	77 (82.8)	38 (86.4)	39 (79.6)	0.423	25 (83.3)	52 (82.5)	0.924
Public services	89 (95.7)	42 (95.5)	47 (95.9)	0.912	29 (96.7)	60 (95.2)	0.751

(24.7% and 54.2%, respectively), the latter is more pronounced in the second year than in the first year (70.6% vs. 14.3%; p = 0.023).

Sleep habits

Sleep quality is poor among the evaluated students. About 10% go to sleep and wake up at a regular time, 14% fall asleep easily at bedtime, and 30% wake up during the night and fall back asleep. No significant differences were found based on gender or academic year.

Regarding gender, a higher proportion of men than women report having time (68% vs. 35%; p = 0.001) and mental control (66% vs. 39%; p = 0.009) when it comes to getting adequate sleep. Regarding academic year, the second-year students less frequently fall asleep easily (8% vs. 27%; p = 0.013) and have less mental control when trying to sleep properly (44% vs. 67%; p = 0.045).

Sexuality and contraception

In the last year, 88.2% of participants reported having one or more sexual partners, with a higher percentage of men reporting having had two or more (50% vs. 20.4%; p = 0.006). A high percentage of students reported not using condoms (18%) or contraceptive

Table 4. Dietary habits

Usual weekly frequency	Total (n = 93)	Gender			Academic year		
		Male (n = 44)	Female (n = 49)	p	First (n = 30)	Second (n = 63)	p
Fruit and vegetables, n (%)							
Most days	52 (55.9)	20 (45.5)	32 (65.3)	0.065	16 (53.3)	36 (57.1)	0.835
Some days	40 (43.0)	24 (54.5)	16 (32.7)		14 (46.7)	26 (41.3)	
No days	1 (1.1)	0	1 (2.0)		0	1 (1.6)	
Fast food, n (%)							
Most days	26 (28.0)	13 (29.6)	13 (26.5)	0.975	7 (23.3)	19 (30.2)	0.637
Some days	66 (70.9)	31 (70.4)	35 (71.4)		23 (76.7)	43 (68.2)	
No days	1 (1.1)	0	1 (2.1)		0	1 (1.6)	
Soft drinks and artificial beverages, n (%)							
Most days	26 (28.0)	14 (31.8)	12 (24.5)	0.486	3 (10.0)	23 (36.5)	0.009
Some days	60 (64.5)	28 (63.6)	32 (65.3)		25 (83.3)	35 (55.6)	
No days	7 (7.5)	2 (4.6)	5 (10.2)		2 (6.7)	5 (7.9)	
8 glasses of water, n (%)							
Most days	40 (43.1)	20 (45.5)	20 (40.8)	0.901	17 (56.7)	23 (36.5)	0.086
Some days	40 (43.1)	18 (40.9)	22 (44.9)		8 (26.7)	32 (50.8)	
No days	13 (13.8)	6 (13.6)	7 (14.3)		5 (16.6)	8 (12.7)	
Eat breakfast, lunch and dinner at regular times. n (%)							
Most days	41 (44.1)	20 (45.4)	21 (42.9)	0.967	16 (53.3)	25 (39.7)	0.464
Some days	41 (44.1)	19 (43.2)	22 (44.9)		11 (36.7)	30 (47.6)	
No days	11 (11.8)	5 (11.4)	6 (12.2)		3 (10.0)	8 (12.7)	
Skipping main meals, n (%)							
Most days	26 (27.9)	15 (34.1)	11 (22.4)	0.446	12 (40.0)	14 (22.2)	0.192
Some days	54 (58.1)	23 (52.3)	31 (63.3)		14 (46.7)	40 (63.5)	
No days	13 (14.0)	6 (13.6)	7 (14.3)		4 (13.3)	9 (14.3)	
Stop eating, despite being hungry, n (%)							
Most days	11 (11.8)	6 (13.6)	5 (10.2)	0.711	5 (16.7)	6 (9.5)	0.008
Some days	40 (43.0)	20 (45.5)	20 (40.8)		6 (20.0)	34 (54.0)	
No days	42 (45.2)	18 (40.9)	24 (49.0)		19 (63.3)	23 (36.5)	
Overeating, despite not feeling hungry, n (%)							
Most days	6 (6.5)	3 (6.8)	3 (6.1)	0.025	2 (6.7)	4 (6.4)	0.994
Some days	46 (49.5)	28 (63.6)	18 (36.8)		15 (50.0)	31 (49.2)	
No days	41 (44.0)	13 (29.6)	28 (57.1)		13 (43.3)	28 (44.4)	
Vomiting or using laxatives after overeating, n (%)							
Some days	6 (6.5)	0	6 (12.2)	0.028	2 (6.7)	4 (6.4)	0.999
No days	87 (93.5)	44 (100)	43 (87.8)		28 (93.3)	59 (93.6)	
In the last year have you, n (%)							
Followed diets without professional supervision Taken	19 (20.4)	7 (15.9)	12 (24.5)	0.306	6 (20.0)	13 (20.6)	0.943
products to lose/gain weight	23 (24.7)	8 (18.2)	15 (30.6)	0.165	6 (20.0)	17 (27.0)	0.466
Reasons for eating healthily, n (%)							
To lose weight	14 (15.1)	4 (9.1)	10 (20.4)	0.155	6 (20.0)	8 (12.7)	0.357
Improving physical/mental performance	32 (34.4)	16 (36.4)	16 (32.7)	0.707	12 (40.0)	20 (31.8)	0.433
Maintain good health	38 (40.9)	19 (43.2)	19 (38.8)	0.666	10 (33.3)	28 (44.4)	0.308
Reasons for NOT eating healthily, n (%)							
Maintaining or improving figure	15 (16.1)	6 (13.6)	9 (18.4)	0.536	6 (20.0)	9 (14.3)	0.484
Does not like dietary restrictions	24 (25.8)	15 (34.1)	9 (18.4)	0.084	7 (23.3)	17 (27.0)	0.707
Inability to control food intake	15 (16.1)	7 (15.9)	8 (16.3)	0.956	6 (20.0)	9 (14.3)	0.484
Does not think about the consequences of poor nutrition	24 (25.8)	9 (20.5)	15 (30.6)	0.264	8 (26.7)	16 (25.4)	0.896
Resources for proper nutrition, n (%)							
Money	54 (58.1)	26 (59.1)	28 (57.1)	0.849	19 (63.3)	35 (55.6)	0.477
Time	46 (49.5)	21 (47.7)	25 (51.0)	0.751	20 (66.7)	26 (41.3)	0.022
Healthy food at the institution	17 (18.3)	11 (25.0)	6 (12.2)	0.112	6 (20.0)	11 (17.5)	0.767
Adequate facilities at the institution	54 (58.1)	26 (59.1)	28 (57.1)	0.849	22 (73.3)	32 (50.8)	0.039
Knowledge for choosing foods	67 (72.0)	32 (72.7)	35 (71.4)	0.889	22 (73.3)	45 (71.4)	0.848
Availability of healthy food at home	70 (75.3)	34 (77.3)	36 (73.5)	0.671	24 (80.0)	46 (73.0)	0.466

methods (31%) during the past year, women being more likely to always use contraceptive methods compared to men (57% vs. 20.5%; p = 0.003). Regarding the resources available for appropriate contraception and sexuality, no differences were found based on gender or academic year, however, at the population level, only 65.6% of participants reported having the financial means for this.

Mental state

12%, 13%, and 15% of participants report constantly feeling sadness, anger, or loneliness, respectively. At the same time, 10% and 13% report feeling joy or hope, respectively. These findings do not differ based on gender or academic year.

Discussion

This research revealed a high prevalence of sedentary behavior, lack of self-care, poor quality of diet, tobacco and alcohol use, inadequate quality of sleep, inconsistent contraceptive use, and intense emotional states among radiology students. These findings reflect unhealthy lifestyle habits, and if maintained long-term, they could combine with occupational exposure to ionizing radiation and increase the incidence of diseases such as cancer and cardiovascular conditions.

Factors influencing cancer development include individual characteristics (such as age and genetics), environmental factors (such as radiation and viruses), and lifestyle. This link is explained by mechanisms such as chronic inflammation and hyperinsulinemia, which promote cell proliferation and genetic instability. To reduce cancer risk, a key preventive measure is to maintain a healthy weight through regular physical activity and a diet rich in fiber but low in processed and sugary foods. In this regard, the university years represent a crucial time to foster the adoption of healthy habits that help mitigate the risk of chronic diseases in adulthood and improve quality-of-life indicators.[10,11]

To the best of our knowledge, there are no published studies regarding healthy lifestyles among radiology technology students. However, these findings align with other studies on university students in Colombia, a group characterized by high levels of sedentary behavior, poor dietary habits, consumption of harmful substances (e.g., alcohol and tobacco), inadequate sleep patterns, infrequent medical check-ups, and risky sexual behaviors.

In this sense, the findings coincide with studies conducted at other universities. Research at Caribbean universities revealed a diet high in sugar and fat but low in fruits and vegetables, along with skipped meals and regular exercise in 29% of the cohort.[12] Similarly, in Medellín, 57% of students monitor their weight, 74% exercise, and 33% have a positive perception of their dietary habits and physical activity level.[13] In the case of universities in Bogotá, one institution[14] found that 30% of students had a poor-quality diet, while a study across three of the city's universities reported that nearly 60% regularly consumed carbonated beverages, 80% consumed sugar-free carbonated drinks, and 65% consumed packaged juice-style drinks.[15] Concurrently, first-semester students showed high rates of cardiovascular risk factors, including excess weight.[16] Regarding physical activity, another university found that 45%, 35%, and 20% of students engaged in low, high, and moderate levels of physical activity, respectively,[17] while programs with a high presence of female students presented higher rates of low physical activity and low fruit consumption.[18]

Overall, these data indicate that radiology students exhibit lifestyles similar to those of other healthcare professionals. It is crucial to note that, during their academic training, these students are also occupationally exposed to ionizing radiation, a factor that theoretically increases cancer risk compared to other professions. In other words, while students in various health-related careers may share similar lifestyles, exposure to ionizing radiation represents a distinguishing risk factor for those pursuing careers in radiology.[19,20] Therefore, training in protection measures should not only focus on the use of personal protective equipment (lead-shielded items, diagnostic reference levels, and the use of dosimeters, among others) but should also include training on healthy lifestyle habits.

To the best of our knowledge, there are no available studies on the effects of interventions aimed at fostering healthy habits among radiology technology students. Given that the findings are similar to those observed in other healthcare students, interventions proven effective for university students could serve as a reference for future studies and strategies, such as programs for developing cognitive-behavioral skills,[21] mindfulness,[22] sports education models,[23] or mHealth (the use of mobile smart devices for health interventions).[24]

Finally, the high proportion of students reporting sleep difficulties, feelings of sadness or stress, and a lack of adequate resources for healthy eating within the

institution indicates that structural factors also play a significant role. Therefore, intervention strategies must go beyond individual education and consider improvements to the institutional environment, such as the availability of healthy food options, spaces for physical activity, and psychological support services.

Strengths and limitations

The study's primary strength lies in its ability to describe the lifestyle scenario of radiology technology students;[25] covering physical activity, use of medications, medical care, smoking, diet, sleep habits, alcohol consumption, oral care, and sexual health. A second strength is the differentiation of healthy practices by gender and academic year, which allows for a distinction in behavior and enables the targeting of interventions in the short and medium term.

The fundamental limitation of this research is the inability to delve into the specifics of each healthy behavior, such as the number of cigarettes smoked or the grams of alcohol consumed, etc. It is important to note that such depth can only be achieved through studies specifically designed for that purpose. Consequently, future research needs to investigate healthy lifestyles in greater detail.

Conclusions

Students of Radiology and Diagnostic Imaging Technology exhibit unhealthy lifestyles. Women showed lower levels of physical activity but higher usage of sunscreen and contraceptive methods, whereas men exhibited higher rates of smoking and a lower perception of risk regarding sexual practices. These differences must be considered in university health promotion programs.

Funding

The authors declare that this research was funded by the *Fundación Tecnológica Autónoma* de Bogotá.

Conflicts of interest

The authors declare no conflicts of interest.

Ethical considerations

Protection of human subjects and animals. The authors declare that the procedures followed were in accordance with the ethical standards of the responsible committee on human experimentation and with the World Medical Association and the Declaration of Helsinki. The procedures were authorized by the Institutional Ethics Committee.

Confidentiality, informed consent, and ethical approval. The authors have followed their institution's confidentiality protocols, obtained informed consent from all patients, and secured approval from the Ethics Committee. SAGER guidelines have been followed as applicable to the nature of the study.

Declaration on the use of artificial intelligence. The authors declare that no generative artificial intelligence was used in the writing or creation of the content of this manuscript.

References

1. Mu H, Sun J, Li L, Yin J, Hu N, Zhao W, et al. Ionizing radiation exposure: hazards, prevention, and biomarker screening. Environ Sci Pollut Res [Internet]. 2018 [cited 15 nov 2024];25(16):15294-306. Available from: http://link.springer.com/10.1007/s11356-018-2097-9
2. Baudin C, Vacquier B, Thin G, Chenene L, Guersen J, Partarrieu I, et al. Occupational exposure to ionizing radiation in medical staff: trends during the 2009-2019 period in a multicentric study. Eur Radiol [Internet]. 2023 [cited 15 nov 2024];33(8):5675-84. Available from: https://link.springer.com/article/10.1007/s00330-023-09541-z
3. Li Y, Schoufour J, Wang DD, Dhana K, Pan A, Liu X, et al. Healthy lifestyle and life expectancy free of cancer, cardiovascular disease, and type 2 diabetes: prospective cohort study. BMJ [Internet]. 2020 [cited 15 nov 2024];l6669. Available from: https://www.bmj.com/lookup/doi/10.1136/bmj.l6669
4. Marino P, Mininni M, Deiana G, Marino G, Divella R, Bochicchio I, et al. Healthy lifestyle and cancer risk: modifiable risk factors to prevent cancer. Nutrients [Internet]. 2024 [cited 15 nov 2024];16(6):800. Available from: https://www.mdpi.com/2072-6643/16/6/800
5. Rock CL, Thomson C, Gansler T, Gapstur SM, McCullough ML, Patel AV, et al. American Cancer Society guideline for diet and physical activity for cancer prevention. CA Cancer J Clin [Internet]. 2020 [cited 15 nov 2024];70(4):245-71. Available from: https://acsjournals.onlinelibrary.wiley.com/doi/10.3322/caac.21591
6. García-Pérez L, Villodres GC, Muros JJ. Differences in healthy lifestyle habits in university students as a function of academic area. J Public Health [Internet]. 2023 [cited 15 nov 2024];45(2):513-22. Available from: https://academic.oup.com/jpubhealth/article/45/2/513/6806167
7. Palenzuela-Luis N, Duarte-Clíments G, Gómez-Salgado J, Rodríguez-Gómez JÁ, Sánchez-Gómez MB. International comparison of self-concept, self-perception and lifestyle in adolescents: a systematic review. Int J Public Health [Internet]. 2022 [cited 15 nov 2024];67:1604954. Available from: https://www.ssph-journal.org/articles/10.3389/ijph.2022.1604954/full
8. De Luna-Bertos E. Hábitos de vida saludable en la población universitaria. Nutr Hosp [Internet]. 2015 [cited 15 nov 2024];(5):1910-9. Available from: https://doi.org/10.3305/nh.2015.31.5.8608
9. Equipo de Investigación CEVJU Colombia. Evaluación de las conductas de salud en jóvenes universitarios. Rev Salud Pública. 2020; 12(4):599-611.
10. Ferlay J, Colombet M, Soerjomataram I, Parkin DM, Piñeros M, Znaor A, et al. Cancer statistics for the year 2020: An overview. Int J Cancer [Internet]. 2021 [cited 11 oct 2025];149(4):778-89. Available from: https://onlinelibrary.wiley.com/doi/10.1002/ijc.33588
11. Clinton SK, Giovannucci EL, Hursting SD. The World Cancer Research Fund/American Institute for Cancer Research Third Expert Report on Diet, Nutrition, Physical Activity, and Cancer: Impact and Future Directions. J Nutr [Internet]. 2020 [cited 11 oct 2025];150(4): 663-71. Available from: https://www.sciencedirect.com/science/article/pii/S0022316622020995?via%3Dihub
12. Pinillos-Patiño Y, Rebolledo-Cobos R, De Ávila-Quintana L, Ariza-Egea S, Viecco-Montero L, Herazo-Beltrán Y, et al. Caracterización de hábitos alimentarios y de actividad física en jóvenes de la Región Caribe Colombiana. Nutr Clínica Dietética Hosp [Internet]. 2022 [cited 22 mar 2024];42(3). Available from: https://doi.org/10.12873/423pinillos

13. Universidad de Antioquia, Rodríguez-Espinosa H, Restrepo-Betancur LF, Universidad de Antioquia, Deossa-Restrepo GC, Universidad de Antioquia. Conocimientos y prácticas sobre alimentación, salud y ejercicio en universitarios de Medellín-Colombia. Perspect En Nutr Humana [Internet]. 2015 [cited 22 mar 2024];17(1). Available from: https://revistas.udea.edu.co/index.php/nutricion/article/view/25434
14. Vinaccia S. Mediterranean diet adherence in Colombian university population. Nutr Clin Diet Hosp [Internet]. 2019 [cited 22 mar 2024];(1):93-100. Available from: https://doi.org/10.12873/391vinaccia
15. Ramírez-Vélez R, Ojeda ML, Tordecilla MA, Peña JC, Meneses JF. El consumo regular de bebidas azucaradas incrementa el perfil lipídico-metabólico y los niveles de adiposidad en universitarios de Colombia. Rev Colomb Cardiol [Internet]. 2016 [cited 22 mar 2024];23(1):11-8. Available from: https://www.sciencedirect.com/science/article/pii/S0120563315000959
16. Zea Robles AC, León-Ariza H, Botero-Rosas DA, Afanador-Castañeda HD, Pinzón-Bravo LA. Factores de riesgo cardiovascular y su relación con la composición corporal en estudiantes universitarios. Rev Salud Pública [Internet]. 2014 [cited 22 mar 2024];16(4):505-15. Available from: http://www.revistas.unal.edu.co/index.php/revsaludpublica/article/view/38878
17. Díaz-Muñoz GA. Caracterización de los hábitos alimentarios y nivel de actividad física en estudiantes universitarios. Rev Salud Bosque [Inter-net]. 2018 [cited 22 mar 2024];8(1):8. Available from: http://revistasaludbosque.unbosque.edu.co/article/view/2371
18. Díaz-Muñoz GA, Pérez Hoyos AK, Cala Liberato DP, Mosquera Rentería LM, Quiñones Sánchez MC. Diferencia de los niveles de actividad física, sedentarismo y hábitos alimentarios entre universitarios de diferentes programas de la salud de una universidad privada en Bogotá, Colombia. Rev Esp Nutr Humana Dietética [Internet]. 2021 [cited 22 mar 2024];25(1):8-17. Available from: https://www.renhyd.org/index.php/renhyd/article/view/1007
19. Avila-Carrillo VP. Alteraciones clínicas en la salud del personal expuesto a radiaciones ionizantes en los hospitales. Rev San Gregor. 2022;1(50):133-47.
20. Barros-Astudillo T, Hidalgo-Gualán E, Tello-Calle A, Olmedo-Raza N. Conocimiento y aplicación de normas de protección radiológica, bioseguridad y riesgos para la salud en la academia. Rev Fac Cienc Médicas Quito [Internet]. 2023 [cited 11 oct 2025];48(2):16-25. Available from: https://revistadigital.uce.edu.ec/index.php/CIENCIAS_MEDICAS/article/view/5439
21. Mazurek-Melnyk B, Hoying J, Tan A. Effects of the MINDSTRONG© CBT-based program on depression, anxiety and healthy lifestyle behaviors in graduate health sciences students. J Am Coll Health [Internet]. 2022 [cited 4 feb 2026];70(4):1001-9. Available from: https://www.tand-fonline.com/doi/full/10.1080/07448481.2020.1782922
22. Soriano-Ayala E, Amutio A, Franco C, Mañas I. Promoting a healthy lifestyle through mindfulness in university students: a randomized controlled trial. Nutrients [Internet]. 2020 [cited 4 feb 2026];12(8):2450. Available from: https://www.mdpi.com/2072-6643/12/8/2450
23. Liao CC, Hsu CH, Kuo KP, Luo YJ, Kao CC. Ability of the sport education model to promote healthy lifestyles in university students: a randomized controlled trial. Int J Environ Res Public Health [Internet]. 2023 [cited 4 feb 2026];20(3):2174. Available from: https://www.mdpi.com/1660-4601/20/3/2174
24. Andargeery SY, El-Rafey DS. A randomized controlled trial of the effectiveness of the mHealth program in improving the lifestyle of nursing students. Sci Rep [Internet]. 2025 [cited 4 feb 2026];15(1):9765. Available from: https://www.nature.com/articles/s41598-024-80982-2
25. Gallardo-Pino C, Arroyo-Acevedo HV, Martínez-Pérez AM. Marco competencial en promoción y educación para la salud: experiencias iberoamericanas. España: Dykinson; 2021.

AUSTRAL JOURNAL OF IMAGING
REVISTA CHILENA DE RADIOLOGÍA

PERMANYER

Check for updates

ORIGINAL ARTICLE

Bibliometric analysis of the *Revista Chilena de Radiología/Austral Journal of Imaging* (1995-2025)

Análisis bibliométrico de la Revista Chilena de Radiología/Austral Journal of Imaging (1995-2025)

Juan Olivos-Pérez[1], Carlos Toledo-Riquelme[1], Graciela C. Sandoval-Martínez[2], Sofía Klein-Díaz[2], Emilia A. Amar-Cerna[3], and Catalina F. Rivas-Pizarro[2]*

[1]Department of Medical Specialties, Faculty of Medicine, Universidad de Concepción, Concepcion, Chile; [2]Doctoral Program in Health Sciences, Universidad de Murcia, Murcia, Spain; [3]Faculty of Medicine. Universidad de Concepción, Concepcion, Bio Bio; [4]Faculty of Medicine, Universidad San Sebastián, Santiago. Chile

Abstract

Introduction: *The Revista Chilena de Radiología, Chile's leading journal for radiological scientific dissemination since 1995, has reflected the evolution of the specialty over the past three decades.* **Objective:** *To analyze the scientific production published in the journal between 1995 and 2025 through a descriptive bibliometric study.* **Material and methods:** *A total of 788 articles retrieved from SciELO Chile and the archives of the Chilean Society of Radiology were analyzed. Variables included publication volume, article type, radiological subspecialties, imaging techniques, authorship characteristics, institutional affiliation, and academic collaboration.* **Results:** *Review articles predominated (41.0%), followed by original research (27.0%), with major thematic areas in abdominal/pelvic, musculoskeletal, and educational radiology. Computed tomography (23.9%) and multimodal imaging studies (38.3%) were the most frequently reported techniques. Most publications had exclusively Chilean authorship (82.6%), while international collaboration remained limited (2.0%). Female first authorship showed a progressive increase over time.* **Conclusions:** *These findings demonstrate the editorial consolidation of the journal and highlight ongoing challenges related to internationalization, strengthening original research production, gender equity, and institutional diversification, within a context of increasing international projection.*

Keywords: *Bibliometrics. Radiology. Latin America.*

Resumen

Introducción: *La Revista Chilena de Radiología, principal órgano de difusión científica radiológica en Chile desde 1995, ha reflejado durante tres décadas la evolución disciplinar de la especialidad en el país.* **Objetivo:** *Analizar la producción científica publicada en la revista entre 1995 y 2025 mediante un estudio bibliométrico descriptivo.* **Material y métodos:** *Se analizaron un total de 788 artículos, recuperados de SciELO Chile y de los archivos de la Sociedad Chilena de Radiología. Se evaluó la producción, tipología de artículos, subespecialidades abordadas, técnicas de imagen empleadas, características de autoría, filiación institucional y colaboración académica.* **Resultados:** *Predominaron los artículos de revisión (41,0%) sobre los originales (27,0%), con mayor representación temática en abdomen/pelvis, musculoesquelético y educación. La tomografía computarizada (23,9%) y los estudios multimodales (38,3%) fueron las técnicas más frecuentemente reportadas. El 82,6% de las publicaciones tuvo autoría exclusivamente chilena, mientras que la colaboración internacional fue limitada (2,0%). La participación femenina como primer autor mostró una tendencia creciente a lo largo del periodo analizado.*

***Correspondence:**
Juan Olivos-Pérez
E-mail: jolivos@udec.cl

Date of reception: 29-12-2025
Date of acceptance: 07-05-2026
DOI: 10.24875/AJI.25000085

Available online: 26-10-2026
Austral J. Imaging. (Engl. ed.). 2026;32(4):191-197
www.resochradi.com

2810-708X / © 2026 Sociedad Chilena de Radiología. Published by Permanyer. This is an open access article under the CC BY-NC-ND license (https://creativecommons.org/licenses/by-nc-nd/4.0/).

Conclusiones: *Los hallazgos evidencian la consolidación editorial de la revista y plantean desafíos en internacionalización, fortalecimiento de la producción de estudios originales, equidad de género y diversificación institucional, en un contexto de creciente proyección internacional.*

Palabras clave: *Bibliometría. Radiología. América latina.*

Introduction

In 1995, to mark the centenary of Wilhelm C. Roentgen's discovery of X-rays, the *Sociedad Chilena de Radiología* (SOCHRADI) founded the *Revista Chilena de Radiología* (RChR), as the official instrument for scientific dissemination within the specialty and to foster the exchange of local experiences, with a primary focus on enriching the Chilean radiological field across technical as well as clinical and professional aspects.[1]

Initially published solely in print, the journal was indexed in SciELO Chile in 2002, thereby expanding its regional visibility.[1] In 2024 it adopted the name Austral Journal of Imaging (AJI), maintaining editorial continuity while broadening its scope to an international level.

In general, scientific journals, more than simply publishing research findings, enable the analysis of a discipline's thematic evolution, its authorship dynamics, and collaboration networks.[2] In this context, bibliometric studies have proven to be useful methodological tools for quantitatively assessing these aspects and providing evidence for editorial management and the analysis of academic impact,[3,4] enabling the identification of strengths and weaknesses, and detecting patterns in subspecialties, gender, institutional affiliation, and academic cooperation.

Similar journals in the field such as *Radiología* published by the *Sociedad Española de Radiología Médica* (Spanish Society of Medical Radiology)[5] and the *Revista Colombiana de Radiología* (Colombian Journal of Radiology)[6] have already been the subject of bibliometric studies. However, in Chile, as yet there has been no systematic study regarding the editorial evolution of the RChR, despite the sustained growth of national radiology over the last 30 years, a period marked by technological advances and increasing clinical and academic complexity.

Given that a journal's publication output reflects the maturity of its scientific community, it is pertinent to examine how the publication of our country's primary instrument for disseminating radiological science has evolved over time. Analyzing publication patterns, subspecialties covered, imaging techniques reported, and authorship characteristics makes it possible to visualize trends, identify gaps, and guide strategic editorial and institutional decision-making.

In reply to this, the present study aims to analyze the evolution of scientific output published in the RChR between 1995 and 2025, describing trends in publication volume, article types, subspecialties, imaging techniques employed, authorship by gender, institutional affiliation, and national and international academic collaboration.

Material and methods

A descriptive, retrospective bibliometric study was conducted, encompassing all articles published in the RChR between March 1995 and December 2025.

- Data sources. Articles were identified using two primary sources: the SciELO Chile database[7] and the historical archives available on the Chilean Society of Radiology website.[8] A database was created in Microsoft Excel 365, systematically recording all articles published from Volume 1, Number 1 (1995) to Volume 31, Number 4 (2025).
- Exclusion criteria. Editorials and letters to the editor were excluded because they did not contain information suitable for bibliometric analysis.
- Variables analyzed. The following variables were extracted for each article:
  - Bibliographic data: year of publication and article title.
  - Editorial classification: article type (original, review, case series, case report).
  - Radiological subspecialty: abdomen and pelvis, musculoskeletal, cardio/thoracic, neuroradiology, education, and others.
  - Predominant imaging technique: computed tomography (CT), magnetic resonance imaging (MRI), ultrasound, plain radiography, and combined techniques.
  - Authorship and affiliation: gender of the first author, type of institution (university/clinical care), institutional role (public, private, mixed), and country of origin.
  - Academic collaboration: national (between Chilean institutions) or international (with foreign institutions).
- Definition of thematic categories. The "Education" category was created as a transversal thematic

concept to group articles whose content did not fit a specific subspecialty but shared a common educational focus. This category included publications on university teaching, resident training, clinical simulation, virtual learning, artificial intelligence applied to teaching, competency assessment, and other educational or management initiatives within the field of radiology.

- Analysis procedure. Descriptive statistics were applied using Microsoft Excel 365, calculating absolute frequencies, percentages, medians, and ranges. The temporal evolution of scientific output over time was represented using line graphs, while categorical variables were visualized using bar and pie charts. Articles were classified independently by two authors. Discrepancies were resolved by consensus to ensure data reliability.
- Ethical considerations. Ethics committee approval was not required. No sensitive data or personally identifiable information was used.

Results

Annual scientific output

A total of 788 published articles were identified between March 1995 and December 2025. An initial upward trend in annual scientific output was observed, peaking in 2009 with 33 articles. A plateau in output was identified during the 2000s, with a median of 29 articles per year (mean: 28; range: 14-33) and a second peak in 2008 with 32 articles per year. From 2013 onwards, a progressive decline in output was evident, with figures ranging from 10 to 28 articles per year (Fig. 1).

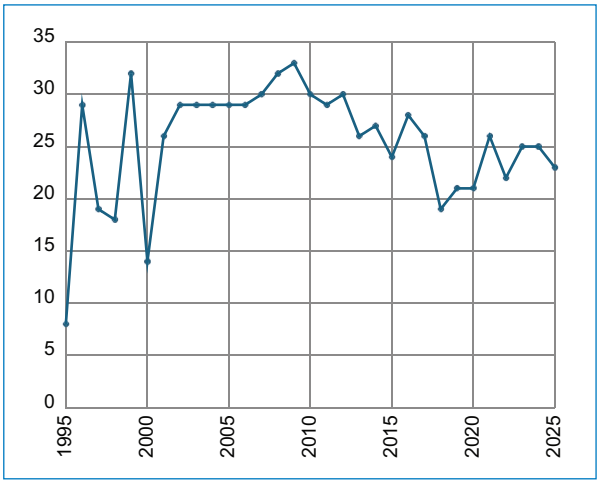

Figure 1. Trend in annual scientific output based on the number of articles published per year.

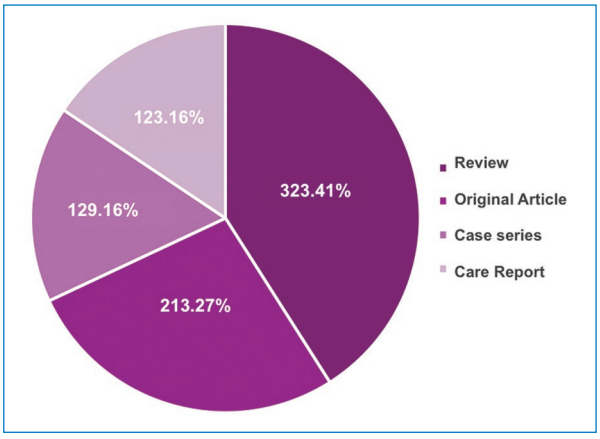

Figure 2. Percentage distribution of total scientific output by article type.

Article type

Of the 788 articles analyzed, reviews predominated with 323 publications (41.0%), followed by original articles with 213 (27.0%), case series with 129 (16.4%), and case reports with 123 (15.6%). The percentage distribution is shown in figure 2.

Radiology subspecialties

Five areas accounted for 84% of the total publications: abdomen and pelvis (29.4%), musculoskeletal (18%), cardio/thoracic (11.5%), and neuroradiology (11.4%). A sustained presence of articles classified under the Education category (13.2%) was observed. The remaining subspecialties accounted for 127 articles (16.1%). This category grouped less frequent subspecialties, including interventional radiology, oncologic imaging, breast imaging, pediatric imaging, and nuclear medicine, among others. The distribution in absolute values is shown in figure 3.

Imaging techniques

The most frequent technique was CT, with 188 articles, followed by MRI with 128 articles, ultrasound with 94 articles, and plain radiography with 78 articles. The combined techniques category, which included articles using more than one technique, accounted for 302 publications. The percentage distribution is shown in figure 4.

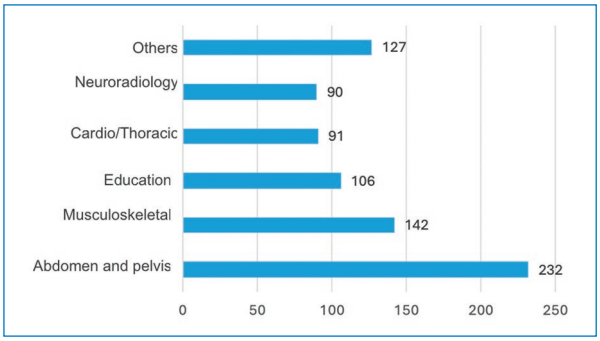

Figure 3. Distribution of scientific content by radiological specialty in absolute values.

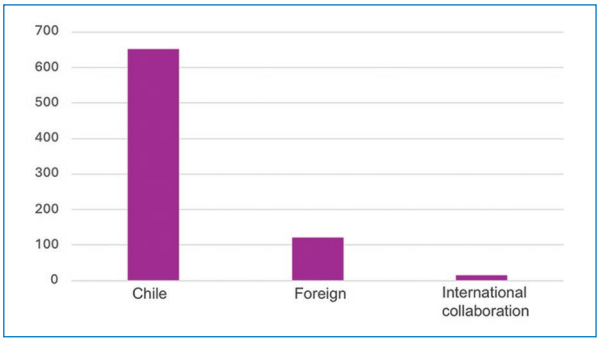

Figure 5. Distribution in absolute values of publication provenance, within or outside of Chile.

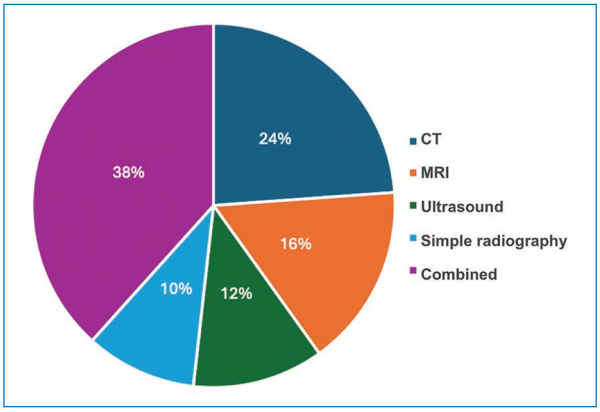

Figure 4. Percentage distribution of scientific output according to the imaging technique used. MRI: magnetic resonance imaging; CT: computed tomography.

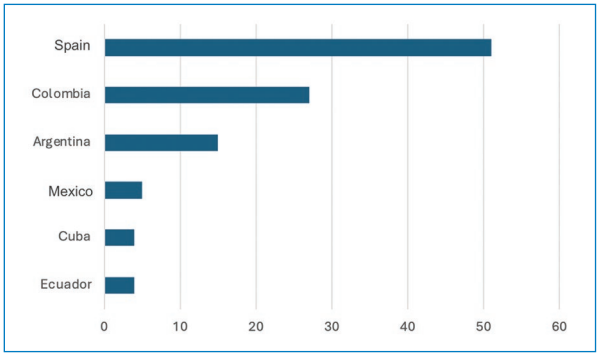

Figure 6. Representation of the main foreign collaborating countries, based on the absolute number of published articles.

Academic collaboration

Most of the articles were exclusively Chilean in origin (82.6%). 15.4% of the publications were of foreign origin, and only 2.0% involved mixed collaboration between Chilean and foreign authors (Fig. 5). The most frequent countries involved in international collaboration were Spain, Colombia, and Argentina (Fig. 6). Throughout the study period, the participation of foreign authors remained low overall. However, in more recent years, a greater relative presence of foreign publications has been observed compared to earlier stages, coinciding with the launch of the journal's English-language version in 2022 (Fig. 7).

First authorship gender

A marked male predominance was observed among first authorship gender, with 521 articles (66.1%) compared to 267 publications led by women (33.9%) (Fig. 8). Female participation remained high at the beginning of the period, followed by a decline during the first half of the previous decade and an upward trend in recent years (Fig. 9).

Institutional affiliation in Chile

Of the total 788 articles, 651 (82.6%) showed a Chilean institutional affiliation. Of these, 351 articles (53.9%) originated from university institutions or associated centers, while 300 (46.1%) (Fig. 10) came from healthcare institutions with no reported direct university affiliation. Throughout the study period, sustained participation from both types of institutions was observed, with no marked variations in their contribution relative to the journal's scientific output. Regarding the institutional type, scientific output was concentrated in private institutions, followed by the public sector and, to a lesser extent, collaborations between both sectors. This distribution remained relatively stable over time, showing no substantial changes in each sector's contribution to the journal's scientific output (Fig. 11). Within the university

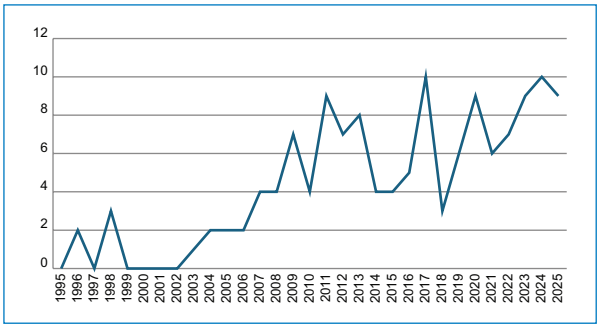

Figure 7. Historical trend of foreign participation in the journal's publications.

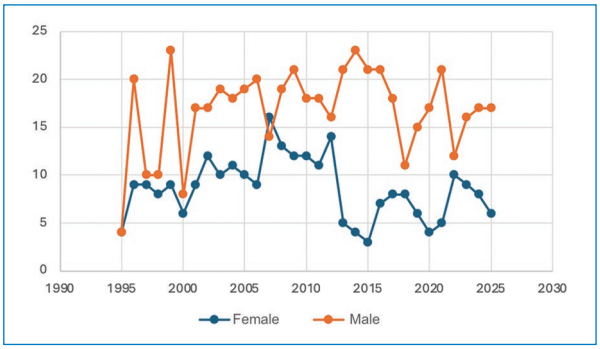

Figure 9. Distribution of the number of articles published per year, by first authorship gender.

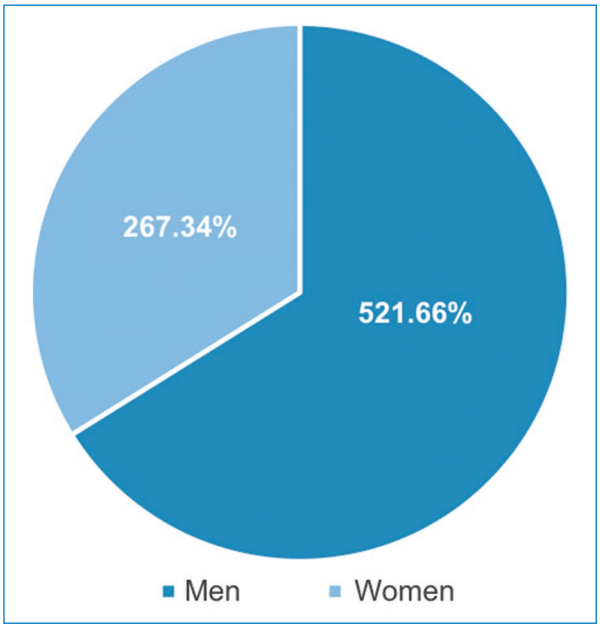

Figure 8. Gender distribution of the first authorship across all scientific publications.

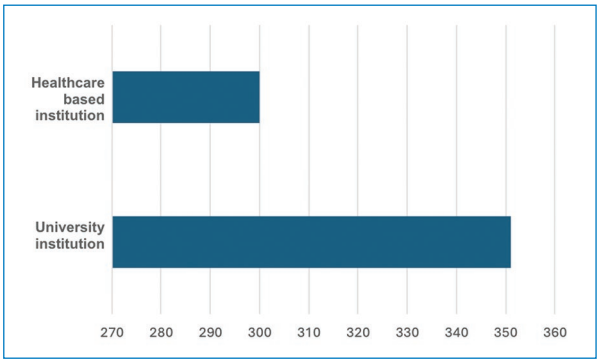

Figure 10. Representation of total scientific output according to university affiliation.

context, the most productive institutions were the *Universidad de Chile* (92 articles; 26.2% of the national total), the *Pontificia Universidad Católica de Chile* (75; 21.4%), and the *Universidad del Desarrollo* (68; 19.4%).

Discussion

Our study offers insight into the editorial evolution of the RChR over its three-decade history, being the first comprehensive bibliometric analysis applied to the journal, which allows its publication patterns to be contextualized within the dynamics described in medical and radiological journals at both regional and international levels. The observed trajectory shows an initial rise in publications, followed by a productivity plateau in the 2000s and a progressive decline in recent years, a pattern consistent with phenomena described in bibliometric literature, where factors such as competition to publish in higher-impact journals and changes in indexing systems directly influence annual scientific output.[2]

The predominance of review articles over original research articles represents one of the analysis's most significant findings. This pattern mirrors that of other Latin American radiology journals, such as the *Revista Colombiana de Radiología*, where synthesis and update articles have historically outnumbered original research studies.[9] Such a distribution may reflect an academic system oriented more toward consolidating and updating knowledge than generating primary evidence, a common phenomenon in countries facing funding limitations and constraints on applied clinical research.[10] However, bibliometric literature emphasizes that the production of original studies is a central component to increasing a journal's visibility and impact,[3] therefore strengthening this type of contribution should be a strategic priority.

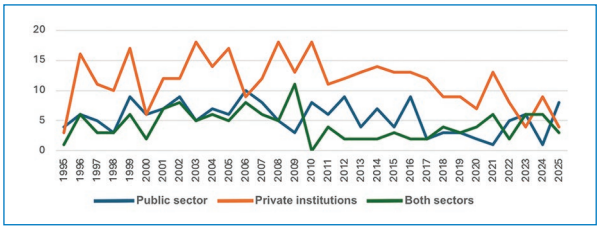

Figure 11. Distribution of institutional affiliation for Chilean articles (1995-2025).

Regarding the predominant subspecialties, abdominal and pelvic, musculoskeletal, cardio-thoracic, and neuroradiology accounted for the largest proportion of publications, which aligns with clinical practice patterns and coincides with findings from other studies showing that the highest volume of publications is concentrated in areas of high clinical/healthcare demand.[2,3] A notable finding is the sustained contribution of articles related to radiology education,[11] reflecting the community's growing interest in medical training, this being a distinguishing feature that positions the RChR as a journal responsive to the educational needs of the local community, aligning with the increasing importance the literature places on continuing education in clinical settings.[3]

Regarding imaging techniques, the predominance of CT and MRI replicates the technological transition radiology has undergone over the last two decades, characterized by a shift from conventional methods toward more technologically complex techniques.[9,12] This pattern reflects both the technological resources available in our healthcare centers and the steady increase in the diagnostic complexity of clinical practice.

Results regarding authorship reveal a historical male predominance, with an increase in female participation in recent years. This shift is consistent with internationally observed trends toward greater equity in scientific output.[8] Nevertheless, structural barriers to achieving gender parity persist, particularly in medical specialties traditionally dominated by men, presenting both a challenge and an opportunity for editorial boards to adopt inclusive policies.

In terms of institutional affiliation, the private sector accounts for the largest share of articles. This pattern correlates with findings from previous studies, which show that scientific output tends to be concentrated in private centers with extensive technological resources.[13] Universities also demonstrate strong academic participation, which contributes significantly to the advancement of radiological research.

Finally, a particularly significant finding is the low level of international collaboration, with a figure that is notably low by international standards, representing a potential structural weakness or a lack of international dissemination of the RChR. Previous bibliometric studies in radiology and the health sciences highlight that internationalization is one of the key factors for boosting a journal's impact, citation rates, and editorial standing.[2] This suggests the need to promote strategies that facilitate linkages with foreign networks, considering that international collaboration is a positive predictor of visibility.

Conclusions

This bibliometric study demonstrates that the RChR has played a significant role in consolidating the academic identity of Chilean radiology and disseminating knowledge of the discipline throughout its three decades of existence. The evolution of its output, marked by an initial growth, a plateau, and a recent decline, aligns with dynamics observed in other regional journals, likely influenced by the indexing processes and editorial competition.

While the prevalence of review articles over original studies has contributed to consolidating educational content, it also highlights the need to strengthen the generation of primary evidence. Furthermore, the thematic concentration on traditional clinical subspecialties and the focus on radiological education stand out as strengths that bridge clinical practice and academic activity.

Progress regarding gender equity, the participation of universities and healthcare centers, and the widespread use of advanced techniques reflect positive transformations. However, the level of international collaboration observed remains low, despite a growing presence of foreign authorship in recent years, a trend likely driven by the introduction of the journal's English-language version in 2022.

Compared to editorial experiences in Colombia, Spain, and other specialized journals in the region, the RChR is well-established, but critical challenges remain in enhancing its standing as a scientific journal at both local and international levels.

Strengths and limitations

A key strength of this study is the comprehensive review of three decades of publications, involving systematic manual coding undertaken by two independent

reviewers in accordance with established methodological recommendations. Recognized limitations include the absence of impact indicators such as citation counts or the h-index. Additionally, the dataset was restricted to SciELO and SOCHRADI's historical archives, excluding international platforms like Scopus or WoS, which limits comparative analysis with other indexed journals. Finally, the study did not employ specialized tools for analyzing co-authorship networks or keywords, thereby limiting the visualization of complex collaborative dynamics.

Future projections

The findings of this study suggest lines of action to strengthen the RChR's editorial standing in the medium and long term. Firstly, there is a need to encourage the publication of original studies, whether in clinical, diagnostic, or educational research, that demonstrate high methodological rigor. This type of output enhances the scientific value of the published content and boosts the journal's citation potential and international standing. Secondly, it is suggested that editorial policies incorporating a gender equity perspective be implemented to reduce persistent gaps in female authorship. These measures could include calls for papers on specific themes, support for emerging female researchers, and efforts to highlight female leadership within the discipline.

Finally, strengthening international collaboration is identified as a priority. To this end, it would be beneficial to actively invite foreign authors, establish partnerships with international scientific societies, and participate in joint editorial projects. Progress in these three areas will be crucial to consolidating the RChR as a leading international scientific journal.

Funding

The authors declare that they have not received funding.

Conflicts of interest

The authors declare no conflicts of interest.

Ethical considerations

Protection of human subjects and animals. The authors declare that no experiments on humans or animals were performed for this research.

Confidentiality, informed consent, and ethical approval. This study does not involve personal patient data, medical records, or biological samples, and does not require ethical approval. SAGER guidelines do not apply.

Declaration on the use of artificial intelligence. The authors declare that they used artificial intelligence in the drafting of this manuscript. The ChatGPT 5.1 tool (OpenAI) was used exclusively for the grammatical, orthographic, and stylistic review of the manuscript, without involvement in the generation of scientific content or analysis of the results.

References

1. Ladrón de Guevara D. Origins and history of the Austral Journal of Imaging: Revista Chilena de Radiología. Austral J Imaging. 2024; 30(4):167-9.
2. Alcalá-Albert GJ, Parra-González ME. Bibliometric analysis of scientific production on nursing research in the Web of Science. Educ Sci. 2021; 11(9):455.
3. Donthu N, Kumar S, Mukherjee D, Pandey N, Lim WM. How to conduct a bibliometric analysis: an overview and guidelines. J Bus Res. 2021;133:285-96.
4. García-Villar C, García-Santos JM. Indicadores bibliométricos para evaluar la actividad científica. Radiología. 2021;63(3):228-35.
5. Fornell-Pérez R, Merino-Bonilla JA, Morandeira-Arrizabalaga C, Marín-Díez E, Rovira F, Ros-Mendoza LH. Análisis bibliométrico de la revista Radiología en el periodo 2010-2019. Radiología. 2021;63(3): 209-17.
6. Moreno-Mejía AM, Puerta-Gaviria LM, Canas-Arboleda AM, García-García HC. Análisis bibliométrico de la Revista Colombiana de Radiología: periodo 2005-2018. Rev Colomb Radiol. 2019;30(3):5187-93.
7. Revista Chilena de Radiología [Internet]. Santiago: SciELO Chile; desde 2002 [cited 27 jul 2025]. Available from: https://www.scielo.cl/scielo.php?script=sci_serial&pid=0717-9308
8. Rev Chil Radiol [Internet]. Santiago: Sociedad Chilena de Radiología; desde 2002 [cited 27 jul 2025]. Available from: https://sochradi.cl/revista
9. LILACS - Literatura Latinoamericana y del Caribe en Ciencias de la Salud [Internet]. São Paulo: BIREME/OPS/OMS; desde 1986 [cited 27 jul 2025]. Available from: https://lilacs.bvsalud.org/es
10. Selva-Pareja L, Ramos-Pla A, Mercadé-Melé P, Espart A. Evolution of scientific production on health literacy and health education: a bibliometric analysis. Int J Environ Res Public Health. 2022;19(7):4356.
11. Aksoy S, Aksoy U, Orhan K. An overview of the 35 years of research in the oral radiology: a bibliometric analysis. Oral Radiol. 2022;38:183-91.
12. Navarro-Ballester A, Merino-Bonilla JA, Ros-Mendoza LH, de-la-Puente-Gómez R, López-Sánchez JR, de-la-Puente-Gómez M et al. Publications on COVID-19 in radiology journals in 2020 and 2021: bibliometric citation and co-citation network analysis. Eur Radiol. 2023;33:3103-14.
13. Vitón-Castillo AA, Casabella-Martínez S, Germán-Flores L, García-Villacampa G, Bravo-Malagón Y. Análisis bibliométrico de la producción científica de la Revista Universidad Médica Pinareña, 2014-2017. Rev Univ Méd Pinareña. 2018;14(3):238-47.

AUSTRAL JOURNAL OF IMAGING
REVISTA CHILENA DE RADIOLOGÍA

PERMANYER

Check for updates

REVIEW ARTICLE

Protection of the lens in fluoroscopic procedures: international standards, implementation gaps, and roadmap for Chile

Protección del cristalino en procedimientos fluoroscópicos: estándares internacionales, brechas de implementación y prioridades para Chile

Sergio Ramos-Avasola[1], Nayareth Cardenas[1], Alexis Flores[1], Ignacio Galaz[1], Sebastián Ortega[1], Andrea Ovando-Tellez[2], Cristóbal Guerrero[3], Jorge Gamarra[4], and Nitza Espinosa[5]*

[1]School of Medical Technology, Faculty of Sciences, Universidad San Sebastián, Santiago; [2]School of Medical Technology, Faculty of Medicine, Universidad de Valparaíso, Valparaiso; [3]Department of Occupational Health, Instituto de Salud Pública; [4]Irradiation Department, Dosimetry Department, Comisión Chilena de Energía Nuclear. Santiago; [5]Hemodynamics Unit, Hospital Regional Dr. Juan Noé Crevani, Arica. Chile

Abstract

Interventional fluoroscopy exposes clinical teams to ionizing radiation, primarily to scattered radiation generated by the interaction of the X-ray beam with the patient, which constitutes the main source of occupational exposure for the operator. The eye lens is a critical organ because of its radiosensitivity and location outside the protection provided by the lead apron. Epidemiological evidence among interventional personnel has documented a higher frequency of posterior subcapsular opacities and cataracts, with patterns consistent with exposure geometry and evidence of a dose-response relationship. These findings supported the reduction in the occupational dose limit for the eye lens recommended by the International Commission on Radiological Protection and the strengthening of radiation protection measures, including specific dosimetric monitoring. This review integrates radiobiological and epidemiological evidence with international standards applicable to fluoroscopic procedures and examines the Chilean context, characterized by a regulatory framework that is not fully aligned with recent international recommendations and by gaps in specific monitoring, including the operational quantity Hp(3), and in the use of eye protection. Strengthening eye lens protection through regulatory updates, dosimetric standardization, optimization of practices, continuous training, and occupational ophthalmologic surveillance is proposed to reduce cumulative exposure and prevent radiation-induced lens damage.

Keywords: *Fluoroscopy. Eye lens. Radiation protection. Personal dosimetry. Radiation-induced cataract.*

Resumen

La fluoroscopía intervencionista expone a los equipos clínicos a radiación ionizante dispersa por el paciente, principal fuente de exposición ocupacional para el operador. El cristalino constituye un órgano crítico por su radiosensibilidad y ubicación fuera de la protección del delantal plomado. La evidencia epidemiológica en personal intervencionista ha documentado mayor frecuencia de opacidades subcapsulares posteriores y cataratas, con patrones compatibles con la geometría de exposición y evidencia de relación dosis-respuesta. Estos hallazgos sustentaron la reducción del límite ocupacional para el cristalino recomendada por la Comisión Internacional de Protección Radiológica y el fortalecimiento de medidas de radioprotección, incluida la vigilancia dosimétrica específica. Esta revisión integra evidencia radiobiológica y epidemiológica con estándares internacionales aplicables a procedimientos fluoroscópicos y analiza la situación chilena, caracterizada por un

***Correspondence:**
Sergio Ramos-Avasola
E-mail: sergioramosavasola@gmail.com

Date of reception: 06-03-2026
Date of acceptance: 16-07-2026
DOI: 10.24875/AJI.26000019

Available online: 26-10-2026
Austral J. Imaging. (Engl. ed.). 2026;32(4):198-206
www.resochradi.com

2810-708X / © 2026 Sociedad Chilena de Radiología. Published by Permanyer. This is an open access article under the CC BY-NC-ND license (https://creativecommons.org/licenses/by-nc-nd/4.0/).

marco normativo no plenamente alineado con recomendaciones internacionales recientes y brechas en el monitoreo específico, incluida la magnitud Hp(3), y en el uso de protección ocular. Se propone fortalecer la protección del cristalino mediante actualización normativa, estandarización dosimétrica, optimización de prácticas, capacitación continua y vigilancia oftalmológica ocupacional, orientadas a reducir la exposición acumulativa y prevenir el daño lenticular.

Palabras clave: *Fluoroscopía. Cristalino. Radioprotección. Dosimetría personal. Catarata radioinducida.*

Introduction

Fluoroscopy-guided interventional procedures are central in interventional cardiology, interventional radiology, and endovascular surgery. However, the sustained increment in the complexity and volume of these procedures has increased the occupational exposure to ionizing radiation among healthcare personnel, particularly for operators positioned close to the patient and the scattered radiation field[1]. Consequently, the lens of the eye (crystalline lens) has assumed critical importance in radiation protection due to its radiosensitivity and its location in the head region, an area frequently exposed and partially unprotected against scattered radiation[2,3].

From a radiobiological perspective, the lens of the eye is an avascular tissue whose transparency depends on the structural organization of proteins and the functional integrity of lens epithelial cells. Due to its limited capacity for repair and cellular turnover, damage accumulates progressively following chronic exposure, even at low doses[4].

Consistent with this biological susceptibility, epidemiological evidence among interventional personnel has documented an increase in posterior subcapsular opacities and cataracts. Cross-sectional studies of interventional cardiologists show higher prevalences of these alterations compared to controls[5,6]. Furthermore, several studies describe a predominance of left-eye involvement, consistent with the geometry of occupational exposure[5,7].

Cohort evidence involving radiological technologists has demonstrated a significant increase in cataract risk, with a dose-response gradient associated with the cumulative workload of interventions[8]. Likewise, quantitative syntheses reinforce this association: a meta-analysis revealed a significant excess of cataracts among interventional personnel[9], and subsequent analyses in another review confirmed an increased risk of lens opacities after adjusting for confounders[10]. Furthermore, systematic reviews indicate that this risk can be observed even within dose ranges consistent with previous occupational limits[11].

Collectively, these findings prompted a revision of the international radiation protection standards. The International Commission on Radiological Protection (ICRP) recommended lowering the occupational limit for the lens of the eyes to 20 mSv/year averaged over 5 years, with a maximum of 50 mSv in any single year[12]; this recommendation was specifically reinforced for interventional procedures[13]. Various jurisdictions have adopted these criteria[14,15], yet in Chile, the *Decreto Supremo (DS)* (Supreme Decree/law) No. 3 of 1985 issued by the *Ministerio de Salud/MINSAL* (Ministry of Health) maintains a limit of 300 mSv/year[16]. Although there exist technical guidelines aligned with international standards[17], challenges persist regarding the standardization of specific monitoring[18] and the systematic implementation of eye protection[6,19]. Against this backdrop, this article includes the radiobiological and epidemiological evidence with international regulatory developments to examine national gaps and identify guidelines aimed at strengthening ocular radiation protection in interventional procedures.

Information sources and synthesis approach

This manuscript is a narrative review with a structured approach, aimed at integrating evidence relevant to clinical practice and policy formulation regarding occupational radiation protection. To do this, scientific literature, international and national regulations, as well as technical documents concerning radiation-induced lens damage in personnel exposed to interventional fluoroscopy procedures, were reviewed.

A structured, though not systematic, bibliographic search was conducted across the PubMed/MEDLINE, Web of Science, EBSCO, Scopus, Cochrane, and SciELO databases for the 2010–2025 time period, using terms related to the eye lens dose (“Hp(3)”), interventional fluoroscopy, radiation-induced cataracts, and radiation protection. The search initially identified 3,217 records, 994 of which were duplicates. Following the selection process, 2,223 records were examined and 69 full-text articles were evaluated, and the search was

further supplemented via citation chasing, which added six additional records. Ultimately, the narrative synthesis was based on 21 studies deemed methodologically relevant to the objectives of this review. The identified evidence was analyzed based on methodological quality, clinical relevance, and applicability to the review's goals. Special emphasis was placed on meta-analyses, cohort studies, and regulatory reference documents, including publications from the ICRP, the International Atomic Energy Agency, and Directive 2013/59/Euratom, complemented by current Chilean regulations.

Although a structured process for identifying and selecting literature was applied to enhance the search's transparency and reproducibility, this remains a narrative review; consequently, the final selection of evidence was guided by its methodological quality, clinical relevance, and contribution to the objectives of the synthesis, rather than by the formal inclusion and exclusion criteria characteristic of a systematic review.

The information was synthesized into five thematic areas: 1) regulatory limits; 2) dosimetric quantities and monitoring; 3) collective and personal protection measures; 4) training and occupational surveillance; and 5) gaps in the implementation of these standards within the Chilean context.

Radiobiological basis of eye lens damage

Radiation-induced damage to the lens of the eye (crystalline) is classified as a tissue reaction characterized by progressive structural alterations that compromise lens transparency. Although a threshold dose for such effects was traditionally postulated, evidence derived from chronic low-dose-rate exposures has led to a re-evaluation of its actual magnitude in occupational settings[20].

At the cellular level, ionizing radiation induces persistent oxidative stress, nuclear and mitochondrial DNA damage, and alterations in gene expression within the lens epithelial cells[21,22]. These cells regulate the differentiation into mature lens fibers, a process essential for maintaining lens transparency. Sustained disruption of these mechanisms promotes the accumulation of misfolded proteins and insoluble aggregates, particularly in the posterior subcapsular region, the subtype most consistently associated with occupational exposure[5,11].

The susceptibility of the ocular lens is related to its avascular nature, limited capacity for cellular turnover, and the absence of effective mechanisms for clearing damaged cells. Furthermore, experimental and observational studies indicate that repeated low-dose exposures can produce cumulative subclinical changes, which have challenged the historically established thresholds for radiation-induced cataracts, thereby justifying a review of dose limits[6,12,23].

In interventional procedures, the ocular dose depends primarily on scattered radiation originating from the patient. The spatial and angular distribution of this radiation is dynamic. Furthermore, it is influenced by the projection used, tube angulation, table height, detector position, and the operator's movements during the procedure[1,3], factors that determine the actual cephalic exposure.

Consequently, ocular exposure must be interpreted as the result of a dynamic geometric scenario[3,12], reinforcing the need for appropriate anatomical positioning of the dosimeter, ideally close to the dominant eye or at the level of the head or neck. Furthermore, when there is significant asymmetry in the exposure, the use of double dosimetry may be considered to improve the estimation of the dose to the lens of the eye.

Consistency between the cellular mechanisms described for crystalline lens damage and the clinical patterns observed in epidemiological studies, especially the predominance of posterior subcapsular opacities and the lateral asymmetry of exposure, has been documented in interventional cardiology personnel occupationally exposed to ionizing radiation[5,7].

Epidemiological evidence regarding personnel exposed to fluoroscopy

Epidemiological evidence concerning occupational damage to the lens in interventional fluoroscopy has been established through cross-sectional studies involving standardized ophthalmological assessment, occupational cohort studies, and quantitative syntheses.

Early cross-sectional studies documented high prevalences of posterior subcapsular opacities among interventional cardiologists and cardiac catheterization laboratory (cath lab) personnel, with significant differences compared to control groups[5,6]. Likewise, in several studies a predominance of left-eye involvement was observed, consistent with the operator's spatial positioning relative to the patient and the X-ray tube[5,7] (Fig. 1).

Cohort evidence adds methodological robustness. In a retrospective cohort of radiology technologists in the United States of America, participation in fluoroscopy-guided procedures was associated with a significant increase in cataract risk, with a dose-response

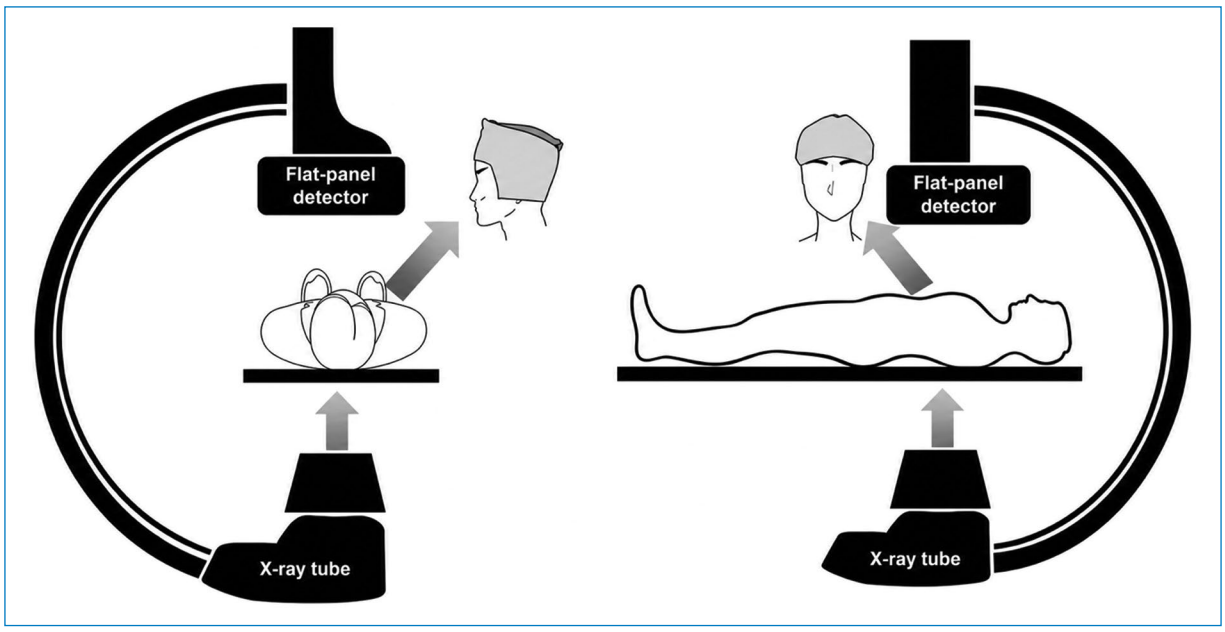

Figure 1. Diagram of scattered radiation generated by the patient and its preferential impact on the operator's left eye lens.

gradient based on the cumulative number of assisted interventions[8].

Quantitative syntheses reinforce these findings. A meta-analysis by Elmaraezy et al.[9] identified a significant increase in cataract risk among interventional personnel, while Alhasan et al.[10] confirmed an elevated risk of lens opacities after adjusting for relevant confounding factors. On one hand, the systematic review by Della Vecchia et al.[11] reports that the majority of included studies described an increased risk of cataracts and posterior subcapsular opacities among exposed healthcare workers, also observing these findings even at low cumulative doses, which has contributed to questioning the adequacy of the protection provided by historical limits (Table 1).

Overall, the existence of a dose-response gradient and the consistency with described radiobiological mechanisms[8,21,22] constitute a body of evidence that has supported the revision of international standards for protection of the eye lens during fluoroscopy-guided interventional procedures.

Evolution and current status of international standards for protection of the eye lens: from ICRP 26 to ICRP 118

International standards for protection of the lens of the eye have evolved alongside the accumulation of radiobiological and epidemiological evidence regarding occupational damage to the lens. In 1977, the ICRP established an annual limit of 300 mSv in its *Publication 26*, based on the assumption of relatively high thresholds for radiation-induced cataracts[24]. Subsequently, this limit was reduced to 150 mSv/year in *Publication 60*, reflecting a more conservative interpretation of the available evidence[20].

A turning point was reached with *Publication 118*, which recommended reducing the occupational dose limit for the eye lens limit to 20 mSv/year averaged over 5 years, with a maximum of 50 mSv in any single year. This recommendation was based on evidence of crystalline lens damage observed at doses below previously considered thresholds, particularly in scenarios of chronic, low-dose-rate exposure. Consequently, the emphasis for radiation protection shifted toward specific monitoring of the crystalline lens and the systematic optimization of interventional procedures[12].

Recommendations for interventional procedures and dosimetric monitoring (ICRP 139)

ICRP *Publication 139* reinforced the operational application of these recommendations in interventional procedures, emphasizing that eye protection must be integrated into occupational radiation protection programs for

Table 1. Meta-analyses and systematic reviews on radiation-induced cataracts in personnel exposed to fluoroscopy

Author (year)	Type of synthesis	Population included	Studies and subjects	Risk estimates or main quantitative finding	Key findings
Elmaraezy et al.[9] (2017)	Meta-analysis	Interventional cardiologists and hemodynamics personnel	8 studies, 2559 subjects	RR: 3.21; 95% CI: 2.14-4.83	Increased risk of opacity or posterior subcapsular cataract in interventional cardiologists
				RR: 0.85; 95% CI: 0.55-1.30	No significant differences in the frequency of nuclear opacities were observed between exposed workers and controls
Alhasan et al.[10] (2022)	Meta-analysis	Occupationally exposed physicians and healthcare workers	15 studies, > 8500 subjects	RR: 4.96; 95% CI: 4.23-5.82	Increased risk of cataract in healthcare workers exposed to ionizing radiation
				RR: 3.26; 95% CI: 2.39-4.43	Increased risk of posterior subcapsular opacity, even after adjustment for confounding factors
Della Vecchia et al.[11] (2020)	Systematic review	Cronically exposed healthcare workers	15 studies, > 20.000 subjects	Most of the included studies reported an increased risk of cataracts and posterior subcapsular cataracts in exposed workers; lens opacities were observed even at low cumulative doses (no pooled RR).	Increased risk even at low cumulative doses; questions the adequacy of historical limits

95% CI: 95% confidence interval; RR: relative risk (pooled RR was available only for meta-analyses).

fluoroscopy suites[13]. The ICRP highlights that ocular risk cannot be addressed solely through quantities based on whole-body effective dose, as the eye lens often lies outside the area protected by lead aprons and can receive significant doses of scattered radiation[1,3,13]. Consequently, *Publication 139* underscores the need to implement specific dosimetric monitoring for the eye lens and systematic optimization strategies within the procedure room.

From a metrological perspective, monitoring of the eye lens has increasingly been linked to the quantity Hp(3), designed to approximate the dose equivalent at a depth of 3 mm, whereas Hp(10) targets penetrating radiation and Hp(0.07) targets superficial or weakly penetrating tissues[18]. Its implementation requires the standardization of quantities, devices, and dosimeter positioning, particularly in environments with high geometric variability[1,3].

Implementation in Europe, Japan, and the United States of America

The adoption of ICRP recommendations has varied across jurisdictions. In Europe, Directive 2013/59/Euratom incorporated the new limit and established obligations regarding radiation protection monitoring and optimization, including worker classification and dosimetric control programs tailored to high-risk practices[14].

Similarly, Japan adopted the limit of 20 mSv/year averaged over 5 years and developed specific technical guidelines for monitoring the eye lens, promoting standardization and traceability in high exposure scenarios[15].

In contrast, the United States maintains a federal limit of 150 mSv/year[25], reflecting a discrepancy relative to the recommendations in ICRP publications 118 and 139, although there is growing recognition of the occupational risk to the lens of the eye during interventional procedures (Table 2).

Overall, contemporary international standards are converging toward more protective dose limits[12,13], specific dosimetric monitoring of the eye lens[3,18], and the systematic optimization of interventional practice.

Current situation in Chile

Existing regulatory framework

In Chile, occupational radiation protection for healthcare workers exposed to ionizing radiation is historically based on *MINSAL Decreto Supremo* (Ministry of Health

Table 2. International comparison of eye lens dose limits and monitoring in personnel exposed to fluoroscopy

Jurisdiction	Lens occupational dose limit	Formal incorporation pf ICRP 118/139	Recommended quantity for monitoring	Implementation status in interventional procedures	Key gaps
European Union (Euratom 2013/59)	20 mSv/year (5 year average)	Yes (mandatory)	Explicit Hp (3)	Specific guidelines in various countries	Variability among member States
Japan	20 mSv/year (5 year average)	Yes	Hp (3) with national guidelines	Advanced implementation in high dose areas	Need for continuous monitoring
United States of America (10 CFR 20)	150 mSv/year	No (fully updated)	Predominantly Hp (10); emerging Hp (3)	Growing acceptance of the problem	Limit still high compared to ICRP
Chile (DS N.º 3/1985 and ISP criteria)	300 mSv/year legal standard; 20 mSv operational (ISP)	Partial (not included in the decree/ law)	Hp (3) not universally required	Heterogeneous implementation	Lack of formal mandatory requirements and systematic auditing

DS: decreto supremo; ISP: public health institute.

Supreme Decree) No. 3 of 1985, which establishes an annual equivalent dose limit of 300 mSv[16] for the lens of the eye. This value, aligned with international standards from the 1970s[24], contrasts with the current consensus, which lowered the occupational limit to 20 mSv/year averaged over five years[12,13]. More than just a numerical difference, this gap has direct implications for the design of occupational monitoring programs and for the institutional prioritization of radiation protection for the lens of the eye.

Although more conservative technical criteria, aimed at aligning with international recommendations, have been adopted at the operational level, structural challenges persist. In this context, the issue is not limited to updating a legal text, but ensuring that clinical practice incorporates auditable requirements, such as identifying high-risk workstations, effectively using protective barriers, implementing specific lens dosimetry monitoring, and maintaining systematic occupational health monitoring[13,14].

Dosimetric monitoring and the Hp(3) quantity

In interventional fluoroscopy, eye exposure arises primarily from scattered radiation originating from the patient[1,3,13]. Therefore, the current standard emphasizes direct monitoring of the eye lens using operational quantities designed for this purpose, specifically Hp(3)[13,18], which estimates the equivalent dose at a depth of 3 mm and requires calibration on a head phantom with metrological traceability and uncertainty estimation. Furthermore, this calibration must be performed using geometric configurations representative of clinical scattered radiation, as the spatial and angular distribution of the field in the head region is dynamic and depends on the projection used, the C-arm angulation and the operator's relative position during the procedure. Key international recommendations regarding lens dosimetry monitoring, including the purpose of the measurement, the suggested number of dosimeters, and their recommended anatomical placement, are summarized in figure 1 of the Supplementary data.

In Chile, lens dosimetry monitoring has traditionally relied on operational quantities used for whole-body dosimetry, particularly Hp(10), which are designed to estimate dose in deep tissues. However, metrological literature and international recommendations highlight the advisability of using quantities specific to the lens, such as Hp(3), which approximates the equivalent dose at a depth of 3 mm in ocular tissue. Therefore, when the eye dose is estimated based on conventional whole-body measurements, it is necessary to evaluate the validity of this approach through comparative studies between Hp(10) and Hp(3) conducted under actual operating conditions. This need is particularly relevant in interventional fluoroscopy procedures, where the exposure geometry may differ significantly from the assumptions of conventional body dosimetry[13,18].

Literature indicates that the dosimetric assessment of the eye lens requires appropriate anatomical positioning of the dosimeter, preferably on the head or neck, to provide a representative approximation of the

eye dose equivalent. Furthermore, in situations involving asymmetric exposure, the use of double dosimetry may be considered to improve the estimation of the occupational dose to the eye lens[3,13].

Robust monitoring also requires standardization of the dosimetric quantity, appropriate detector placement, and metrological traceability, particularly in units with high procedure volumes[12,13]. Moreover, the systematic implementation of Hp(3) requires the development of national metrological capacity, including accredited laboratories (e.g., under ISO/IEC 17025), a documented traceability chain, and characterization of the dosimetry system's uncertainty. Finally, in scenarios involving exposure asymmetry or high geometric variability, double dosimetry may be considered a complementary measure to improve the representativeness of the eye lens dose estimate.

Available national evidence

Evidence published in Chile regarding eye dose and eye lens protection in interventional settings remains limited, although available results are consistent with international evidence. The head region can receive significant doses, and eye protection measures do not always ensure sufficient dose reduction without systematic optimization within the procedure room. A national study evaluated eye doses using dosimeters placed in front of and behind leaded eyewear, observing partial reductions attributable to this protection, with variability between measurements[26]. However, the comparison with currently applicable standards depends on the operational quantity used and the calibration scheme employed, factors that are decisive for estimating dose equivalents to Hp(3)[13,18]. Consequently, rather than a mere lack of epidemiological studies, the primary national gap lies in the discrepancy between what should be measured to adequately manage ocular risk and what is currently measured in a standardized manner.

In the absence of national epidemiological studies, the interpretation of occupational risk must rely on available international evidence, which has consistently documented an increased risk of cataracts and lens opacities among personnel exposed during interventional procedures[8-11].

These observations reinforce the importance of implementing specific ocular monitoring programs and promoting the systematic use of protective barriers/screens, particularly during procedures involving a high fluoroscopic workload[13].

Implementation gaps in the national context

Comparing international standards with the national situation reveals four interrelated, yet operationally distinct gaps.

The first corresponds to a regulatory gap. The continued application of an historical dose limit for the lens of the eye[16] establishes a less stringent framework than those recommended internationally[12,13], a situation that tends to limit the institutional prioritization of ocular radiation protection in the absence of explicit regulatory obligations and formal audit mechanisms.

The second corresponds to a metrological gap. Specific monitoring using Hp(3), recommended for interventional procedures[13,18], is not implemented consistently. Consequently, estimating ocular dose based on Hp(10) can introduce uncertainty when the actual exposure depends on the procedure's geometry and the effective use of protective barriers[1,3,13].

The third corresponds to an operational gap regarding the implementation of in-room protective measures. Evidence shows that protective barriers, when used correctly, significantly reduce the dose to the eye lens[1,3]. However, their effectiveness depends on the clinical team's behavior, equipment availability, and the institutional safety culture. Furthermore, leaded eyewear varies in efficacy depending on design and fit[27], whereas structural comprehensive protection strategies allow for even greater reductions in occupational exposure[28].

The fourth corresponds to a gap in occupational monitoring. Eye lens monitoring requires specific dosimetry and periodic ophthalmological evaluations to detect subclinical changes[5-7,9-11]. In the absence of systematic monitoring programs, both the early detection of lens damage and the assessment of the effectiveness of preventive measures are limited.

Strategies to strengthen lens protection in Chile

Strengthening ocular radiation protection in Chile requires aligning standards, measurement, and clinical practice within a framework applicable to actual fluoroscopy suites. It is a priority to establish a coherent national standard that translates the internationally recommended limit into enforceable operational criteria for interventional units, including the identification of high-risk workstations and the definition of dosimetric investigation levels[12-14,16]. This operationalization must be complemented by audits focused on the actual implementation of in-suite

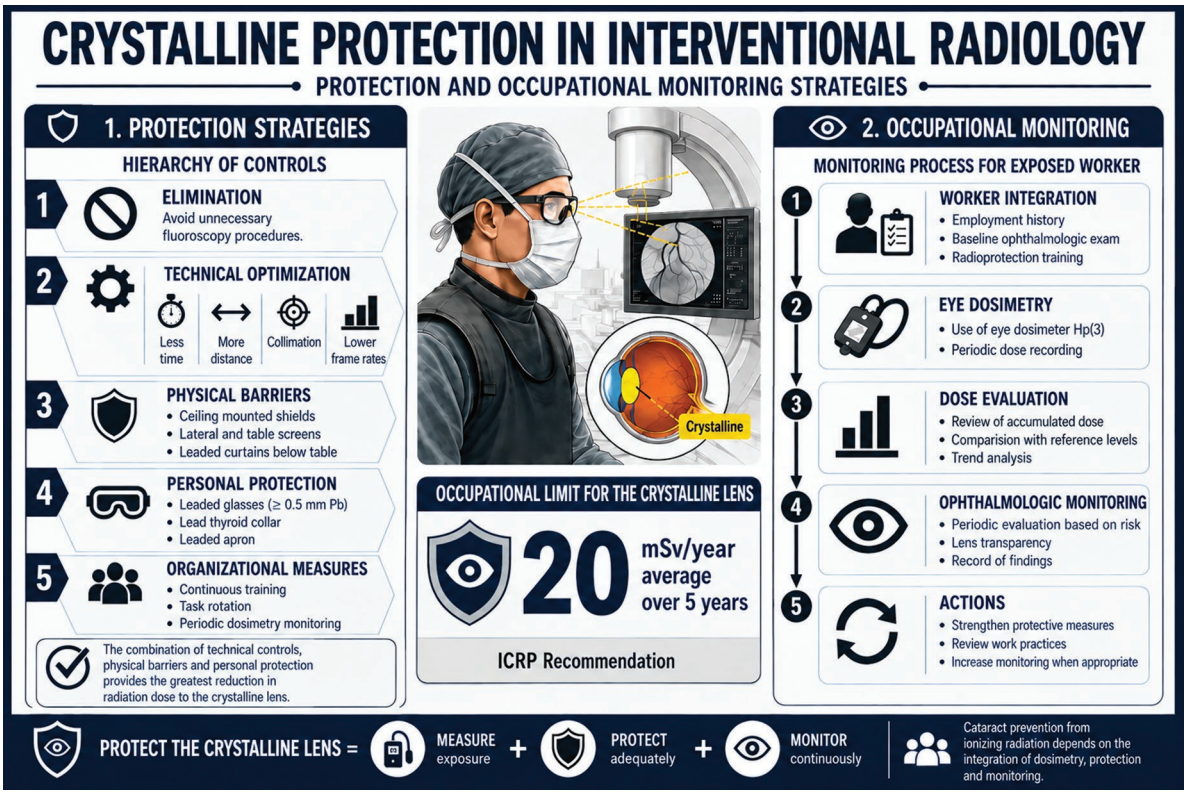

Figure 2. Integrated strategies for lens (crystalline) protection in interventional radiology procedures.

protection measures. Recommendations can be integrated into an operational framework combining dosimetric positioning, protection strategies, and periodic occupational monitoring (Fig. 2).

Dosimetric monitoring must move toward standardized protocols that prioritize direct measurement using appropriate quantities, ideally Hp(3), defining specific anatomical positioning and interpretation criteria for interventional procedures[13,18]. This requires traceable metrological capabilities to estimate lens dose under actual scattered radiation conditions.

Dose reduction must be addressed at the source through the systematic optimization of the practice. Properly used suspended screens and shields reduce head and neck exposure[29]. Eye protection must be part of a comprehensive strategy, taking into account its variations in design and fit, particularly regarding oblique scattered radiation[27]. Furthermore, engineering solutions and comprehensive protection measures can lower occupational exposure and reduce reliance on lead aprons[28].

Finally, available epidemiological evidence has documented an increased risk of lens opacities and cataracts among personnel exposed to radiation during interventional procedures, which reinforces the need for occupational monitoring programs that include specific lens dosimetry and periodic ophthalmological evaluations for the early detection of subclinical changes[5-7,9-11].

Limitations

This text is a review based on secondary evidence and regulatory documents. It does not include standardized national primary measurements of lens dose using Hp(3), nor does it include systematic audits of barrier use or optimization practices in Chilean fluoroscopy suites. Also, the national epidemiological evidence regarding radiation-induced cataracts in interventional personnel is limited, which restricts the direct risk estimation and quantitative assessment of the impact of interventions. Additionally, some of the literature employs exposure proxies and exhibits methodological heterogeneity.

Conclusions

Radiation protection of the lens during fluoroscopy-guided interventional procedures is a priority supported by consistent radiobiological and epidemiological evidence. The reduction of the occupational limit recommended by the ICRP entails the implementation of specific dosimetric monitoring and systematic

optimization within the procedure lab. In Chile, a gap persists between the historical legal framework and contemporary standards, together with heterogeneity in eye monitoring and metrological standardization.

Overcoming these gaps requires enforceable national criteria, specific lens dose measurement using Hp(3), effective use of protective barriers, and periodic ophthalmological monitoring for at-risk personnel.

Funding

The authors declare that they have not received funding.

Conflicts of interest

The authors declare no conflicts of interest.

Ethical considerations

Protection of human subjects and animals. The authors declare that no experiments on humans or animals were performed for this research

Confidentiality, informed consent, and ethical approval. This study does not involve personal patient data, medical records, or biological samples, and does not require ethical approval. SAGER guidelines do not apply.

Declaration on the use of artificial intelligence. The authors declare that an artificial intelligence tool, specifically ChatGPT, was used to improve wording, punctuation, and spelling. After using this tool, the authors reviewed and edited the content as necessary and assume full responsibility for the content of the publication.

Supplementary data

Supplementary data are available at *Austral Journal of Imaging/Revista Chilena de Radiología* (DOI: 10.24875/AJI.26000019). These data are provided by the corresponding author and published online for the benefit of the reader. The contents of supplementary data are the sole responsibility of the authors.

References

1. Vañó E, Gonzáles L, Fernández JM, Haskal ZJ. Eye lens exposure to radiation in interventional suites: caution is warranted. Radiology. 2008;248:945-53.
2. Hamada N. Ionizing radiation sensitivity of the ocular lens and its dose rate dependence. Int J Radiat Biol. 2017;93:1024-34.
3. Martin CJ. Eye lens dosimetry for fluoroscopically guided clinical procedures: practical approaches to protection and dose monitoring. Radiat Prot Dosimetry. 2016;169:286-91.
4. Hammer GP, Scheidemann-Wesp U, Samkange-Zeeb F, Wicke H, Nerishi K, Blettner M. Occupational exposure to low doses of ionizing radiation and cataract development: a systematic literature review and perspectives on future studies. Radiat Environ Biophys. 2013;52:303-19.
5. Ciraj-Bjelac O, Rehani MM, Sim KH, Liew HB, Vañó E, Kleiman NJ. Risk for radiation-induced cataract for staff in interventional cardiology: is there reason for concern? Catheter Cardiovasc Interv. 2010;76:826-34.
6. Vañó E, Kleiman NJ, Duran A, Rehani MM, Echeverri D, Cabrera M. Radiation cataract risk in interventional cardiology personnel. Radiat Res. 2010;174:490-5.
7. Jacob S, Boveda S, Bar O, Brézin A, Maccia C, Laurier D, et al. Interventional cardiologists and risk of radiation-induced cataract: results of a French multicenter observational study. Int J Cardiol. 2013;167:1843-7.
8. Velázquez-Kronen R, Borrego D, Gilbert ES, Miller DL, Moysich KB, Freudenheim JL, et al. Cataract risk in US radiologic technologists assisting with fluoroscopically guided interventional procedures: a retrospective cohort study. Occup Environ Med. 2019;76:317-25.
9. Elmaraezy A, Morra ME, Mohammed AT, Al-Habbaa A, Elgebaly A, Ghazy AA, et al. Risk of cataract among interventional cardiologists and catheterization laboratory staff: a systematic review and meta-analysis. Catheter Cardiovasc Interv. 2017;90:1-9.
10. Alhasan AS, Aalam WA. Eye lens opacities and cataracts among physicians and healthcare workers occupationally exposed to radiation. Saudi Med J. 2022;43:665-77.
11. Della-Vecchia E, Modenese A, Loney T, Muscatello M, Silva-Paulo M, Rossi G, et al. Risk of cataract in health care workers exposed to ionizing radiation: a systematic review. Med Lav. 2020;111:269-84.
12. International Commission on Radiological Protection. ICRP statement on tissue reactions and early and late effects of radiation in normal tissues and organs: threshold doses for tissue reactions in a radiation protection context. ICRP Publication 118. Ann ICRP. 2012;41:1-322.
13. International Commission on Radiological Protection. Occupational radiological protection in interventional procedures. ICRP Publication 139. Ann ICRP. 2018;47:1-118.
14. European Society of Radiology. Summary of the European Directive 2013/59/Euratom: essentials for health professionals in radiology. Insights Imaging. 2015;6:411-7.
15. Yokoyama S, Tsujimura N, Hashimoto M, Yoshitomi H, Kato M, Kurosawa T, et al. The Japan Health Physics Society guideline on dose monitoring for the lens of the eye. J Radiat Prot Res. 2022;47:1-7.
16. Chile. Ministerio de Salud. Aprueba Reglamento de Protección Radiológica de Instalaciones Radioactivas. Decreto Supremo N.o 3. Santiago: Biblioteca del Congreso Nacional de Chile; 1985. (Consultado el 06-07-2026.) Available from: https://www.bcn.cl/leychile/navegar?idNorma=1026879.
17. Instituto de Salud Pública de Chile. Departamento de Salud Ocupacional. Elementos para considerar en un programa de vigilancia epidemiológica de trabajadores ocupacionalmente expuestos a radiaciones ionizantes. Santiago: Instituto de Salud Pública de Chile; 2023.
18. Ubeda C, Nocetti D, Inzulza A, Oyarzún C, Alarcón R. Magnitudes y unidades para dosimetría del personal ocupacionalmente expuesto en radiodiagnóstico e intervencionismo. Rev Chil Radiol. 2018;24:5-11.
19. Andreassi MG, Piccaluga E, Guagliumi G, Del Greco M, Gaita F, Picano E. Occupational health risks in cardiac catheterization laboratory workers. Circ Cardiovasc Interv. 2016;9:e003273.
20. International Commission on Radiological Protection. 1990 Recommendations of the International Commission on Radiological Protection. ICRP Publication 60. Ann ICRP. 1991;21:1-201.
21. Ainsbury EA, Bouffler SD, Dörr W, Graw J, Muirhead CR, Edwards AA, et al. Radiation cataractogenesis: a review of recent studies. Radiat Res. 2009;172:1-9.
22. Ainsbury EA, Dalke C, Hamada N, Benadjaoud MA, Chumak V, Ginjaume M, et al. Radiation-induced lens opacities: epidemiological, clinical and experimental evidence, methodological issues, research gaps and strategy. Environ Int. 2021;146:106213.
23. Kleiman NJ. Radiation cataract. Ann ICRP. 2012;41:80-97.
24. International Commission on Radiological Protection. Recommendations of the International Commission on Radiological Protection. ICRP Publication 26. Ann ICRP. 1977;1:1-53.
25. United States Nuclear Regulatory Commission. Standards for protection against radiation: 10 CFR Part 20. Subpart C – Occupational dose. Washington (DC): United States Nuclear Regulatory Commission; 2006. Available from: https://www.govinfo.gov/app/collection/cfr/2006?utm
26. Zett-Lobos C, Vera-Muñoz F, Arriola-Álvarez K, Díaz-Ramos O, Gamarra J, Fernández-Palomo C, et al. Protección contra la radiación ionizante mediante gafas de vidrio plomado durante cardiología intervencionista. Rev Med Chil. 2013;141:63-9.
27. Honorio da Silva E, Martin CJ, Vanhavere F, Dabin J, Buls N. An investigation into potential improvements in the design of lead glasses for protecting the eyes of interventional cardiologists. J Radiol Prot. 2022; 42-(3):031509.
28. Fattal P, Goldstein JA. A novel complete radiation protection system eliminates physician radiation exposure and leaded aprons. Catheter Cardiovasc Interv. 2013;82:11-6.
29. Fetterly KA, Magnuson DJ, Tannahill GM, Hindal MD, Mathew V. Effective use of radiation shields to minimize operator dose during invasive cardiology procedures. JACC Cardiovasc Interv. 2011;4:1133-9.

AUSTRAL JOURNAL OF IMAGING
REVISTA CHILENA DE RADIOLOGÍA

PERMANYER

Check for updates

REVIEW ARTICLE

Radiomics in lung cancer: advances and challenges in clinical practice

Radiómica en cáncer de pulmón: avances y desafíos en la práctica clínica

Fernando A. Ramos-Zaga

Research Directorate, Universidad Privada del Norte, Lima, Peru

Abstract

Artificial intelligence–based radiomics has emerged as an approach capable of transforming medical imaging into quantitative biomarkers, in a context where lung cancer remains the leading cause of cancer-related mortality worldwide. The objective of this article is to analyze the current state of this technology as a non-invasive phenotypic characterization tool, assessing its ability to extract biomarkers and the standardization challenges that condition its clinical implementation. The findings indicate that radiomic models can predict relevant molecular alterations, estimate response to immunotherapy, and improve prognostic stratification with clinically meaningful performance; however, limitations persist related to variability in image acquisition, tumor segmentation, reproducibility, and model interpretability. It is concluded that, although its potential is substantial, the clinical adoption of radiomics requires robust standardization, multicenter validation, and governance frameworks to ensure its safe integration into precision medicine.

Keywords: *Quantitative imaging biomarkers. Deep learning. Clinical translation.*

Resumen

La radiómica basada en inteligencia artificial ha emergido como un enfoque capaz de transformar la imagen médica en biomarcadores cuantitativos, en un contexto donde el cáncer de pulmón continúa siendo la principal causa de mortalidad oncológica global. El objetivo del artículo es analizar el estado actual de esta tecnología como herramienta de caracterización fenotípica no invasiva, evaluando su capacidad para extraer biomarcadores y los desafíos de estandarización que condicionan su implementación clínica. Los resultados muestran que los modelos radiómicos permiten predecir alteraciones moleculares, estimar la respuesta a la inmunoterapia y mejorar la estratificación pronóstica con desempeño clínicamente relevante; sin embargo, persisten limitaciones asociadas a la variabilidad en la adquisición de imágenes, la segmentación, la reproducibilidad y la interpretabilidad. Se concluye que, aunque su potencial es sustantivo, la adopción clínica de la radiómica requiere una estandarización robusta, una validación multicéntrica y unos marcos de gobernanza que garanticen su integración segura en la medicina personalizada.

Palabras clave: *Biomarcadores de imagen cuantitativos. Aprendizaje profundo. Traslación clínica.*

Correspondence:
Fernando A. Ramos-Zaga
E-mail: fernandozaga@gmail.com

Date of reception: 31-07-2025
Date of acceptance: 25-06-2026
DOI: 10.24875/AJI.25000058

Available online: 26-10-2026
Austral J. Imaging. (Engl. ed.). 2026;32(4):207-215
www.resochradi.com

2810-708X / © 2026 Sociedad Chilena de Radiología. Published by Permanyer. This is an open access article under the CC BY-NC-ND license (https://creativecommons.org/licenses/by-nc-nd/4.0/).

Introduction

Lung cancer is the leading cause of cancer-related mortality worldwide and produces a significant impact in terms of years of life lost due to disability.[1,2] The population of interest comprises patients with lung neoplasms, specifically non-small cell lung cancer, whose classification has traditionally guided therapeutic management. Given the marked biological heterogeneity of these tumors, a need has arisen for personalized medicine approaches focused on the individual characteristics of each case. Such an approach seeks to optimize risk classification and treatment selection in order to reduce mortality and improve survival and quality of life.

Radiomics is defined as the extraction and analysis of large amounts of quantitative data from medical images using advanced computing systems.[3,4] This field enables the transformation of standard radiological studies into complex numerical information using statistical models and neural networks. Two main approaches are identified: the use of mathematical measures predefined by human experts and the application of deep learning, in which the system autonomously identifies patterns.[5,6] Its clinical usefulness has been explored in the diagnosis, the identification of molecular profiles, and the prediction of the response to treatment.

In oncological practice, radiomics addresses the limitations of physical biopsies, which may be incomplete due to intratumoral heterogeneity or entail risks for the patient.[7] This technology has demonstrated the ability to non-invasively identify genetic alterations, such as *EGFR* or *ALK* mutations, as well as to estimate the presence of immunological markers like PD-L1.[8,9] Its integration as a complementary tool facilitates prognostic classification and the anticipation of response to immunotherapy, thereby providing added value to clinical care planning.

Despite this potential, methodological challenges exist that hinder the widespread clinical use of these biomarkers. The lack of uniformity in image acquisition and data processing raises questions regarding whether the results obtained at one center can be successfully replicated at another.[10] Questions also persist regarding the stability of these measurements and about the clarity with which the results generated by complex artificial intelligence systems can be interpreted.

This article aims to analyze the current state of artificial intelligence-based radiomics as a tool for non-invasive phenotypic characterization in lung cancer, evaluating its capacity to extract quantitative biomarkers and the standardization challenges affecting its clinical implementation. The analysis seeks to synthesize the fundamentals of this technology and the limitations that must be overcome to consolidate its role in personalized medicine.

Method

A narrative review was conducted to analyze the current state of artificial intelligence-based radiomics applied to lung cancer.

In line with this methodological framework, the search strategy was applied to international biomedical databases, including PubMed, Scopus, and Web of Science. The following search string was used: ("*radiomics*" OR "*radiogenomics*") AND ("*artificial intelligence*" OR "*machine learning*" OR "*deep learning*") AND ("*lung cancer*" OR "*non-small cell lung cancer*"). Articles published in English between 2012 and 2026 were included, a period that coincides with the introduction of the radiomics concept and its development in thoracic oncology.

Based on this identification strategy, the inclusion criteria encompassed original studies, reviews, and meta-analyses addressing the application of radiomics or radiogenomics in lung cancer, with emphasis on biomarker extraction, clinical prediction, or aspects of standardization. Studies with insufficient information, duplicates, non-peer-reviewed publications, and works focusing on other neoplasms without specific lung analysis were excluded.

Using these criteria, document selection was carried out by reviewing titles, abstracts, and full texts. Data extraction considered variables related to model type, clinical applications, performance metrics, and technical limitations. The analysis was conducted through thematic synthesis, grouping the evidence into conceptual categories. As this was a narrative review based on secondary sources, ethics committee approval was not required.

Fundamentals of radiomics in non-invasive tumor characterization

Radiomics proposes a fundamental paradigm shift by transforming medical imaging from a simple visual depiction into a source of highly complex quantitative data.[4] This conceptual evolution implies that each voxel, the basic volumetric unit of a three-dimensional image, contains biological information that goes beyond

traditional anatomical observation. Thus, a digital substrate is created in which the tumor biology is encoded in patterns imperceptible to the human eye.[7] The central premise is that these imaging characteristics reflect specific biological differences related to critical processes such as cell growth and division.[11]

The measurement process is organized through the systematic extraction of descriptors, mathematical parameters that characterize the image, grouped into clear categories. First-order characteristics analyze the statistical distribution of the gray levels without considering pixel position, while the shape descriptors measure three-dimensional geometric properties such as tumor volume and sphericity.[12] Meanwhile, the texture characteristics calculate spatial organization patterns that allow for the detection of tumor tissue heterogeneity at a mesoscopic scale that is visibly imperceptible to the clinician.[13]

Building on this methodological foundation, the application of mathematical filters to the original image adds an analytical layer by highlighting information on various spatial scales. For instance, wavelet filters decompose the image to isolate fine or coarse details, while other operators accentuate lesion boundaries.[14] This processing capability generates hundreds of data points per lesion, necessitating rigorous selection methods to ensure that the resulting models are reliable and easy to interpret by the medical team.[3]

Continuing with this development, the field has evolved from a manual approach, where experts defined what to measure, to the use of deep learning architectures. While the traditional approach relies on prior medical knowledge, modern neural networks autonomously learn to identify the patterns most useful for predicting the behavior of the disease.[5] This shifts the nature of the biomarker, that goes from being a direct mathematical measurement to a complex representation autonomously processed by the artificial intelligence.[6]

As an extension of this shift, three-dimensional artificial intelligence models have further advanced the field by processing the entire tumor volume, capturing spatial details that planar images overlook.[15] Recently, it has been proposed to treat computed tomography scans as if they were video sequences, applying networks trained to recognize motion in order to extract information regarding deep volumetric texture.[16] These tools generate representations that offer prognostic insights independent of tumor size or conventional clinical stage.[5]

In that same line of conceptual refinement, a recent proposal is the so-called "tensor radiomics", which seeks to avoid the rigidity of using a single value for each characteristic. Instead, the system analyzes multiple variants (or *flavors*) of a same descriptor under different technical configurations.[17] This approach allows the model to select the most suitable context for each data point, maintaining the clarity of traditional measures while leveraging the immense computing power of artificial intelligence.[17]

From an integrative perspective, the link between digital data and the tumor microenvironment forms the conceptual foundation of this discipline. Internal tumor heterogeneity manifests simultaneously at the molecular, cellular, and radiological levels.[7] Texture measures capture these variations, while shape data reflect biological processes linked to the cancer's invasive potential.[18] These imaging patterns have been shown to correlate with fundamental biological pathways, such as the cellular metabolism and the response of the immune system.[19]

In spatial terms, the interface between the tumor and healthy parenchyma has emerged as an area of high informational value. This transition zone at the tumor margin contains critical data regarding cell infiltration and the lesion's aggressive potential.[9] Including the regions surrounding the tumor in the analysis allows for the integration of valuable information about the disease microenvironment, substantially improving the predictive capacity of current models.[20]

Given these foundations, the conceptual development of radiomics as a system for extracting quantitative biomarkers from medical imaging lays the groundwork for its clinical application. However, the validity of this approach cannot rest solely on plausibility, rather it must be verified by robust empirical evidence in real-world clinical settings. Consequently, the following section explicitly addresses the predictive capacity of radiogenomic signatures in lung cancer, evaluating their performance in the identification of molecular alterations, prognosis stratification, and prediction of the therapeutic response.

Predictive capacity of radiogenomic biomarkers in thoracic oncology

Radiogenomics enables the integration of quantitative imaging features with tumor molecular profiles, establishing a digital biopsy method capable of identifying actionable genetic alterations without resorting to invasive procedures.[21] This approach is crucial in

non-small cell lung cancer, where the biological variability of mutations prevents an isolated tissue sample from reflecting the lesion's overall reality, often leading to sampling errors with direct consequences on therapy.[7]

Based on this premise, the non-invasive prediction of epidermal growth factor receptor (EGFR) mutations stands out as one of the most robust applications of this technology. Models based on tomography data have achieved accuracy levels (area under the curve) exceeding 0.80, allowing for the identification of patients eligible for specific treatments with clinically relevant reliability.[8] This way, texture patterns obtained from image-processing filters are combined with clinical variables, such as smoking history, demonstrating that the use of multiple data sources outperforms the efficacy of any single parameter analyzed in isolation.[22]

Complementarily, this discriminatory capability extends to ALK gene alterations, the detection of which is critical for selecting specific drugs such as crizotinib or alectinib. Advanced analysis models have proven capable of identifying imaging patterns associated with the EML4-ALK translocation, serving as a supportive tool that complements traditional molecular testing.[23] This evidence supports the utility of non-invasive genetic characterization in cases where tissue sampling is insufficient, or the risk associated with biopsy is high.[21]

In parallel, assessing the tumor's immunological profile using these tools has gained significant importance given the increasing use of immunotherapy. Predicting PD-L1 expression using artificial intelligence models has achieved an accuracy of 0.84 in identifying patients with a high probability of responding to checkpoint inhibitors.[24] This methodology surpasses the limitations of conventional immunohistochemistry, particularly regarding the uneven distribution of PD-L1 within the tumor, which often leads to false-negative results in needle biopsies.[9]

Based on this foundation, the assessment of the response to immunotherapy has proven effective in various cancer types, identifying a common response pattern in both lung cancer and melanoma.[9] The most valuable data are obtained by analyzing the transition zone between the tumor margin and healthy tissue, which provides information on immune system activity that cannot be detected using conventional visual criteria, such as the RECIST (*Response Evaluation Criteria in Solid Tumors*) system.[25] These imaging signatures surpass the predictive power of the clinical stage or the mutational stage alone.[9]

Regarding prognosis, prediction via quantitative image analysis has been validated in large patient cohorts over the long term. Models integrating contrast-enhanced computed tomography data with clinical variables achieve high concordance in predicting overall survival, generating individualized risk curves.[26] Applying image-processing filters to texture data enhances the ability to distinguish disease behavior, capturing biological variations linked to oncological prognosis.[7] Furthermore, distinguishing between the main histological subtypes of lung cancer, such as adenocarcinoma and squamous cell carcinoma, is also possible using these techniques. Systems based on shape and texture parameters achieve accurate classification in independent studies.[18] This clinical differentiation has a direct therapeutic impact, as it allows for the adjustment of chemotherapy regimens and the selection of patients suitable for targeted therapies.[27]

From a surgical perspective, the preoperative detection of tumor dissemination through air spaces is a relevant application of 3D computational analysis. This pathological finding is a key factor in deciding between limited resection or lobectomy. Artificial intelligence models applied to contrast-enhanced CT scans have proven to be superior to traditional assessment methods.[15] This technology enables the detection of spatial patterns associated with microscopic invasion, bridging the macroscopic imaging with the patient's cellular reality.[5]

In a therapeutic context, the use of these tools in stereotactic radiotherapy planning allows for the prediction of tumor sensitivity to treatment. Models based on advanced logic have achieved high accuracy rates in identifying patients likely to respond favorably at early stages.[28] Incorporating respiratory motion analysis during data acquisition enhances the stability of these models in front of patient-specific physiological variability.[21]

Accumulated evidence regarding radiogenomics performance demonstrates significant clinical potential across multiple domains, including molecular characterization, prediction of treatment response, and prognosis estimation. However, the heterogeneity of the results and their dependence on specific technical conditions necessitate a critical examination of the methodological robustness of these findings. Consequently, the following section explicitly introduces an analysis of the technical limitations and reproducibility problems associated with radiomic biomarkers, emphasizing the sources of variability that affect their generalizability.

Technical limitations and reproducibility of radiomic biomarkers

The clinical consolidation of radiomics faces its primary obstacle in the technical fragility of quantitative data, the stability of which depends on a complex chain of physical, mathematical, and calibration processes. Heterogeneity in computed tomography (CT) acquisition protocols constitutes the primary source of variability. Technical parameters, such as voltage, tube current, slice thickness, and reconstruction algorithms, substantially alter the measurement values obtained for the same lesion.[29] This technical sensitivity means that examinations performed on different scanners can generate incompatible results, thereby compromising the feasibility of applying predictive models in different institutions.[10]

Given this initial variability, studies using standard test objects or phantoms have documented significant variations in texture characteristics when physical acquisition parameters are altered. This demonstrates that biomarker stability cannot be assumed without prior verification.[29] Factors such as radiation dose, scan time, and the patient's respiratory phase introduce technical variations that propagate throughout the analysis process, generating artifacts that can obscure the tumor's true biological information.[30] This vulnerability necessitates the harmonization of protocols prior to any use in routine clinical practice.[20]

Considering these sources of error, the image reconstruction process introduces another layer of variability that has been systematically characterized. Comparisons between classical diagnostic algorithms and advanced methods based on Bayesian statistics or deep learning have shown that only a small subset of measures maintains consistent robustness. Indeed, only 27 features meet strict technical stability criteria.[31] Features analysing tissue texture tend to be more resistant to image noise, whereas intensity-based measures exhibit marked fluctuations in response to changes in equipment signal levels.[31] Within this context of instability, tumor segmentation, or lesion delineation, represents an additional critical factor. Since data are derived from the contoured volume, any variation in the boundaries directly impacts the final result. Manual delineation introduces inter-observer bias, with levels of agreement that drop significantly for lesions with irregular margins or those located near blood vessels.[32] This limitation particularly affects features that measure tumor shape and those obtained using advanced processing filters.[12]

To address this limitation, although automated segmentation methods have improved consistency, their performance can still decline in tumors with poorly defined boundaries.[33] One strategy to ensure reliability is the use of stress tests, such as applying slight rotations or artificial changes to the contour, to identify only those measurements that withstand these variations.[19] Only the features maintaining a stability greater than 90% in the face of these alterations can be considered legitimate candidates to be used as clinical biomarkers.[10]

From a technical standpoint, the lack of uniformity among the software tools employed is also a significant source of variability. Two different software platforms can yield different values for the same image. To address this, the Image Biomarker Standardisation Initiative (IBSI) coordinated 25 international teams to unify the definitions of 169 radiomic features.[10] This effort achieved an excellent reproducibility in computed tomography, magnetic resonance imaging, and nuclear medicine, ensuring that results do not depend on the specific software used.[10]

Continuing these efforts, this framework has recently been extended to the use of processing filters, establishing strict mathematical definitions for tools that highlight fine details or structural edges.[14] This technical consensus allows, for the first time, the comparison of studies conducted anywhere in the world. However, software standardization is only an initial step, as physical variability during scanning remains a challenge that requires comprehensive harmonization solutions.[14]

Given the persistence of this heterogeneity, statistical methods exist that are designed to mitigate inter-hospital differences following image acquisition. The ComBat algorithm, adapted from the field of genetics, allows data obtained at different centers to be aligned without altering the patient's biological information.[34] Its application in lung cancer has enabled the pooling of data from multiple institutions to create more robust and reliable prediction models.[24] This technical correction is crucial when it is not possible to standardize imaging equipment, although its success depends on the quality of the statistical analysis applied.[35]

From a comprehensive evaluation perspective, the scientific quality of the field is analyzed using the *Radiomics Quality Score* (RQS), a tool that assesses the accuracy of the studies from image acquisition to its validation in real patients.[11] Recent analyses reveal that the majority of published literature achieves only one-third of the maximum score, which highlights shortcomings in external validation and the transparency of

reports.[36] The new version of this evaluation system incorporates principles of trust in artificial intelligence, focusing on robustness, traceability, and the fairness of the results.[37]

In line with these methodological requirements, adherence to reporting guidelines, such as TRIPOD (Transparent Reporting of a multivariable prediction model for Individual Prognosis Or Diagnosis) and CLAIM (CheckList for Artificial Intelligence in Medical imaging), is essential to ensure transparency and the possibility to replicate the findings in other medical settings.[38] Integration of these technical standards with rigorous documentation establishes the foundation for the necessary scientific legitimacy. Only in this way will it be possible to transform the promise of radiomics into auditable, reliable evidence for application in personalized oncology.[39]

Due to these limitations, the identification of vulnerabilities in the data acquisition and processing chain demonstrates that reproducibility is an essential requirement for the clinical validation of radiomics. Despite advances in standardization, challenges remain that hinder its uniform implementation across institutions. This realization necessitates expanding the analysis beyond technical aspects. Therefore, the following section explicitly introduces the factors influencing clinical translation, including model interpretability, its integration into healthcare systems, and the governance frameworks required for its safe adoption.

Integration and governance challenges in clinical radiomics

The transition of radiomics from research to clinical practice faces challenges that extend beyond the purely technical. Obstacles arise from the interaction between professionals and technology, as well as from the structure of healthcare institutions. The lack of transparency in complex models, often referred to as the “black box” problem, is a barrier to medical trust. Professionals need to understand the logic behind the predictions that guide the critical therapeutic decisions.[40] In oncology, responsibility for the patient rests with the medical team, and not with the computer system.[41]

Faced with this interpretative limitation, explainable artificial intelligence emerges as a response to the challenge by offering tools to measure the extent to which each image characteristic contributes to the final result. By using mathematical models that break down the algorithm’s decision into understandable components, an opaque process is transformed into an auditable clinical support tool.[42] In the context of lung cancer, specific measures of texture and shape complexity have been shown to be reliable predictors of malignancy. This facilitates the integration of system data with conventional medical reasoning.[43]

Given the need to make these decisions intelligible so that the models can be supervised, methods operating at various levels are required. Visual importance maps allow for the identification of regions of the image that most strongly influence the system’s decision. This inspection capacity is highly valuable in radiology, as it enables verification that the algorithm is focusing on structures with biological significance.[44] Consistency between the areas analyzed by the system and the findings of the human observer constitutes an essential criterion for clinical validity.[40]

Alongside these interpretability requirements, the technical connection between analysis systems and hospital infrastructure represents another critical dimension. Picture Archiving and Communication Systems (PACS) form the foundation of modern radiology. Any artificial intelligence tool must integrate into these workflows without causing disruptions.[45] The use of structured reporting standards facilitates the communication of algorithmic results in formats compatible with electronic health records, allowing predictions to be incorporated into traditional radiology reports.[22]

In parallel with this operational integration, the use of cloud-based storage and processing platforms helps manage the heavy data loads required by these models. This allows the heavy computational workload to be shifted from local computers to external servers with greater capacity, thereby facilitating the analysis of large patient cohorts.[22] This structure enables the creation of standardized, easily replicable processes, ensuring that other medical centers can achieve similar results.[46] However, the use of these services raises debates regarding data control and costs that could affect centers with less resources.[22]

As an alternative to these structural limitations, federated learning is a strategy for training models without the need to move sensitive data out of the hospitals. This resolves privacy concerns and enables the aggregation of information from multiple centers to improve system accuracy.[47] This strategy is particularly relevant in oncology, where personal data protection regulations are very strict.[48] In the context of lung cancer, this method has enabled the creation of models that are as accurate as traditional ones, while complying with all the legal security requirements.[46]

Amidst this technological expansion, the regulations governing the approval of these algorithms as medical devices have evolved to adapt to their changing nature. Guidelines from international agencies now mandate continuous monitoring once a system enters active use, as well as clear protocols for updates.[49] This legal and institutional framework aims to ensure the technology's transition from the testing phase to becoming a certified, safe clinical tool.[50]

On the other hand, the algorithm fairness is a growing concern, as models trained on data from limited groups may not perform equally well for other patients.[51] Current international standards require studies to report the demographic characteristics of the patients used to develop the model. It is essential to systematically evaluate whether system performance varies across different population subgroups.[37] This ethical requirement is crucial for ensuring that the technology's deployment is fair and beneficial for everyone.[52]

Regarding this dimension of fairness and actual use, integrating these systems into the patient care cycle requires linking imaging information with clinical and genetic data. Electronic health records (EHRs) are the natural setting for this integration, although the lack of uniformity between different hospital systems poses a significant challenge.[53] The use of modern data communication standards helps ensure that information is structured and reusable across different platforms.[54]

As a corollary to this progressive integration, the training of healthcare professionals in the use of these tools is the final requirement for their success. Radiologists and oncologists must possess the necessary competencies to critically evaluate system results, understand their limitations, and explain uncertainty to the patient.[55] Incorporating content on artificial intelligence into specialized medical training is key to the responsible use of the technology. This enables the physician to move beyond being a passive user and become a critical agent capable of supervising the system in their daily practice.[41]

Conclusions

The transformation of conventional medical images into quantifiable biological datasets marks a turning point in thoracic oncology. AI-driven radiomics consolidates a shift from subjective visual assessment to objective phenotypic characterization of lesions. This approach facilitates the capture of tumor microenvironment heterogeneity in lung cancer with a level of detail previously unattainable. This creates a scenario in which diagnostic imaging evolves to position itself as an active and indispensable instrument in precision medicine.

The ability to infer underlying tumor biology without relying exclusively on invasive procedures redefines the scope of medical imaging. Representations generated by deep learning algorithms enable the establishment of quantifiable correlations between anatomical patterns, molecular alterations, and immune profiles. This organization between macroscopic imaging data and cellular biological processes creates a more integrated interpretive framework. Consequently, the spatial organization of the neoplasm can be understood as a carrier of prognostic and predictive information relevant to characterizing the disease.

In the clinical setting, these developments translate into stratification tools aimed at optimizing therapeutic decision-making. The ability to anticipate responses to immunotherapy or predict microscopic spread prior to surgery illustrates their direct usefulness in patient management. However, the systematic adoption of these tools requires that analytical models be transparent for the clinician. The treating physician's confidence depends on explainable systems that justify their predictions and integrate seamlessly into existing hospital information systems.

Advancing the field requires overcoming the methodological fragility associated with technical variability across different acquisition systems and healthcare institutions. Consequently, future research must prioritize validating these models within multicenter cohorts that ensure an adequate demographic representation and promote algorithmic fairness. Furthermore, the implementation of federated learning architectures emerges as a crucial avenue for development. This approach will enable the training of robust predictive systems on a large-scale while strictly safeguarding clinical data privacy.

The progressive integration of algorithmic rigor with stringent clinical validation has the potential to reshape the oncology care ecosystem. The use of artificial intelligence is envisioned not as a substitute for clinical judgment, but as a support tool that enhances the physician's capabilities through auditable digital biomarkers. The translational maturity of this technology will depend on its ability to consistently mitigate diagnostic uncertainty. Achieving this will allow healthcare professionals to focus their efforts on truly comprehensive and personalized patient care.

Funding

The author declares that they have not received funding.

Conflicts of interest

The author declares no conflicts of interest.

Ethical considerations

Protection of human and animal subjects. The author declares that no experiments on humans or animals were performed for this research.

Confidentiality, informed consent, and ethical approval. This study does not involve personal patient data, medical records, or biological samples, and does not require ethical approval. SAGER guidelines do not apply.

Declaration on the use of artificial intelligence. The author declares the use of OpenAI's GPT-5.3 large language model to identify and correct grammatical and spelling errors. The prompt used was: "detect and correct all writing and spelling errors." Upon receiving the system's output, the resulting text was reviewed to ensure it maintained the tone and intent of the original manuscript.

References

1. Bray F, Laversanne M, Sung H, Ferlay J, Siegel RL, Soerjomataram I, et al. Global cancer statistics 2022: GLOBOCAN estimates of incidence and mortality worldwide for 36 cancers in 185 countries. CA Cancer J Clin. 2024;74:229-63.
2. Zhou J, Xu Y, Liu J, Feng L, Yu J, Chen D. Global burden of lung cancer in 2022 and projections to 2050: incidence and mortality estimates from GLOBOCAN. Cancer Epidemiol. 2024;93:102693.
3. Lambin P, Rios-Velazquez E, Leijenaar R, Carvalho S, van Stiphout RGPM, Granton P, et al. Radiomics: extracting more information from medical images using advanced feature analysis. Eur J Cancer. 2012;48:441-6.
4. Gillies RJ, Kinahan PE, Hricak H. Radiomics: images are more than pictures, they are data. Radiology. 2016;278:563-77.
5. Hosny A, Parmar C, Quackenbush J, Schwartz LH, Aerts HJWL. Artificial intelligence in radiology. Nat Rev Cancer. 2018;18:500-10.
6. Avanzo M, Wei L, Stancanello J, Vallières M, Rao A, Morin O, et al. Machine and deep learning methods for radiomics. Med Phys. 2020; 47:e185-e202.
7. Aerts HJWL, Velazquez ER, Leijenaar RTH, Parmar C, Grossmann P, Carvalho S, et al. Decoding tumour phenotype by noninvasive imaging using a quantitative radiomics approach. Nat Commun. 2014;5:4006.
8. Wang S, Shi J, Ye Z, Dong D, Yu D, Zhou M, et al. Predicting EGFR mutation status in lung adenocarcinoma on computed tomography image using deep learning. Eur Respir J. 2019;53:1800986.
9. Trebeschi S, Drago SG, Birkbak NJ, Kurilova I, Călin AM, Delli Pizzi A, et al. Predicting response to cancer immunotherapy using noninvasive radiomic biomarkers. Ann Oncol. 2019;30:998-1004.
10. Zwanenburg A, Vallières M, Abdalah MA, Aerts HJWL, Andrearczyk V, Apte A, et al. The image biomarker standardization initiative: standardized quantitative radiomics for high-throughput image-based phenotyping. Radiology. 2020;295:328-38.
11. Lambin P, Leijenaar RTH, Deist TM, Peerlings J, de Jong EEC, van Timmeren J, et al. Radiomics: the bridge between medical imaging and personalized medicine. Nat Rev Clin Oncol. 2017;14:749-62.
12. Van Griethuysen JJM, Fedorov A, Parmar C, Hosny A, Aucoin N, Narayan V, et al. Computational radiomics system to decode the radio-graphic phenotype. Cancer Res. 2017;77:e104-7.
13. Kumar V, Gu Y, Basu S, Berglund A, Eschrich SA, Schabath MB, et al. Radiomics: the process and the challenges. Magn Reson Imaging. 2012;30:1234-48.
14. Whybra P, Zwanenburg A, Ayotte A, Andrearczyk V, Schaer R, Apte AP, et al. The image biomarker standardization initiative: standardized convolutional filters for reproducible radiomics and enhanced clinical insights. Radiology. 2024;310:e231319.
15. Tao J, Liang C, Yin K, Fang J, Chen B, Wang Z, et al. 3D convolutional neural network model from contrast-enhanced CT to predict spread through air spaces in non-small cell lung cancer. Diagn Interv Imaging. 2022;103:535-44.
16. Chen J, Wee L, Dekker A, Bermejo I. Using 3D deep features from CT scans for cancer prognosis based on a video classification model: a multi-dataset feasibility study. Med Phys. 2023;50:4220-33.
17. Rahmim A, Toosi A, Salmanpour MR, Dubljevic N, Janzen I, Shiri I, et al. Tensor radiomics: paradigm for systematic incorporation of multi-flavoured radiomics features. Quant Imaging Med Surg. 2023;13:7680-94.
18. Wu W, Parmar C, Grossmann P, Quackenbush J, Lambin P, Bussink J, et al. Exploratory study to identify radiomics classifiers for lung cancer histology. Front Oncol. 2016;6:71.
19. Wang J, Dai G, Ren X, Shi R, Luo R, Liu J, et al. Assessing the reproducibility, stability, and biological interpretability of multimodal computed tomography image features for prognosis in advanced non-small cell lung cancer. iRadiology. 2024;2:e56.
20. Hatt M, Tixier F, Pierce L, Kinahan PE, Cheze Le Rest C, Visvikis D. Characterization of PET/CT images using texture analysis: the past, the present… any future? Eur J Nucl Med Mol Imaging. 2017;44:151-65.
21. Safarian A, Mirshahvalad SA, Nasrollahi H, Jung T, Pirich C, Arabi H, et al. Impact of [18F]FDG PET/CT radiomics and artificial intelligence in clinical decision making in lung cancer: its current role. Semin Nucl Med. 2025;55:156-66.
22. Bontempi D, Nuernberg L, Pai S, Krishnaswamy D, Thiriveedhi V, Hosny A, et al. End-to-end reproducible AI pipelines in radiology using the cloud. Nat Commun. 2024;15:6931.
23. Yamamoto S, Korn WA, Oklu R, Migdal C, Gotway MB, Weiss GJ, et al. ALK molecular phenotype in non-small cell lung cancer: CT radiogenomic characterization. Radiology. 2014;272:568-76.
24. Saber R, Tonneau M, Salko O, Liberman M, Malo J, Elkrief A, et al. Multi-institutional CT scan-based radiomics for predicting tumor PD-L1 expression in patients with advanced and limited non-small cell lung cancer. Cancers. 2026;18:552.
25. Sun R, Limkin EJ, Vakalopoulou M, Dercle L, Champiat S, Han SR, et al. A radiomics approach to assess tumour-infiltrating CD8 cells and response to anti-PD-1 or anti-PD-L1 immunotherapy: an imaging biomarker, retrospective multicohort study. Lancet Oncol. 2018;19:1180-91.
26. Hou KY, Chen JR, Wang YC, Chiu MH, Lin SP, Mo YH, et al. Radiomics-based deep learning prediction of overall survival in non-small-cell lung cancer using contrast-enhanced computed tomography. Cancers. 2022;14:3798.
27. Parmar C, Grossmann P, Bussink J, Lambin P, Aerts HJWL. Machine learning methods for quantitative radiomic biomarkers. Sci Rep. 2015;5:13087.
28. Yakar M, Etiz D, Gulbandilar E, Duruer K, Erden E. Radiomic-assistant response prediction to stereotactic body radiotherapy in early stage lung cancer. Int J Hematol Oncol. 2025;35:27-40.
29. Mackin D, Fave X, Zhang L, Fried D, Yang J, Taylor B, et al. Measuring computed tomography scanner variability of radiomics features. Invest Radiol. 2015;50:757-65.
30. Traverso A, Wee L, Dekker A, Gillies R. Repeatability and reproducibility of radiomic features: a systematic review. Int J Radiat Oncol Biol Phys. 2018;102:1143-58.
31. Liu Y, Wang G, Yan X, Wang H, Li T, Yang S, et al. Effect of reconstruction settings on radiomics feature robustness in positron emission tomography images: a clinical study. Quant Imaging Med Surg. 2025; 15:9515-33.
32. Pavic M, Bogowicz M, Würms X, Glatz S, Finazzi T, Riesterer O, et al. Influence of inter-observer delineation variability on radiomics stability in different tumor sites. Acta Oncol. 2018;57:1070-4.
33. Primakov SP, Ibrahim A, van Timmeren JE, Wu G, Keek SA, Beuque M, et al. Automated detection and segmentation of non-small cell lung cancer computed tomography images. Nat Commun. 2022;13:3423.
34. Orlhac F, Boughdad S, Philippe C, Stalla-Bourdillon H, Nioche C, Champion L, et al. A postreconstruction harmonization method for multi-center radiomic studies in PET. J Nucl Med. 2018;59:1321-8.
35. Da-ano R, Visvikis D, Hatt M. Harmonization strategies for multicenter radiomics investigations. Phys Med Biol. 2020;65:24TR02.
36. Spadarella G, Stanzione A, Akinci D'Antonoli T, Andreychenko A, Fanni SC, Ugga L, et al. Systematic review of the radiomics quality score applications: an EuSoMII radiomics auditing group initiative. Eur Radiol. 2023;33:1884-94.
37. Lambin P, Woodruff HC, Mali SA, Zhong X, Kuang S, Lavrova E, et al. Radiomics quality score 2.0: towards radiomics readiness levels and clinical translation for personalized medicine. Nat Rev Clin Oncol. 2025;22:831-46.

38. Mongan J, Moy L, Kahn CE. Checklist for artificial intelligence in medical imaging (CLAIM): a guide for authors and reviewers. Radiol Artif Intell. 2020;2:e200029.
39. Park JE, Kim D, Kim HS, Park SY, Kim JY, Cho SJ, et al. Quality of science and reporting of radiomics in oncologic studies: room for improvement according to radiomics quality score and TRIPOD statement. Eur Radiol. 2020;30:523-36.
40. Reyes M, Meier R, Pereira S, Silva CA, Dahlweid FM, von Tengg-Kobligk H, et al. On the interpretability of artificial intelligence in radiology: challenges and opportunities. Radiol Artif Intell. 2020;2:e190043.
41. Ghassemi M, Oakden-Rayner L, Beam AL. The false hope of current approaches to explainable artificial intelligence in health care. Lancet Digit Health. 2021;3:e745-50.
42. Lundberg SM, Lee SI. A unified approach to interpreting model predictions. Adv Neural Inf Process Syst. 2017;30:4765-74.
43. Raptis S, Ilioudis C, Theodorou K. Uncovering the diagnostic power of radiomic feature significance in automated lung cancer detection: an integrative analysis of texture, shape, and intensity contributions. BioMedInformatics. 2024;4:2400-25.
44. Selvaraju RR, Cogswell M, Das A, Vedantam R, Parikh D, Batra D. Grad-CAM: visual explanations from deep networks via gradient-based localization. Int J Comput Vis. 2020;128:336-59.
45. Kohli M, Prevedello LM, Filice RW, Geis JR. Implementing machine learning in radiology practice and research. AJR Am J Roentgenol. 2017;208:754-60.
46. Pati S, Baid U, Edwards B, Sheller M, Wang SH, Reina GA, et al. Federated learning enables big data for rare cancer boundary detection. Nat Commun. 2022;13:7346.
47. Rieke N, Hancox J, Li W, Milletari F, Roth HR, Albarqouni S, et al. The future of digital health with federated learning. NPJ Digit Med. 2020; 3:119.
48. Sheller MJ, Edwards B, Reina GA, Martin J, Pati S, Kotrotsou A, et al. Federated learning in medicine: facilitating multi-institutional collaborations without sharing patient data. Sci Rep. 2020;10:12598.
49. Larson DB, Harvey H, Rubin DL, Irani N, Tse JR, Langlotz CP. Regulatory frameworks for development and evaluation of artificial intelligence-based diagnostic imaging algorithms: summary and recommendations. J Am Coll Radiol. 2021;18:413-24.
50. Vasey B, Nagendran M, Campbell B, Clifton DA, Collins GS, Denaxas S, et al. Reporting guideline for the early-stage clinical evaluation of decision support systems driven by artificial intelligence: DECIDE-AI. Nat Med. 2022;28:924-33.
51. Chen RJ, Chen TY, Lipkova J, Wang JJ, Williamson DFK, Lu MY, et al. Algorithmic fairness in artificial intelligence for medicine and healthcare. Nat Biomed Eng. 2023;7:719-42.
52. Lekadir K, Feragen A, Fofanah AJ, Frangi AF, Buyx A, Emelie A, et al. FUTURE-AI: international consensus guideline for trustworthy and deployable artificial intelligence in healthcare. BMJ. 2025;388:e081554.
53. Topol EJ. High-performance medicine: the convergence of human and artificial intelligence. Nat Med. 2019;25:44-56.
54. Bibault JE, Xing L, Giraud P, Doust R, Maingon Y, Mahe JP, et al. Radiomics: a primer for the radiation oncologist. Cancer Radiother. 2020;24:403-10.
55. Pesapane F, Codari M, Sardanelli F. Artificial intelligence in medical imaging: threat or opportunity? Radiologists again on the forefront of innovation in medicine. Eur Radiol Exp. 2018;2:35.

AUSTRAL JOURNAL OF IMAGING
REVISTA CHILENA DE RADIOLOGÍA

PERMANYER

Check for updates

CASE SERIES

Postoperative pseudothyroid on ultrasound: avoiding misinterpretation of the surgical bed

Pseudotiroides posoperatoria ecográfica: evitando la sobreinterpretación del lecho quirúrgico

Luis Canales-Franco[1,2], David Astudillo-Jara[1,2], Roberto Rouhana-Monagas[3], and David Astudillo-Ortega[2,4]*

[1]Imaging Unit, Hospital Regional de Ñuble, Chillan; [2]Faculty of Medicine, Universidad Católica de la Santísima Concepción, Concepcion; [3]Medical and Home Hospitalization Services; [4]Otolaryngology Service. Hospital Regional de Ñuble, Chillan. Chile

Abstract

Postoperative pseudothyroid is a transient ultrasound finding observed in the surgical bed after thyroidectomy. It is characterized by occupation of the operative bed by a variable mixture of hemostatic material, organized hemorrhage, inflammatory reaction, and fibroconnective tissue undergoing maturation. This combination may acquire echogenicity and morphology similar to those of a normal thyroid gland, creating the impression of a "false" gland. Recognition of this finding is particularly relevant for radiologists in training, as it may mimic residual thyroid tissue or tumor recurrence.

Keywords: *Pseudothyroid. Thyroidectomy. Postoperative. Neck ultrasound.*

Resumen

La pseudotiroides posoperatoria corresponde a un hallazgo ecográfico transitorio observado en el lecho quirúrgico tras una tiroidectomía. Se caracteriza por la ocupación del lecho operatorio por una mezcla variable de material hemostático, hemorragia organizada, reacción inflamatoria y tejido fibroconectivo en proceso de maduración. Este conjunto puede adquirir una ecogenicidad y una morfología semejantes a las de una glándula tiroidea normal, generando la impresión de una «falsa» glándula. Su reconocimiento es especialmente relevante para radiólogos en formación, dado que podría simular un remanente glandular o una recurrencia tumoral.

Palabras clave: *Pseudotiroides. Tiroidectomía. Posoperatorio. Ecografía cervical.*

***Correspondence:**
Luis Canales-Franco
E-mail: luiscanalesf@gmail.com

Date of reception: 08-02-2026
Date of acceptance: 22-06-2026
DOI: 10.24875/AJI.26000015

Available online: 26-10-2026
Austral J. Imaging. (Engl. ed.). 2026;32(4):216-220
www.resochradi.com

2810-708X / © 2026 Sociedad Chilena de Radiología. Published by Permanyer. This is an open access article under the CC BY-NC-ND license (https://creativecommons.org/licenses/by-nc-nd/4.0/).

Introduction

Cervical ultrasound is the primary tool for the postoperative follow-up of patients who have undergone thyroidectomy, particularly in the monitoring of thyroid cancer. However, its diagnostic accuracy depends heavily on the operator's experience and their detailed knowledge of cervical anatomy, lymph node compartments, relevant differential diagnoses, and normal postsurgical changes, its variations and potential imitators (mimics) of residual or recurrent disease[1,2].

The postoperative thyroid bed can present multiple benign findings that create diagnostic uncertainty, such as scar tissue, suture granulomas, residual hemostatic material, and transient inflammatory phenomena[2]. In this context, we propose the term "postoperative pseudo-thyroid" to describe a transient ultrasound pattern characterized by a pseudo-glandular appearance of the surgical space contents, resulting from the reorganization of hemostatic material, organized hemorrhage, inflammatory reaction, and fibroconnective tissue following thyroid resection[3,4].

This ultrasound finding has been consistently identified in patients monitored at the *Hospital Regional de Ñuble* (Ñuble Regional Hospital), with reproducible ultrasound characteristics and documented resolution during follow-up. To the best of our knowledge, this pattern has not been formally described in the literature as a specific semiological condition, despite its relevance in ultrasound follow-up.

Case series

Imaging follow-up was conducted on nine patients who had undergone thyroidectomy (total or partial) for thyroid cancer between 2022 and 2025, and whose follow-up ultrasound scans revealed images consistent with a "pseudo-thyroid", with the aim to characterize the behavior and evolution of these findings over time. All cases involved small papillary variant tumors (10-17 mm), and the thyroidectomies were performed using Surgicel™ (oxidized regenerated cellulose) as a hemostatic agent for the surgical bed (two sheets measuring approximately 1 × 3 cm). The finding presents a relatively narrow window of appearance and consistently resolves spontaneously during follow-up, as shown in table 1.

The ultrasound examinations were performed using high-frequency linear transducers, systematically incorporating color Doppler and power Doppler imaging to assess the thyroid bed and cervical lymph node compartments.

During the postoperative reorganization of the surgical bed, the findings evolve into a uniform sonographic pattern, creating a well-defined pseudo-glandular appearance[1] (Figs. 1 A to D). Following the surgery-induced changes, the contents of the surgical bed may appear on ultrasound as an isoechoic or mildly hyperechoic area with an inverted-triangular or flattened morphology, which occupies the virtual space corresponding to the thyroid gland[1,2] (Fig. 2A) and may also exhibit a peripheral hypoechoic halo (Figs. 2 E and F) and an absence of Doppler signal.

The series demonstrates a relatively predictable temporal pattern, with the appearance of the sonographic "pseudo-thyroid" during the early postoperative follow-up period, specifically between the second and fourth months after thyroidectomy (Figs. 1 B to D, 2 A to C, and 3 C and E). This period coincides with the phase of inflammatory reorganization and scarring of the surgical bed, a stage when the risk of confusion with glandular remnants or tumor recurrence is highest[1,2].

In earlier postoperative phases, that is, within the first 2 months in our series and prior to the reorganization of the surgical bed, the area may appear heterogeneously filled, showing cystic components as well as internal trabeculations, consistent with serohemorrhagic collections and an acute inflammatory process in the postoperative site[1,2] (Fig. 3D).

Ultrasound follow-up was primarily conducted between the sixth and ninth postoperative months; in cases 5 and 9 (Table 1), due to the lack of a follow-up control during that interval, a later ultrasound was performed solely to monitor progression, without affecting the primary temporal analysis.

The spontaneous resolution documented in all patients, generally after the sixth postoperative month, supports the benign and transient nature of this finding (Figs. 1 F, 2 D, and 3 F). The absence of sonographic progression and the observed systematic shrinking reinforce the value of serial ultrasound follow-up as an appropriate strategy to confirm the non-neoplastic nature of the finding and avoid unnecessary invasive diagnostic procedures.

Discussion

The postoperative "pseudo-thyroid" is a transient ultrasound finding observed in the surgical bed following a thyroidectomy. The echogenicity and morphology

Table 1. Temporal ultrasound evolution of the postoperative pseudo-thyroid

Cases	Gender	Age (years)	Ultrasound detection of pseudo-thyroid (postoperative day)	Documented ultrasound resolution (postoperative day)
1	F	46	62	349
2	F	35	44	219
3	F	43	53	191
4	F	43	113	233
5	F	44	59	621
6	M	27	98	390
7	F	31	69	282
8	F	46	90	189
9	F	39	137	546

F: female; M: male.

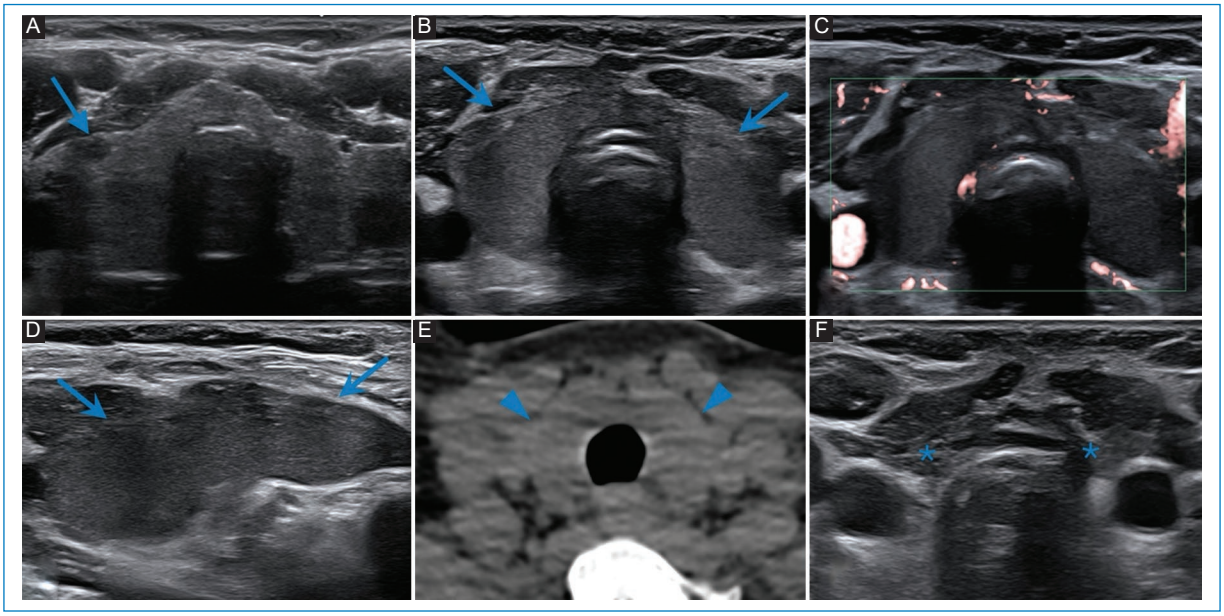

Figure 1. Classic pattern. Case 1: 46-year-old woman with papillary thyroid carcinoma. **A:** preoperative ultrasound showing a right thyroid nodule (arrow). **B:** transverse ultrasound of the surgical bed 62 days postoperatively, showing a homogeneous pseudo-thyroid with echogenicity similar to that of the thyroid parenchyma (arrows). **C:** absence of color Doppler and power Doppler signals in the pseudo-glandular area. **D:** longitudinal plane confirming the pseudo-lobular morphology of the finding (arrows). **E:** non-contrast axial CT scan of the neck showing homogeneous filling of the surgical bed, without the normal glandular hyperdensity. **F:** follow-up ultrasound showing complete resolution of the pseudo-thyroid (asterisks).

of the pseudo-thyroid can closely resemble normal thyroid parenchyma, which creates a potential for diagnostic overinterpretation during follow-up ultrasound examinations, particularly among radiologists in training.

It is important to be familiar with the evolution of post-thyroidectomy changes on ultrasound over time, when performing an examination in the first few months following surgery[1,2,5]. Although international recommendations suggest the first follow-up ultrasound between 6

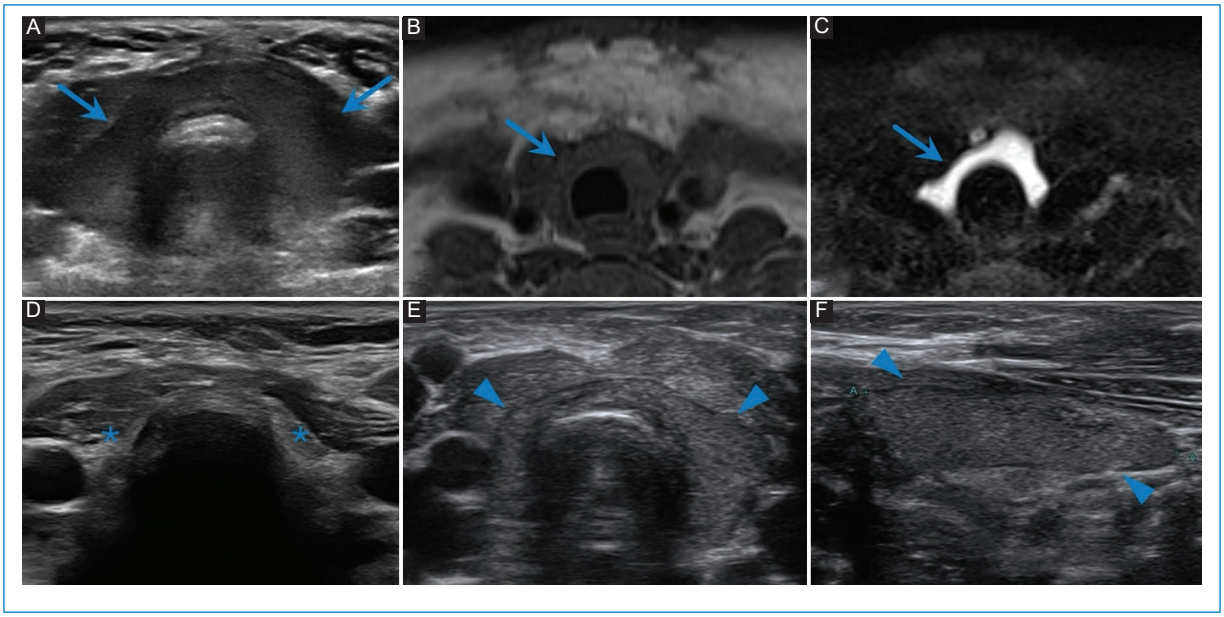

Figure 2. Early phase and multimodal correlation. Case 2: 35-year-old woman who underwent total thyroidectomy for papillary carcinoma. **A:** postoperative ultrasound (day 44) showing homogeneous fluid filling the surgical bed, forming a pseudo-thyroid (arrows). **B** and **C:** axial T1-weighted and T2-weighted STIR MRI (day 80) confirming fluid content. **D:** follow-up ultrasound (day 219) showing resolution of the finding (asterisks). Case 3: 43-year-old woman; transverse and longitudinal ultrasound (**E** and **F**) showing an organized pseudo-thyroid with homogeneous echogenicity and a thin peripheral hypoechoic halo (arrowheads).

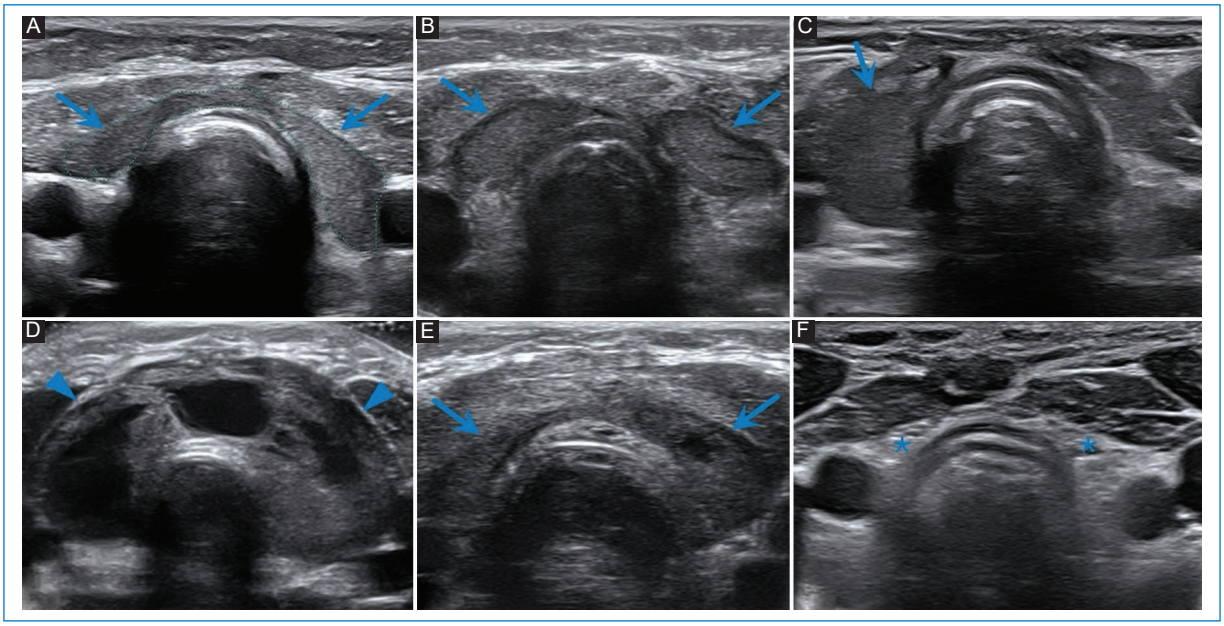

Figure 3. Morphological and evolutionary spectrum. **A:** case 4, 43-year-old woman, asymmetric pseudo-thyroid detected on postoperative day 111. **B:** case 5, 44-year-old woman, discontinuous bilateral pseudo-thyroid, with less prominent isthmic configuration and a peripheral hypoechoic halo. **C:** case 6, 27-year-old man, two-stage thyroidectomy; ultrasound on day 98 after right lobectomy shows a unilateral pseudo-thyroid. **D, E,** and **F:** case 7, 31-year-old woman; early ultrasound (day 16) showing heterogeneous filling, with solid-cystic appearance, of the surgical bed (arrowheads), progression to an organized pseudo-thyroid (arrows) by day 69, and complete resolution of the finding on follow-up (asterisks).

and 12 months post-thyroidectomy, in our clinical practice we identified a number of patients who underwent early ultrasound checks. This situation allowed us to recognize a transient and little-known postoperative finding whose appearance could lead to erroneous interpretations. This also prompted a review of our clinical care protocols, aligning them with the follow-up intervals proposed by international guidelines[6].

The semiological elements that point toward a diagnosis of postoperative pseudo-thyroid include:

- Overall echogenicity similar to that of thyroid parenchyma, without organized internal architecture.
- Presence of a thin hypoechoic halo (Figs. 2 E-F and 3B), consistent with a pseudo-capsule, at the margin of the surgical bed.
- Absence of color or power Doppler signals, both peripherally and centrally (Fig. 1C).
- Stable configuration relative to adjacent structures, without significant mass effect.
- Progressive involution over a period of time, with a decrease in volume on successive follow-up scans.
- Spontaneous resolution of the finding around the sixth postoperative month.

In all cases included in this series, the presence of these criteria and the temporal evolution allowed for the exclusion of tumor recurrence or glandular remnants, thereby avoiding unnecessary invasive diagnostic procedures. Among these criteria, the absence of Doppler signal and the progressive decrease in volume on successive follow-up scans are the most useful indicators.

Conclusions

The postoperative pseudo-thyroid is a benign, transient, and potentially common ultrasound pattern in the thyroid bed following a thyroidectomy, that can mimic residual tissue or tumor recurrence. Recognizing its distinctive ultrasound characteristics and understanding its temporal evolution helps reduce diagnostic overinterpretation, avoid unnecessary additional studies, and optimize the postoperative follow-up.

It is important to note that the risk of diagnostic error is higher during early ultrasound assessments, when the follow-up coincides with the period of highest frequency of detection for this ultrasound pattern, between two and four months postoperatively, the stage in which its pseudo-glandular appearance can lead to greater diagnostic confusion. The structured description of this phenomenon is particularly useful for radiology education, especially for radiologists in training, and facilitates more accurate and safe post-surgical surveillance.

Future longitudinal studies involving a larger number of cases will allow for a more precise definition of the temporal evolution of this finding and confirm its reproducibility.

Funding

The authors declare that they have not received funding.

Conflicts of interest

The authors declare no conflicts of interest.

Ethical considerations

Protection of human subjects and animals. The authors declare that no experiments on humans or animals were performed for this research.

Confidentiality, informed consent, and ethical approval. The authors have obtained approval from the Ethics Committee for the analysis of routinely collected and anonymized clinical data; therefore, individual informed consent was not required. Relevant ethical recommendations have been followed.

Declaration on the use of artificial intelligence. The authors declare that ChatGPT was used for editorial support, such as grammar checking, verifying formal consistency, and word counting, without generating original scientific content.

References

1. Ko MS, Lee JH, Shong YK, Gong GY, Baek JH. Normal and abnormal sonographic findings at the thyroidectomy sites in postoperative patients with thyroid malignancy. AJR Am J Roentgenol. 2010;194:1596-609.
2. Simeone JF, Daniels GH, Hall DA, McCarthy K, Kopans DB, Butch RJ, et al. Sonography in the follow-up of 100 patients with thyroid carcinoma. AJR Am J Roentgenol. 1987;148:45-9.
3. Dolcetti V, Lori E, Fresilli D, Del Gaudio G, Di Bella C, Pacini P, et al. US evaluation of topical hemostatic agents in post-thyroidectomy. Cancers (Basel). 2023;15:2644.
4. Shahin MN, Gupta A. Hemostatic agent mimicking residual thyroid tissue in a patient status post completion thyroidectomy for thyroid cancer. Endocr Pract. 2018;24:500.
5. Kim E, Park JH, Jung JH. Ultrasonographic surveillance following thyroidectomy for differentiated thyroid cancer. J Endocr Surg. 2025;25:47-57.
6. Ringel MD, Sosa JA, Baloch Z, Bischoff L, Bloom G, Brent GA, et al. 2025 American Thyroid Association management guidelines for adult patients with differentiated thyroid cancer. Thyroid. 2025;35:841-985.